



Cite this: *RSC Adv.*, 2024, **14**, 38952

## Advancements in nanotechnology-driven photodynamic and photothermal therapies: mechanistic insights and synergistic approaches for cancer treatment

S. Sameera Shabnum,<sup>a</sup> R. Siranjeevi,<sup>\*,a</sup> C. Krishna Raj,<sup>a</sup> A. Saravanan,<sup>b</sup> A. S. Vickram,<sup>c</sup> Hitesh Chopra<sup>d</sup> and Tabarak Malik  <sup>\*,ef</sup>

Cancer is a disease that involves uncontrolled cell division triggered by genetic damage to the genes that control cell growth and division. Cancer starts as a localized illness, but subsequently spreads to other areas in the human body (metastasis), making it incurable. Cancer is the second most prevalent cause of mortality worldwide. Every year, almost ten million individuals get diagnosed with cancer. Although different cancer treatment options exist, such as chemotherapy, radiation, surgery and immunotherapy, their clinical efficacy is limited due to their significant side effects. New cancer treatment options, such as phototherapy, which employs light for the treatment of cancer, have sparked a growing fascination in the cancer research community. Phototherapies are classified into two types: photodynamic treatment (PDT) and photothermal therapy (PTT). PDT necessitates the use of a photosensitizing chemical and exposure to light at a certain wavelength. Photodynamic treatment (PDT) is primarily based on the creation of singlet oxygen by the stimulation of a photosensitizer, which is then used to kill tumor cells. PDT can be used to treat a variety of malignancies. On the other hand, PTT employs a photothermal molecule that activates and destroys cancer cells at the longer wavelengths of light, making it less energetic and hence less hazardous to other cells and tissues. While PTT is a better alternative to standard cancer therapy, in some irradiation circumstances, it can cause cellular necrosis, which results in pro-inflammatory reactions that can be harmful to therapeutic effectiveness. Latest research has revealed that PTT may be adjusted to produce apoptosis instead of necrosis, which is attractive since apoptosis reduces the inflammatory response.

Received 3rd October 2024  
 Accepted 1st December 2024

DOI: 10.1039/d4ra07114j  
[rsc.li/rsc-advances](http://rsc.li/rsc-advances)

### 1. Introduction

Therapy with light has been practiced for the past three millennia.<sup>1</sup> Light was employed by the ancient Egyptian, Indian, and Chinese cultures to treat a variety of ailments, such as vitiligo, rickets, psoriasis, and skin cancer. Numerous therapies exist that take use of the photochemical, photothermal, or

photomechanical interactions between light and tissues in the body.<sup>2</sup> Thermal therapies have been used to treat cancer cells since the 18th century. A class of disorders known as cancer is defined by abnormal and uncontrolled cell proliferation that can have detrimental effects on health. Depending on the kind and severity of the cancer, many treatment options are available. For example, surgery aids in the removal of cancerous masses or tumours. Drugs are used in chemotherapy to destroy certain cancer cells. Other cancer treatments include immunotherapy, bone marrow transplantation, targeted medication therapy, radiation therapy, hormone therapy, and cryoablation. While there have been some instances when these therapies have been shown to be beneficial, they also have serious negative effects. Finding the most effective cancer medication that has higher efficacy and few to nil side effects is therefore urgently needed.

The raising of temperature over physiological ranges, usually to 40–45 °C, is known as hyperthermia. The major objective of hyperthermia is to provide an environment that makes tumor removal easier while protecting healthy tissues used in cancer

<sup>a</sup>Department of Chemistry, Saveetha School of Engineering, Saveetha Institute of Medical and Technical Sciences, Saveetha University, Chennai-602105, Tamil Nadu, India. E-mail: [jaisiranjeevi.r@gmail.com](mailto:jaisiranjeevi.r@gmail.com)

<sup>b</sup>Department of Sustainable Engineering, Institute of Biotechnology, Saveetha School of Engineering, SIMATS, Chennai-602105, Tamil Nadu, India

<sup>c</sup>Department of Biotechnology, Saveetha School of Engineering, Saveetha Institute of Medical and Technical Sciences, Saveetha University, Chennai-602105, Tamil Nadu, India

<sup>d</sup>Centre for Research Impact & Outcome, Chitkara College of Pharmacy, Chitkara University, Rajpura, 140401, Punjab, India

<sup>e</sup>Department of Biomedical Sciences, Institute of Health, Jimma University, 378, Jimma, Ethiopia. E-mail: [malikitrc@gmail.com](mailto:malikitrc@gmail.com)

<sup>f</sup>Division of Research & Development, Lovely Professional University, Phagwara, 144411, India



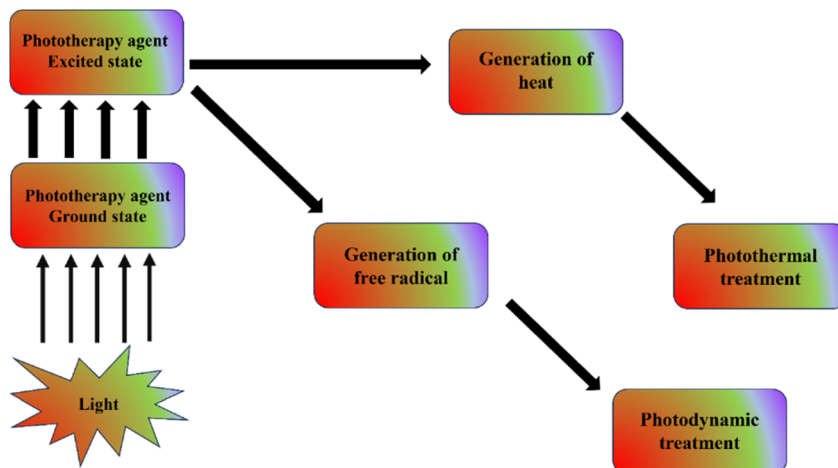


Fig. 1 Simple diagrammatic representation of photodynamic therapy and photothermal therapy mechanism.

therapy. However, the normal tissues are frequently impacted by this treatment. Applying photothermal therapy with laser radiation can make photothermal therapy more applicable for more targeted cancer treatment. The requirement for a powerful laser to kill the tumor cells is a major drawback of this treatment. Modern phototherapy offers advantages including focused therapy, deep penetration, specialized phototherapy, large exposure area, and longer exposure period. It also makes use of nanomaterials like CNT, gold nanoparticles, graphene, and quantum dots. The combination of PDT and PTT is also quickly gaining popularity due to its synergistic benefits, which can help chemotherapy and radiation therapy as an adjuvant treatment method Fig. 1.<sup>3</sup>

Photodynamic therapy (PDT) was developed in the nineteenth century by Niels Finsen. The scientists found that mixing chemicals and light may cause more cell death than usual. Using light-activatable chemicals (or, more recently, nanoparticles) to trigger the production of deadly harmful free radicals or reactive oxygen species—most frequently, singlet-state oxygen, or  $^1\text{O}_2$ —photodynamic treatment (PDT) is based on photochemistry.<sup>4</sup> The main component of photodynamic treatment (PDT) is the use of photosensitizers (PSs), which are activated by light of a wavelength that is long enough to convert oxygen molecules into ROS (hazardous reactive oxygen species), such as singlet oxygen. This process ultimately results in cell death for the cancer cells by oxidative stress.<sup>5</sup>

In contrast, photothermal therapy (PTT) kills cells and tissues primarily by heat using just light, often in the near-infrared range for maximal tissue penetration.<sup>6</sup> PTT is a more discreet and maybe helpful substitute for treating cancer. Applying pulsed laser irradiation within the near-infrared (NIR) range to activate photosensitizing compounds, PTT produces heat for the thermal destruction of cancer tumours with a restricted invasion into neighbouring healthy tissues.<sup>7</sup> Selective heating has been suggested for PTT that contains a photothermal agent. The main requirements for PTT are an NIR light source and a compatible photothermal compound with an exceptionally high absorption co-efficient. The degree of

absorption of the NIR spectrum and the light-excitation coefficient determine the temperature increase in the PTT. Photothermal therapy may eradicate cancer cells from the main tumor or from tumors that have already begun to metastasize, either by alone or in combination.<sup>3</sup>

Cancer is a primary source of illness and mortality globally, necessitating ongoing efforts to innovate and improve treatment options. Traditional cancer treatments, such as chemotherapy, radiation, and surgery, are restricted due to systemic side effects, non-specificity, and, in many cases, treatment resistance. In response, photodynamic therapy (PDT) and photothermal therapy (PTT) have emerged as potential minimally invasive cancer therapies due to their ability to precisely target tumor cells while causing minimum harm to surrounding healthy tissue. PDT uses light-activated photosensitizers to generate reactive oxygen species (ROS), which cause cancer cell death, whereas PTT uses photothermal agents to turn light into heat, resulting in localized hyperthermia and cell ablation. Despite their therapeutic promise, PDT and PTT are restricted by tissue penetration, nonspecific accumulation, and sometimes poor therapeutic effectiveness. These problems have sparked interest in nanotechnology as a way to improve the efficacy and specificity of PDT and PTT.<sup>3,8–10</sup>

Nanomaterials have distinct physicochemical features, such as variable size, surface charge, large surface area, and increased optical properties, making them excellent for improving PDT and PTT. Nanomaterials, such as gold, silver, silica, and silicon nanoparticles, quantum dots, carbon-based nanomaterials, manganese dioxide ( $\text{MnO}_2$ ) nanosheets, and nanoscale metal-organic frameworks (MOFs), have been engineered to enhance the stability, cellular uptake, and therapeutic impact of photosensitizers and photothermal agents. For example, gold nanoparticles have a significant surface plasmon resonance, which improves light absorption and heat production in PTT. Furthermore, their biocompatibility and ease of functionalization make them useful carriers for photosensitizers, facilitating targeted administration and effective ROS generation in PDT. However, the exorbitant cost of gold



nanoparticles, as well as their potential cytotoxicity at high concentrations, limit their use, spurring the search for alternatives.<sup>11–13</sup>

NPs have been discovered to penetrate deep tissues, increasing the increased permeability and retention (EPR) impact. Furthermore, surface features influence bioavailability and half-life by successfully passing through epithelial fenestration.<sup>14</sup> For example, NPs coated with polyethylene glycol (PEG), a hydrophilic polymer, reduce opsonization and avoid immune system clearance.<sup>15,16</sup> It is also feasible to optimise the release rate of medications or active moiety by altering particle polymer properties. Overall, the unique features of NPs influence their therapeutic efficacy in cancer care and therapy.

Drug-targeting pathways are techniques for delivering therapeutic compounds directly to disease locations, boosting therapy efficacy while avoiding unwanted effects. These pathways are classified as passive and active targeting. Passive targeting is based on the spontaneous accumulation of medications in certain tissues due to biological processes such as the Enhanced Permeability and Retention (EPR) effect, which is especially important in malignancies. The EPR effect arises because tumor tissues have leaky vasculature with big holes that allow nanoparticles and drug carriers to collect, and tumors have inadequate lymphatic drainage, which helps to keep these medications for longer. This method is frequently used in cancer therapies, where drug-loaded nanoparticles passively aggregate in tumor tissues without the need for particular targeting mechanisms. Passive targeting simplifies drug carrier design since it does not require specialized ligands to target receptors; nevertheless, its shortcoming is a lack of specificity, as it relies on physiological parameters rather than precision targeting.<sup>17–19</sup>

Active targeting, on the other hand, entails modifying drug carriers with particular molecules such as antibodies, peptides, or ligands that bind preferentially to receptors on target cells' surfaces. By using ligands that bind to receptors overexpressed on sick cells, such as cancer cells, active targeting guarantees that the drug carrier is delivered specifically to the designated region. This method is particularly effective in targeted cancer therapy, as certain cells overexpress identified receptors, allowing for more accurate drug administration. Active targeting has higher specificity and fewer off-target effects, making it highly effective for diseases with distinct cellular markers. However, it requires detailed knowledge of target cell receptors and careful engineering of drug carriers, which can be complex and costly. Both passive and active targeting are critical in developing drug delivery systems, particularly in nanomedicine, since they allow for increased drug accumulation at disease locations and better therapeutic effects.<sup>20,21</sup>

Nanoparticles play an important role in both passive and active drug-targeting techniques because they have unique features that improve drug delivery accuracy and efficiency in modern biomedical research. Nanoparticles used in passive targeting take advantage of tumors' Enhanced Permeability and Retention (EPR) effect. Nanoparticles, because of their tiny size and ability to be tailored to match ideal size and surface features, may easily pass through tumor vasculature and

aggregate more efficiently than standard therapeutic molecules. This has been established in several studies employing nanoparticles such as liposomes, polymeric nanoparticles, and lipid-based nanocarriers to carry chemotherapeutic drugs to malignant cells. Researchers increased medication stability and bioavailability by encapsulating pharmaceuticals in nanoparticles, resulting in more concentrated and extended drug release at the target location.

Nanoparticles are an appropriate platform for active targeting because they may be functionalized with particular ligands, antibodies, or peptides that bind selectively to cell surface receptors on sick cells, such as cancer cells overexpressing certain biomarkers. Gold nanoparticles, quantum dots, and polymeric nanoparticles, for example, have been functionalized with targeting molecules such as folic acid, transferrin, or antibodies to specifically target cancer cells with overexpressed receptors, resulting in more effective and selective delivery. Current research indicates that nanoparticles with these surface changes have the potential to improve drug delivery accuracy, reduce off-target effects, and allow for lower drug dosages, hence lowering possible toxicity to healthy tissues.<sup>22,23</sup>

Furthermore, nanoparticles provide extra functions in targeted treatment due to their inherent features. Certain metallic nanoparticles, such as gold or magnetic nanoparticles, can perform both drug delivery and imaging, enabling for real-time tracking and monitoring of medication distribution inside the body. Others, such as photothermal or photodynamic agents, are intended to release therapeutic chemicals in response to certain stimuli, such as light or heat, allowing for spatiotemporally regulated treatment at the target region. As a result, nanoparticles are crucial to current research on passive and active medication targeting, allowing for a new degree of personalization in treatment techniques that are highly precise, minimally intrusive, and tuned for optimal therapeutic efficacy in disease management.<sup>24–27</sup>

Nanoparticles have considerable benefits in cancer therapy, both as independent medicines and in conjunction with photodynamic therapy (PDT), because of their unique features that allow for targeted, regulated, and multi-functional therapeutic methods. As individual agents, nanoparticles improve drug delivery by allowing both passive and active targeting, resulting in increased drug accumulation in tumors while sparing healthy cells, thereby boosting therapeutic efficacy and lowering adverse effects. Additionally, nanoparticles improve therapeutic solubility and stability, particularly for hydrophobic medicines that are difficult to administer efficiently in traditional forms. They also allow for regulated and prolonged medication release at the tumor site, which reduces the need for frequent dosing and increases patient compliance. Some nanoparticles, such as gold and magnetic nanoparticles, have intrinsic therapeutic capabilities, such as causing localized heating (hyperthermia) in response to specific stimuli, which can either directly kill cancer cells or sensitize them to subsequent therapies. Furthermore, nanoparticles have theranostic capabilities, which means they may perform both therapeutic and diagnostic tasks. For example, iron oxide nanoparticles can



act as MRI contrast agents while also providing heat, allowing for real-time monitoring of the therapy's progression.<sup>28-32</sup>

Silver nanoparticles have also demonstrated potential owing to their antibacterial characteristics and significant light absorption in the near infrared (NIR) region, making them suited for both PDT and PTT. However, worries about their long-term biocompatibility and potential toxicity have yielded inconsistent outcomes in clinical trials. Silica and silicon nanoparticles, on the other hand, offer a biocompatible and cost-effective platform with great thermal stability and drug encapsulation capability, which improves the therapeutic index of PDT and PTT treatments. Quantum dots (QDs) have unique optical characteristics and great photostability, allowing for real-time imaging and monitoring of photosensitizers *in vivo*, enhancing PDT accuracy. However, the toxicity of heavy metals in QDs has limited their usage in clinical applications.<sup>33,34</sup>

Carbon-based nanomaterials, such as graphene and carbon nanotubes, have a high surface area and unique heat conductivity, making them ideal photothermal agents in PTT. These materials have high photothermal conversion efficiency, but they require careful surface modification to increase dispersibility and biocompatibility. Manganese dioxide ( $MnO_2$ ) nanosheets and nanoscale metal-organic frameworks (MOFs) have received interest for their flexibility in PDT and PTT.  $MnO_2$  nanosheets have catalytic activity that increases intracellular oxygen levels, reducing hypoxia in the tumor microenvironment, a recognized obstacle to PDT effectiveness. MOFs, with their high porosity and flexible frameworks, provide variable release profiles for photosensitizers and other therapeutic agents, hence improving both PDT and PTT results. However, there are still hurdles in synthesizing MOFs of uniform quality and stability under physiological circumstances.<sup>35</sup>

In addition to these individual nanoparticles, great progress has been made in mixing numerous nanomaterials to form hybrid systems with complimentary features. For example, incorporating gold nanoparticles into carbon-based materials can improve photothermal stability and efficacy, whereas silica-coated nanoparticles can minimize toxicity and increase circulation times. The combination of PDT and PTT with traditional treatments such as chemotherapy, radiation, and immunotherapy has shown further synergistic effects in cancer treatment, leveraging the strengths of each modality to improve overall therapeutic results. Such combination medicines address several areas of cancer pathophysiology, possibly overcoming challenges such as treatment resistance and immune evasion.<sup>36-38</sup>

When used with PDT, nanoparticles provide additional benefits that increase the therapy's efficacy. They increase photosensitizer transport to tumor locations by raising the concentration of the photosensitizer in cancer cells, improving PDT efficacy while decreasing undesired accumulation in healthy tissues. Encapsulating or attaching photosensitizers to nanoparticles shields them against degradation, increasing photostability and extending their active duration. Furthermore, certain nanoparticles allow for regulated activation *via* dual-modal treatments, in which PDT is paired with photothermal effects, therefore boosting the therapeutic

effectiveness. Nanoparticles also increase reactive oxygen species (ROS) formation in PDT, enhancing the deadly effect on cancer cells. Combining PDT with other nanoparticle features, such as magnetic hyperthermia, allows for multi-modal therapy that can overcome tumor resistance and minimize recurrence. Finally, nanoparticles enable real-time imaging and monitoring, which is useful for tracking photosensitizer location and improving therapy progress. Overall, nanoparticles employed alone or in combination with PDT provide novel options in cancer therapy, providing focused, regulated, and synergistic techniques that may enhance patient outcomes by overcoming the limits of current therapies.<sup>39-41</sup>

The need for this study stems from the potential yet fragmented research environment in nanomaterial-enhanced PDT and PTT. While various studies have looked at individual nanomaterials for these therapies, there is an urgent need to consolidate and critically analyze the benefits, limits, and synergistic potential of these nanomaterials in the context of combined cancer treatments. This study seeks to bridge knowledge gaps and highlight future possibilities in cancer nanomedicine by giving a complete overview of PDT and PTT molecular processes, nanomaterial advances, and combination techniques. This topic was chosen because of its potential to enlighten and inspire focused, effective, and patient-centered cancer treatment tactics, resulting in the development of more resilient and individualized oncological medicines.

## 2. Mechanism of action

### 2.1. Mechanism of action at molecular level of PDT and PTT

Three primary constituents typically necessary for PDT: light, a light-activatable substance (called a photosensitizer, or PS), and, in the case of many PS, oxygen. These three ingredients combine to undergo a photodynamic reaction that results in the production of cytotoxic ROS. A PS molecule absorbs incident light, which changes it from its ground state to excited singlet state with a short half-life ( $\sim ns$ ). This singlet state subsequently crosses the intersystem to become an excited triplet state, which is comparatively more stable ( $\sim ms$ ). Photosensitizer molecules can undergo a type I or type II photodynamic reaction to return from the triplet to the ground state. In the former, different ROS, such as  $O_2^-$  and  $HO_2^-$ , are formed when activated photosensitizers transfer an electron to substrate. A type II reaction produces energy quickly shifted to ground-state molecular oxygen. Numerous biological reactions, such as direct cytotoxicity, vascular events and inflammation, are triggered by the reactive species. Significantly, the diffusion distance of ROS within cells and tissues is remarkably small (less than 50 nm), meaning the photosensitizers often required to be positioned in close range to the target location Fig. 2.<sup>42,43</sup> PDT frequently produces a distinct border separating the necrotic sections that received the TPDT dosage and the viable tissue regions because of the shortened ROS distance of diffusion and targeted light delivery.<sup>44</sup> Furthermore, as photosensitizers prefer to cluster inside cancer cells, PDT produces extremely minimal effects on adjacent neurons and ECM, although when they are in the treatment area.<sup>45</sup> Because of this,



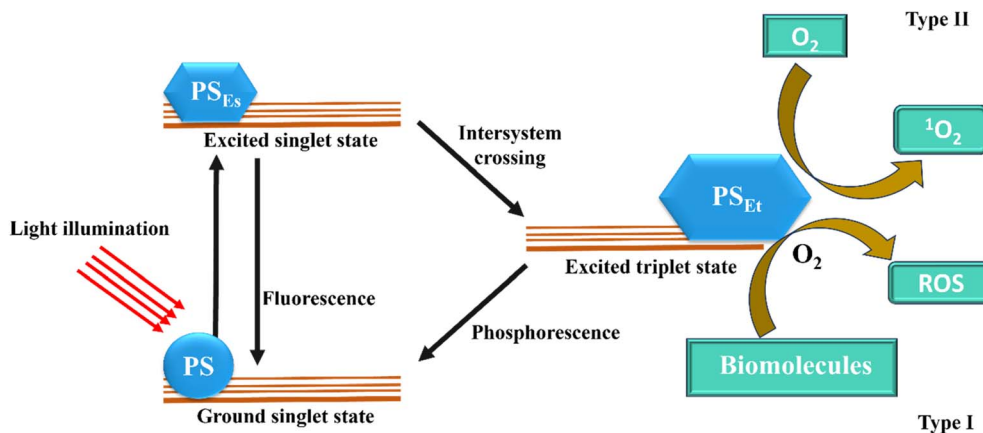


Fig. 2 The PDT's mode of action displays both type I and type II responses. ROS denotes reactive oxygen species, whereas PSEs and PSET denote PS excited singlet and triplet states (Calixto *et al.* 2016).<sup>42</sup>

PDT is appropriate for tumors that are encircled by vital tissues, such as malignancies of the bladder, oesophagus, lung, prostate, pancreatic, and head and neck.<sup>46</sup>

Using light, usually in the near-infrared (NIR) spectrum, photothermal treatment (PTT) raises tissue temperature and causes local photocoagulation. PTT uses comparatively high light intensities to reach temperatures that are either coagulative (55–100 °C) or subcoagulative (43–55 °C), which causes fast cell death by producing disruption to the cell membrane and denaturation of proteins.<sup>47</sup> Milder heating protocols (41–43 °C) are categorized as hyperthermia, which, unless administered for extended periods of time (>1 h), is not tumoricidal on its own. Although hyperthermia is not utilized therapeutically as an independent modality, it may be used to induce HSP and change the tumor perfusion and metabolic status, which can improve the selectivity and effectiveness of other modalities like radiation treatment or chemotherapy.<sup>48</sup>

## 2.2. Mechanisms of cell death *via* PDT

Due to the short-lived ROS that primarily drives PDT-induced cytotoxicity, the prevailing cell death pathways are determined by the chemical structure of the photosensitizer, its subcellular location, and the parameters of light delivery. It is well acknowledged that lysosomal photosensitzers cause protease release, whereas photosensitzers that localize to the mitochondria and endoplasmic reticulum cause apoptosis by release of cytochrome C. It is interesting to note that PDT efficacy is greatly increased by successive targeting of lysosomes as well as mitochondria. This effect may be attributed to increased radical generation within mitochondria as a consequence of photochemically driven iron release by lysosomes.<sup>49</sup> Utilizing this approach, a liposomal PS composition that targets lysosomes, endoplasmic reticulum and mitochondria all at once was created.<sup>50</sup> Photo damage that degrades the Bcl-2 (an anti-apoptotic protein), which triggers a series of downstream pro-apoptotic events, is another mechanism of PDT cytotoxicity. PDT can also induce paraptosis and autophagy along with necrosis and apoptosis.<sup>49,51</sup> Last but not least, some

photosensitzers have the capacity to elicit immunogenic cell death (ICD), as demonstrated by the externalizing of calreticulin (CRT) as well as the ATP, HMGB1, HSP70 and HSP90 are therefore released.<sup>52</sup>

## 2.3. Mechanisms of cell death *via* PTT

Depending on the temperature, time frame, and the usage of external photo-absorbers like nanoparticles, PTT can work through diverse cell death pathways Fig. 3.<sup>53</sup> The main mechanism of PTT cytotoxicity is protein denaturation *via* induction of heat, so the higher the temperature, the more rapidly and efficiently the death of cell occurs. Mild hyperthermia (~41–43 °C) has been shown to induce HSP response, however, it is less damaging if continued over an extended length of time (~1 h).<sup>54,55</sup> It is believed that apoptosis is induced by PTT (55–60 °C), which will be followed with secondary necrosis.<sup>47</sup> The study showed that melanoma cells exposed with gold nanorods exhibited patterns of temperature-dependent cell death. A comparatively minor amount of cell viability was lost with mild heating (43 °C), with 10.2% through apoptosis, 18.3% by necroptosis, and 17.6% of cells *via* necrosis, respectively. Raising the temperature over the coagulative threshold (about 55–60 °C) usually results in tissue necrosis right away because of proteins denaturation and a breakdown of integrity of cell membrane.<sup>56</sup> The real-time visualization of these tissue changes by MRI, ultrasound, or optical modalities is beneficial for therapy adjustment and monitoring.<sup>57</sup>

## 2.4. PDT in tumor cell death

In order to kill target tumor cells, photodynamic therapy (PDT) primarily uses the excited state of a photosensitizer to produce singlet oxygen. PDT is applicable in a number of cancerous conditions.<sup>58</sup> It is a method that makes use of certain substances that function as photosensitzers.<sup>59</sup> These substances are dormant unless exposed to a certain kind of light. Additionally, oxygen must always be present for them to function. ROS are produced by the photosensitizer (PS), that is triggered by light. Consequently, ROS are in charge of effector



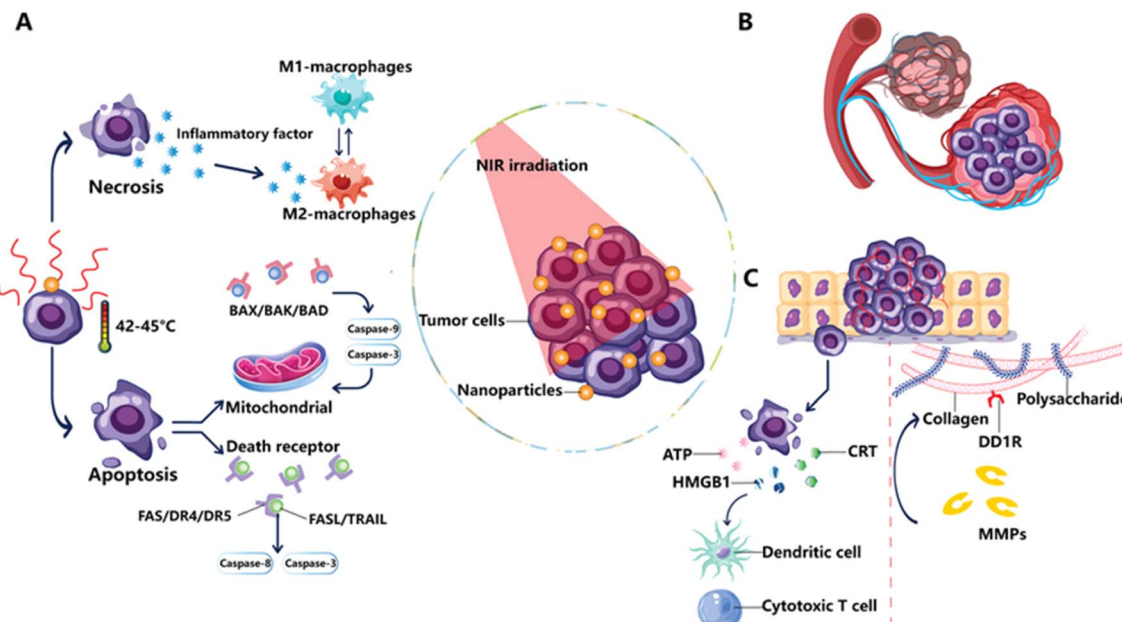


Fig. 3 PTT mechanics as perceived via a medical viewpoint. (A) Tumor cell necrosis and apoptosis: PTT induces necrosis by breaking the tumor cell membrane, which causes the release of inflammatory cytokines and encouraging macrophages to adopt an M2-like phenotype. When a cell goes through apoptosis, the cell envelope remains intact while the death receptor and mitochondrial mechanisms cause cell death. (B) Tumor hypoxia and vascular disruption: PTT disrupts the tumor vasculature, making the tumor hypoxic and encouraging cell death. (C) Extracellular matrix changes and ICD: PTT induces the synthesis of DAMPs, which impact cytotoxic T cells and DCs, resulting in ICD. PTT also promotes ECM rearrangement by damaging collagen, the major component of the ECM, via DDR1 and MMPs (Xiong et al. 2023).<sup>53</sup>

processes like tumor cell death.<sup>60</sup> An electron moves to its initial excited singlet state when the PS is activated by light. An intersystem crossover that comes next produces a triplet state. Reactive singlet oxygen ( ${}^1\text{O}_2$ ) is produced when the triplet PS transmits energy to the triplet oxygen.  ${}^1\text{O}_2$  has a wide variety of effects, including the direct destruction of cancer cells, vascular damage, and immune response induction. PDT can also cause necrosis and apoptosis in cancer cells.<sup>61</sup> Furthermore, PDT may damage the tumor's vascular systems, depriving cancer cells of essential nutrients and causing them to become hypoxic.<sup>62,63</sup> Recent research has demonstrated that ROS have a variety of biological impacts. While direct tumor cell death is one of PDT's most powerful effects, immunological responses generated by PDT also have the ability to significantly impact the treatment's overall efficacy.<sup>60</sup> PDT may ultimately result in either immune system activation or inhibition.<sup>64</sup>

The use of optic fibers, which could penetrate interstitial tumor tissues, solved the challenge of delivering light to the cancer location other than surface ones. These developments made it possible to employ PDT to treat a variety of cancers, such as those of the pancreas, prostate, head and neck, and others.<sup>65</sup> For therapy of interstitial tumors, the PS can be given intravenously or orally. Then, at the targeted tissue region, it is triggered using a certain light wavelength. This may be accomplished with a laser. Through optical fibers contained within clear plastic needles, light may be administered to the desired tissue.<sup>59</sup> PDT can make use of particular kinds of laser or light-emitting diodes (LEDs). The type of light that is employed depends on the type of tumor tissue and its location

inside the body. The placement of the guides, which are often done under general anesthesia, uses ultrasonography to assist the targeting of the tumor tissue accurately. There is a lag time between the patient receiving the medication and the light treatment. Drug-to-light interval refers to this time frame, which can range from hours to days according on the PS being used (e.g., pharmacokinetic properties). The majority of PDT applications are typically carried out in an outpatient environment and do not necessitate hospitalization.<sup>58</sup>

The overall tumor-eradication impact of PDT involves many unique pathways.<sup>61,66</sup> The immune system of the host may be boosted by PDT to combat tumor cells.<sup>60</sup> While most traditional anti-cancer treatment techniques, like radiation and chemotherapy, suppress the immune system, PDT can stimulate inflammation, draw leukocytes to the affected area, and help activate T cells that fight cancer. PDT also reduces the microvasculature of the tumor, depriving the malignant tissue of nutrition and oxygen.<sup>60,67</sup> Finally, but just as importantly, PDT can directly destroy tumor cells by causing necrosis or apoptosis by the use of active  $\text{O}_2$ . Most likely, there are connections between these systems. Certain processes may hold significance in varying therapeutic contexts, contingent upon the tumor type and PS. Not only do tumor tissues have parenchyma, or cancer cells, but they also contain stroma.<sup>68</sup> The components of the tumor microenvironment include extracellular matrix, fibroblasts, vascular structures, and immune cells. The majority of stromal components serve to promote the development of tumors. PDT can have an impact on the majority of tumor milieu components.<sup>58</sup> To a certain extent, PDT can directly

eradicate tumor cells, however this kind of removal can't be accomplished by a single method.<sup>69</sup> PDT has the ability to lower the quantity of tumor cells that are clonogenic. It was observed that immediately following the conclusion of light illumination of photosensitizer-treated tumors, a reduction of up to roughly 72% may be achieved in the overall number of clonogenic cells. PDT directly causes target tumor cells to undergo a combination of necrosis and apoptosis.<sup>61</sup> PDT has the ability to cause apoptosis quickly. Furthermore, it was claimed that PDT might cause autophagy, a crucial conserved cellular recycling system, to cause cancer cells to die.<sup>70</sup> Also, these pathways may manifest simultaneously, contingent upon the kind and concentration of the photosensitizer.<sup>71</sup>

Agarwal *et al.* showed that PDT might cause apoptosis and cause DNA to break down into fragments. Time and dosage had an impact on the DNA fragmentation. They also discovered impairment of cytoplasmic structures and the appearance of chromatin condensation at the nucleus's perimeter.<sup>72</sup> A number of photosensitizers have an impact on the mitochondria, and PDT has been shown to be a powerful inducer of apoptosis under a variety of circumstances. Many studies have looked at the processes underlying PDT-induced cell apoptosis along with the effect of signaling pathways on response to PDT.<sup>73-79</sup> Apoptosis induction mediated by PDT involves caspases and members of the Bcl-2 protein family. On the contrary, while the apoptotic process is blocked or occurs concurrently with apoptosis, autophagy can occur without the involvement of Bax.<sup>71</sup> It is well known that a number of cancer treatments, such as PDT, target apoptotic pathways.<sup>80-86</sup> PDT has the capacity to trigger many apoptotic pathways. PDT-induced apoptosis is linked to both the intrinsic (facilitated by mitochondria) and extrinsic (facilitated by death receptors) pathways. The kind of apoptotic pathway depends on the photosensitizer and cancer cell types. PDT mostly activates caspase-3 or caspase-7 by activating the intrinsic route.<sup>87</sup> The intrinsic route, which causes caspase-dependent and caspase-independent apoptosis in PDT, depends critically on mitochondria. It should be mentioned that PDT mainly initiates apoptotic pathways that are dependent on caspase.<sup>71</sup> The photosensitizer's intracellular location influences the effectiveness of inducing apoptosis in PDT as well. Accordingly, localized photosensitizers on mitochondria are highly effective apoptosis inducers.<sup>61</sup> Numerous investigations have revealed significant information on the critical processes linked to mitochondrial events and the apoptotic pathways which are activated in response to PDT. In the context of PDT, a number of apoptotic mediators and signaling pathways are being discovered.<sup>88</sup> Apart from *in vitro* investigations, other research works shown the *in vivo* apoptotic consequences of photodynamic tumor treatment.<sup>89</sup> The perturbation of the mitochondrial transmembrane potential is one of the early processes in PDT-mediated apoptosis that has been documented. Loss of potential for the mitochondrial membrane may occur quickly after PDT.<sup>90,91</sup> The hypothesis put forth by Kowaltowski *et al.* was that the PDT agent's effects on inner membrane permeation to protons could lead to impairment of mitochondrial membrane potential.<sup>92</sup> According to a number of

studies, photosensitizers targeting the mitochondria may effectively cause apoptosis in PDT.<sup>93-99</sup>

PDT has been linked to mechanisms such as cytochrome c release and caspase activation, particularly caspase-9 and caspase-3.<sup>100,101</sup> These results are consistent with the numerous investigations that have examined the function of caspase-3 in PDT-mediated apoptosis using a range of photosensitizers.<sup>102</sup> Additionally, it has been found that PDT modifies a number of signaling pathways linked to oxidative stress responses.<sup>103</sup> In conclusion, it is clear that PDT has a strong apoptosis-inducing effect.<sup>61</sup> However, PDT's ability to totally eradicate malignancies in a clinical context is still lacking. The current status has been explained in a number of ways. According to some research, the effectiveness of photodynamic therapy (PDT) in killing tumor cells declines as the cells get farther away from the blood supply. This might have serious consequences due to the uneven distribution of photosensitizer inside the tumor tissue.<sup>104</sup> Furthermore, the oxygen quantity and accessibility in the tumor tissue might affect PDT's effectiveness. Many tumor tissues demonstrate hypoxia. Furthermore, PDT employs oxygen in photodynamic processes. Not to add, PDT can injure vascular tissues and cause oxygen deficit. PDT has been observed to produce abrupt decreases in oxygen levels of tissue. According to Pogue *et al.*, the hypoxic tissue regions showed abrupt reduction in partial oxygen pressure following treatment, but the greater partial oxygen pressure regions showed heterogeneity and some parts retained their partial oxygen pressure value. On the other hand, in a situation whereby the photosensitizer was administered three hours before to the administration of light, another study found that the partial oxygen pressure in the tumor tissue rose after the light exposure was completed.<sup>105,106</sup> In actuality, tissue hypoxia could restrict PDT's therapeutic efficacy. The PDT irradiation process may fragment, allowing oxygen to be replenished in the tissue.<sup>107</sup>

## 2.5. PTT in tumor cell death

In photothermal treatment (PTT), laser energy is converted into the heat to destroy cancer cells using nanoparticles placed inside tumors as exogenous energy absorbers. PTT can be a viable substitute for traditional cancer treatment, but in some cases of radiation exposure, it can cause necrosis of cell. This necrosis may elicit pro-inflammatory responses that are detrimental to the treatment's progression. It is desirable when PTT can be adjusted to cause apoptosis instead of necrosis since apoptosis inhibits an inflammatory response, as evidenced by recent research. Several NP compositions are being investigated by researchers as PTT transducers. The ability to capture NIR light, with an extensive absorption cross section to improve light-to-heat exchange, diameter around 30 and 200 nm that promote lengthy circulation and increased tumor growth, and lowest toxicity/maximum biocompatibility are among the main design factors. Although PTT has advanced at an astounding rate from idea to clinical testing, there aren't many in-depth research that look at the fundamental biological response to PTT. To optimize treatment efficacy and reduce the risk of unfavourable side effects, it is critical to comprehend the kinetics and causes of cell death brought on by this method.<sup>108</sup>



Necrosis and apoptosis are the two types of cell death that PTT may cause. The breakdown of plasma membrane stability and consequent leakage of intracellular components such as DAMPs (damage-associated molecular patterns), within the external to cells environment are hallmarks of necrosis. Because of the potential for harmful inflammatory and immunogenic reactions brought on by this aberrant release, necrosis is an undesirable mode of cell death. In contrast, during apoptosis, the reliability of the cell membrane is preserved, and signals such as phosphatidylserine (PS) are sent to the extracellular domain of the membrane, designating a cell for phagocytosis. When apoptotic cells come into contact with phagocytes, they undergo a transformation that inhibits inflammation, which is a different and preferable result than what happens during necrosis. Nevertheless, an apoptotic cell may potentially lose its membrane integrity and discharge its internal contents, including DAMPs, if phagocytes do not quickly remove it. When phagocytes are not present, a process referred to as secondary necrosis can be shown in *in vitro* experiments.<sup>109</sup> Currently, necrosis is the most often documented *in vitro* cellular responses to photothermal therapy (PTT); nevertheless, other research has indicated that, in specific light exposure settings, apoptosis may be the major cause of cell death.<sup>110</sup> The overview of apoptosis by PTT is supported by the following data: (i) Western blotting after PTT shows loss of Bid and increased synthesis of tBid; (ii) flow cytometry after PTT shows impairment of mitochondrial membrane potential; and (iii) FACS after PTT shows activation of caspase-3. First, while PTT activates Bid, the exact method of activation is yet unknown. In the present investigation, administering cells along with caspase-8 inhibitor failed to avert apoptosis following PTT. Normally, caspase-8 activates Bid into the extrinsic apoptosis pathway.<sup>111</sup> The mechanism of Bid–tBid separation is unknown, hence caspase-8 is not needed for PTT-mediated cell death. The most plausible reason is because during PTT, partial penetration or full lysosomal rupture caused by heating of nanoparticles which releases lysosomal cathepsins into the cytosol, that have been demonstrated to directly breakdown Bid.<sup>112</sup> PTT causes cathepsin release and lysosomal disruption, which splits Bid and triggers apoptosis. It will be necessary to do further research on cathepsins to verify this theory. To put it briefly, after laser irradiation, lysosome rupture triggers Bid, which causes Bax/Bak oligomerization along with pore creation in outer membrane of the mitochondria. Apaf-1 facilitates the assembly of apoptosomes once cytochrome c is released. After that, the apoptosome triggers caspase-9, which in turn triggers caspase-3. Subsequently, caspase-3 initiates apoptotic cell death by acting as the executioner.<sup>108</sup>

Even though PTT is now undergoing clinical studies, not much is understood about the mechanisms of cell death that are triggered.<sup>113</sup> The number of research using PTT as a cancer treatment is constantly rising, but there are relatively few publications carrying out a thorough investigation, making it challenging to identify a common mechanism of cell death.<sup>114</sup> Depending on the properties associated with the tumor and the nanoparticles, the degree of internalization, the amount of energy absorbed, and the duration of the radiation, heat

produced by PTT can trigger many pathways. As a result, a complicated biological reaction to PTT is to be expected.<sup>115</sup> It has been demonstrated that apoptosis is induced by moderate temperatures up to 42–47 °C.<sup>116</sup> Necrosis was caused by temperatures over 55 °C.<sup>117</sup> The laser's intensity, the kind of cell, the qualities of the NP (composition, size, shape, and degree of internalization), and the surrounding environment (vascularization) all affect the temperature that is reached during irradiation.<sup>118,119</sup> The simple existence of NPs may also change cell processes; therefore, the action of PTT cannot be solely caused by heat shock.

Numerous investigations have been conducted, concentrating on several mechanisms that may result in cellular death.<sup>120</sup> Excessive light intensity can induce skin burns and subsequently inflammation in both healthy and tumorous cells.<sup>121</sup> Certain nanoparticles (NPs) during PTT increase heat stress, which intensifies the generation of (ROS) that may cause damage to nearby healthy tissues.<sup>122,123</sup> The reaction can be varied by the heat shock's duration and rate of heating (rapid or slow). When comparing radiation dose and duration, shorter radiation exposure times cause a little rise in body temperature and trigger apoptosis. Quite the opposite extending the radiation's duration raises the temperature more quickly, causing skin damage and necrosis. According to one research, PTT alters the phenylalanine route, making cells more susceptible to apoptosis. According to other studies, PTT causes the mitochondria to depolarize.<sup>124</sup> A more thorough investigation has identified the intrinsic apoptotic pathway in which a proapoptotic protein Bid plays an essential part during the permeabilization of mitochondria as the mechanism causing cell death triggered by moderate PTT.<sup>111</sup> Additional research revealed a reduction in Akt and Erk activation, which lowers the action of several proapoptotic protein inhibitors and promotes mitochondrial membrane permeabilization.<sup>124</sup>

**2.5.1. PTT and autophagy.** The stimulation of autophagy as a protective mechanism towards oxidative stress has been linked to gold nanoparticles. Nevertheless, another research on autophagy, which examined the production of autophagosomes as well as the p62 degradation, revealed a buildup of autophagosomes together with a blockage in autophagic flux.<sup>125,126</sup> Damage to proteins and organelles brought on by elevated temperatures triggers autophagy, a defense mechanism against PTT. According to some studies, autophagy inhibition boosts PTT's effectiveness. As a result, designing dual chemo-PTT with autophagy inhibitors might offer a novel way to boost PTT's effectiveness.<sup>127</sup> But taking into account not only individual cells but the entire body, autophagy plays a role in presenting antigens and may thus enhance the immune response to tumors, indicating that autophagy shouldn't be suppressed.<sup>128</sup>

**2.5.2. PTT and heat shock proteins.** HSPs are usually expressed when the temperature rises. The conserved family of chaperones known as HSPs binds to denatured proteins under heat stress to stop them from aggregating and to help them refold when the temperature returns to normal.<sup>129</sup> In non-stressful circumstances, HSF1, a heat shock factor (HSF), binds to HSP90 and HSP70. HSF1 gets released and migrates to the nucleus after which it binds to DNA to activate HSP genes



when HSP90 and HSP70 connect to unfolded proteins during heat shock. Consequently, it is anticipated that HSPs will engage in processes that PTT initiates.<sup>130</sup> Inhibiting apoptosis and protecting against high temperatures, HSP70 binds to unfolded proteins therefore plays a protective function in cellular recovery. Certain malignancies have been shown to overexpress HSPs, and some research lends credence to the theory that blocking them might increase the susceptibility of the tumor to PTT.<sup>131</sup> As previously stated, the immune system cannot be disregarded, though, as HSP70 can convey antigen to DCs and its expression may thus trigger an antitumoral immune response.<sup>132</sup>

**2.5.3. PTT and immune activity.** A potentially effective next-generation therapeutic strategy is cancer immunotherapy. Numerous research has demonstrated the effectiveness of this strategy. However, creating a common approach for many cancer types is challenging due to the intricate immune response. Thankfully, a novel method for eliciting an anticancer immune response by PTT with inorganic NPs has been found.<sup>133</sup> Tumor ablation produces cell residues which can function as tumoral antigens produced *in situ*, which is why PTT is advantageous when used in conjunction with immune treatment. As a result, a single, distinctive method produces several distinct immune responses to a wide range of solid tumors. On the other hand, these tumor antigens have the potential to stimulate an inflammatory response, which might result in either acceleration or repression of tumor development.<sup>134</sup> Furthermore, in order for the immune response to be triggered, a stimulation signal is required. Necrosis cells emit constituents of their own that may be antigens or DAMPs that stimulate DCs and stimulate the immune system as a whole. However, apoptotic cells often do not produce DAMPs and instead display “tolerate me” signals. They additionally deliver antigens to DCs containing phagocytized apoptotic material. As a result, the immunological reaction is inhibited.<sup>135</sup> Co-stimulators enhance the stimulation of the antitumoral immune response when used with PTT. This is the reason why some works include an adjuvant—a material that boosts the immune system's reaction to an antigen—in the construction of the NPs.<sup>136</sup> However, gold nanoparticles have the ability to stimulate DCs and macrophage's immune systems, which increases the release of proinflammatory cytokines. As a result, gold nanoparticles could have advantageous properties that might be used.<sup>137</sup> In order to preserve immunological homeostasis and guard against improper immune response activation, the immune response features checkpoints. PD-1 (Programmed death-1) and CTLA-4 (cytotoxic T lymphocyte-associated antigen-4) are negative regulators of the immune response; hence, blocking them strengthens the immunological response.<sup>138</sup> It is vital to notice that necrosis promotes tumor development whereas apoptosis is thought to be an immunosuppressive method of cell death. As a result, there are differences in the methods used to control the immune response triggered by each cell death pathway. There has to be more research done on the immune response's balance between tumor necrosis and apoptosis since the immune response that is triggered after PTT is not well understood.<sup>111</sup>

### 3. Photosensitizers in PDT

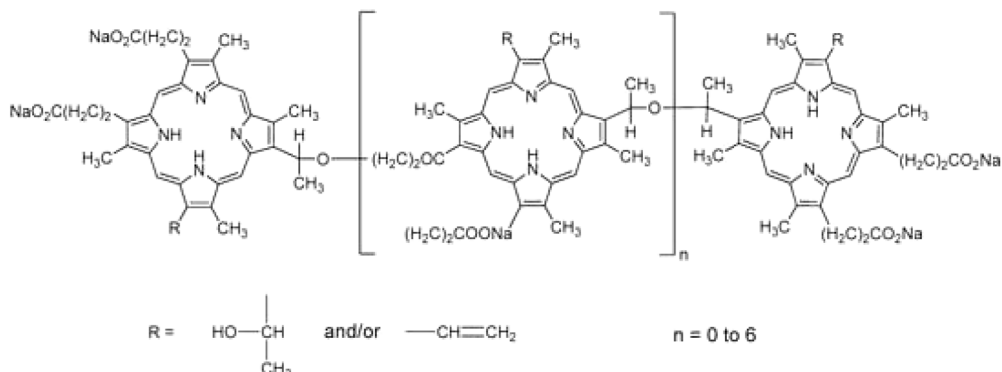
The existence of photosensitizers is essential components of photodynamic therapy (PDT), along with oxygen and light. These elements are described as materials that have the ability to absorb light at a certain wavelength and cause photophysical or photochemical processes.<sup>2</sup>

It is possible to identify a collection of traits and circumstances that characterize the perfect photosensitizer: (i) extremely pure chemical composition, (ii) steadiness at ambient temperature, (iii) the photosensitive effect is only present when a certain wavelength is present, (iv) the photochemical reactivity is high, and the optimal range of wavelengths for maximal light absorption is between 600 and 800 nm. Light having a wavelength greater than 800 nm cannot be sufficiently absorbed to produce further reactive oxygen species or to excite oxygen in its singlet form, (v) a minimum amount of absorption between 400 and 600 nm. By doing this, sunlight-induced hyper photosensitivity is potentially avoided, (vi) no chemical in the human system, including endogenous pigments like melatonin, haemoglobin, or oxyhaemoglobin, should have its absorption bands overlapped, (vii) easy solubility in bodily tissues, (viii) reduced cell death in the dark, (ix) high affinity for neoplastic tissues: to reduce the photo toxic adverse effects of the therapy, the photosensitizer must be rapidly withdrawn from healthy tissues but gradually removed from problematic regions, where it should remain for at least a few hours, (x) easy availability and synthesis at a low cost.<sup>139</sup>

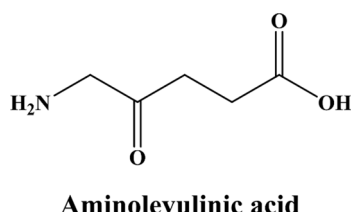
#### 3.1. 1st generation photosensitizers

Oscar Raab, a Munich-based medical student, is credited with pioneering the use of light with a photosensitizing chemical. Raab discovered that fluorescence happens in protozoa that have been dye-treated and subsequently exposed to radiation while conducting studies with acridine dyes. This occurrence caused oxygen to be consumed and had a toxic impact, which killed protozoa. In 1904, Raab showed Professor von Tappeiner his data, and he clarified and labeled this phenomenon as a “photodynamic effect”.<sup>140</sup> Soon after, in 1905, the first successful effort to cure skin cancer with 5% eosin dye was conducted. But this treatment was not widely adopted and was ignored for many years.<sup>141</sup> It was in the 1970s when Dr Thomas Dougherty along with others first commercialized photosensitizers for use in medical therapy.<sup>142</sup> They were evaluating a porphyrin combination known as the “hematoporphyrin derivative” (HpD), which is soluble in water. Separation and chemical treatment of hematoporphyrin (Hp), the very first porphyrin used as PS, produced HpD. When it came to malignancies, HpD exhibited superior tissue selectivity and less photosensitizing capability on the skin than Hp. Later, a blend of dimers and oligomers of porphyrin that were separated from HPD was sold under the brand name “Photofrin.” As of right now, sodium porfimer, also referred to as Photofrin, is still the most widely used PS Fig. 4.<sup>6,143</sup> Even though PDT is widely used, the therapeutic uses are limited by its low purity of chemicals (it is a combination of over 60 compounds) and poor tissue



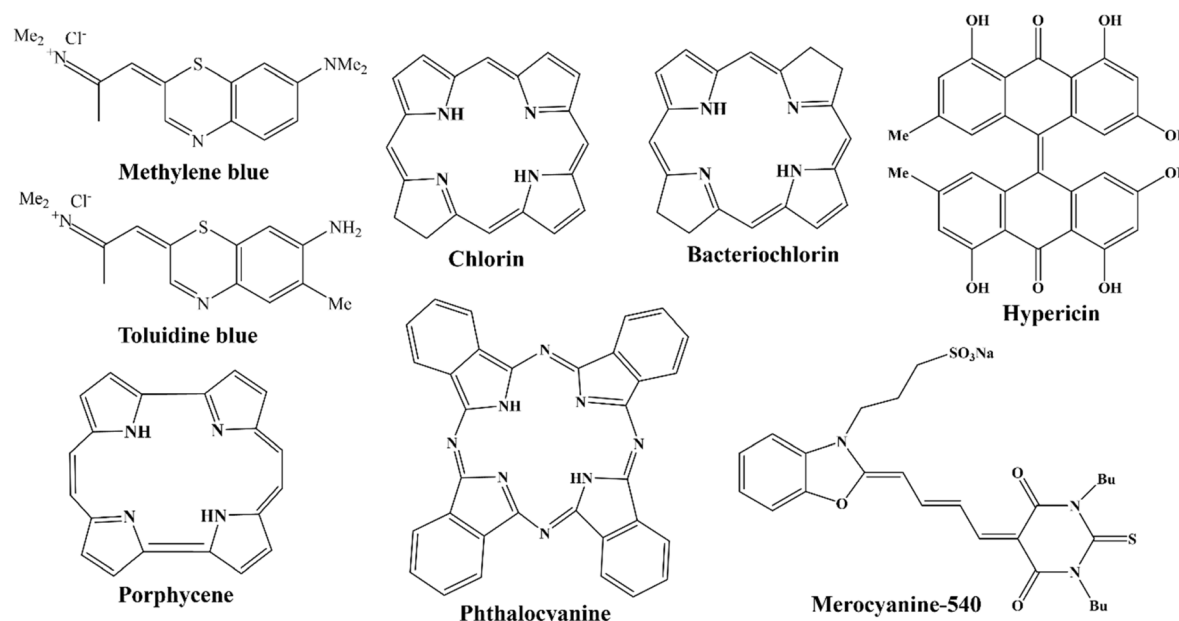
Fig. 4 First generation photosensitizer – Photofrin (Chen *et al.*, 1995).<sup>6</sup>

penetration because of its greatest absorption at 630 nm, a very short wavelength. In addition, a few weeks following PDT, skin becomes hypersensitive to light due to the prolonged half-life of PS and the elevated levels in the skin. The shortcomings associated with the first-generation PS made it necessary to look into other substances, which sparked the creation of a second-generation photosensitizers.<sup>144</sup>

Fig. 5 Structure of aminolevulinic acid (Morton *et al.*, 2002).<sup>147</sup>

### 3.2. 2nd generation photosensitizers

Research on the upcoming generation of photosensitizers started as early as the 1980s. Only a small number of the several hundred compounds with possible photosensitizing qualities that had been suggested have been employed in clinical studies. Even fewer compounds have regulatory approval for clinical use during photodynamic therapy (PDT) against cancer.<sup>145</sup> Derivatives of hematoporphyrin and synthetic photosensitizers, such as texaphyrins, 5-aminolevulinic acid, thiopurine derivatives, benzoporphyrin derivatives, chlorin, and bacteriochlorin analogues and phthalocyanines, are currently included in the category of second-generation photosensitizers Fig. 6.<sup>146</sup> Utilizing 5-aminolevulinic acid (ALA), the precursor to protoporphyrin IX, proved to be a significant finding. ALA is a type of prodrug that requires transformation into a protoporphyrin in order to become an active PS. Because of this, ALA and its esters have a wide range of therapeutic uses, both topically and orally Fig. 5.<sup>147</sup>

Fig. 6 Second generation photosensitizers (Chen *et al.*, 1995).<sup>6</sup>

The photosensitizers of the second generation exhibit enhanced chemical purity, higher levels of generation of singlet oxygen, and superior penetration into deeply situated tissues because of their greatest absorption in the 650–800 nm wavelength range. Because of their increased selectivity for malignant tissues and quicker bodily removal of the photosensitizer, they also show less adverse effects. The primary drawback of second-generation PS is its low water solubility, which severely restricts their use *via* IV and necessitates the development of novel drug delivery strategies.<sup>148</sup>

### 3.3. 3rd generation photosensitizers

The production of materials with a greater affinity for tumor tissue provides the foundation for the creation of third-generation photosensitizers, which lessen harm to nearby, healthy tissues. Preparing a pharmacological process that would allow photosensitizers to be administered parenterally is another obstacle to the broad clinical implementation of photodynamic therapy in cancer. The photodynamic method's bioavailability can be efficiently increased by new drug delivery techniques that are on the rise.<sup>149</sup>

To improve the drug's selectivity, photodynamic treatment is modified in the following ways: (i) combination of targeting agents with second-generation photosensitizers, (ii) mixtures of photosensitizers and low-density lipoprotein, as the growing tumor cells require higher levels of cholesterol in production of their cell walls, (iii) using tumor surface indicators like growth factor receptors, hormones (like insulin), as well as transferrin receptors Fig. 7. (iv) In combination with a photosensitizer and a monoclonal antibody that recognizes cancer cell antigen.<sup>150,151</sup>

## 4. PDT and nanotechnology

In the past ten years, there has been a notable acceleration in the advancement of nanotechnology. The field known as "nanomedicine" employs nanomaterial systems for diagnostic

and therapeutic procedures, which makes it possible to precisely deliver drugs to target tissues and enhance the efficacy of cancer treatment. The incorporation of photosensitizers along with nanomaterials may improve the efficiency of photodynamic therapy and as well get rid of its side effects. The application of nanoparticles allows for the achievement of a targeted method that is focused on particular receptors, which in turn enhances the specificity of photodynamic therapy. PS's can be encapsulated within or immobilized upon nanoplateforms through covalent, noncovalent interactions.<sup>152</sup>

### 4.1. Photosensitizers in photodynamic therapy

The therapeutic uses of traditional organic photosensitizers (PSs) have been mainly restricted by their poor stability and hydrophobicity in the PDT environment, and reduced cell/tissue selectivity, despite the fact that PSs are still frequently employed and have made considerable advancements in PDT. As a result, intriguing nano-agents with optical and physico-chemical qualities have surfaced as a compelling substitute to get over these limitations of conventional photosensitizers. Although certain first-generation PSs have been granted approval for clinical use, their limitations such as hydrophobicity and shallow penetration depth-as well as the decreased cell and tissue specificity of second-generation PSs continue to impede their potential as clinical therapeutics. A lot of focus has been on the study of nanomaterial-based photodynamic therapy (PDT) during the last few years. This is a novel treatment approach that uses nanomaterial as a PS or carrier.

Nanomaterials have several special qualities which render them more effective for PDT as compared to organic PSs.<sup>6</sup> Nanomaterials are radiation-stable and have exceptional optical characteristics that enhance PDT's penetration and effectiveness.<sup>153</sup> Furthermore, molecule-modified nanocarriers can more accurately distribute PS to the targeted cells than conventional PSs, which translates into a better therapeutic benefit and fewer adverse effects.<sup>154,155</sup> Because of their unique

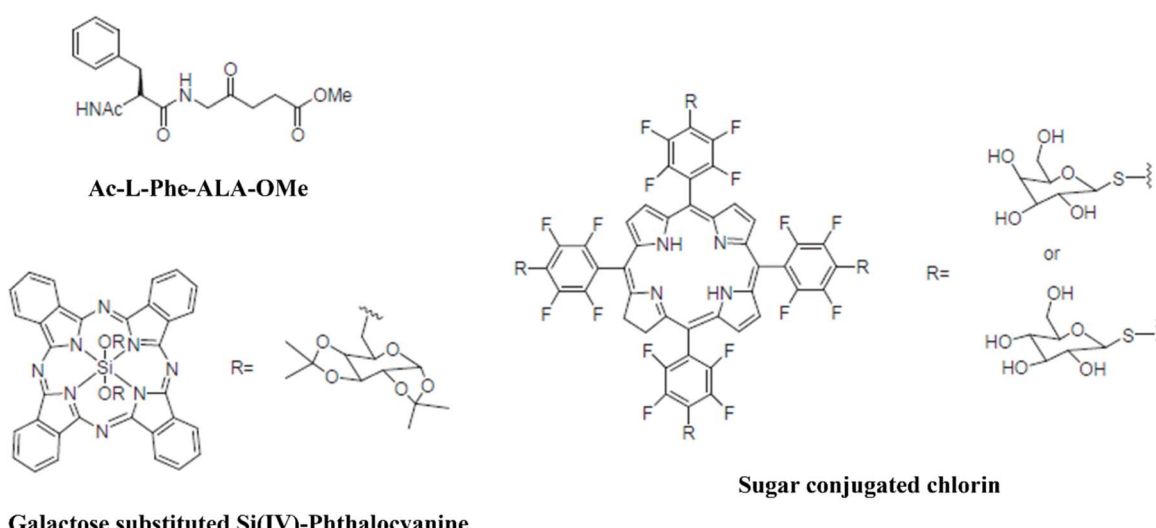


Fig. 7 Several examples of third-generation PSs that have been coupled with targeting agents (Lee *et al.*, 2005).<sup>150</sup>



light absorption characteristics, certain nanomaterials, such as semiconducting nanoparticles, have the innate ability to create ROS through the transfer of energy or electron transfer process.<sup>156</sup> Because of their vast surface area and adaptable surface changes, nanomaterials are increasingly used as PS carriers, enabling targeted distribution of photosensitizers toward the tumor location through improved drug loading efficiency as well as better uptake by the cancer cells.<sup>157</sup>

**4.1.1. Gold nanoparticles.** The simplicity of surface modification using gold-thiol chemistry, biocompatibility, and huge surface areas of these gold nanoparticles have made them the subject of much investigation for years as a means to induce PDT.<sup>158</sup> Since gold nanoparticle's optical dispersion and absorption may be adjusted, they are also being investigated in great detail for diagnostic purposes.<sup>159</sup> The Hwang group reported in 2014 the first application of gold nanorods (Au NRs) for PDT on their own (without using an organic PS). It was discovered that gold nanorods could create singlet oxygen under the stimulation of near-infrared light (915 nm,  $\lambda_1$ ), which caused the B16F0 melanoma cancers in mice to be destroyed. Heat shock protein (HSP 70) generation indicates the activation of gold nanorods at 780 nm ( $\lambda_2$ ) which can raise the temperature surrounding tumor tissues in addition to generating  $^1\text{O}_2$ . This is because photon energy can be converted to heat. Gold nanorods primarily produced the so-called photothermal treatment (PTT) impact in this procedure, which caused cancer cells to undergo apoptosis. PDT and PTT are the two dominant phototherapeutic effects that may be altered by varying the stimulation wavelengths ( $\lambda_1$  or  $\lambda_2$ ) Fig. 8.<sup>160</sup>

Prior research has demonstrated that metal nanoparticles may produce singlet oxygen using the one-photon excitation method. Nevertheless, the surrounding tissues near the tumor site may sustain photodamage as a result of one-photon stimulation. In this regard, two-photon excitation with accurate treatment dosage modification is more desirable.<sup>160,161</sup> Gold nanorod and gold nanosphere aggregates have been evaluated as photosensitizers for two-photon PDT in the work of Jiang and

colleagues. Either, individual or clustered gold nanoparticles were used to demonstrate two-photon induced production of singlet oxygen upon exposure to femtosecond laser pulses at 800 nm. Aggregated gold nanoparticles, however, typically improved the  $^1\text{O}_2$  production capabilities. In other words, aggregated gold nanospheres were 8.3 times more capable of generating  $^1\text{O}_2$  than unaggregated ones.<sup>162</sup>

**4.1.2. Silver nanoparticles.** These days, antimicrobial treatments also make extensive use of silver nanoparticles. The fact that silver nanoparticles often have an extraordinarily high specific surface area – meaning that the surface area of silver that is in contact with microorganisms can be very large is one of its fascinating characteristics. The capacity of silver nanoparticles to produce singlet oxygen has also been discovered, which has led to a lot of research into their application in PDT.<sup>33</sup> According to Hwang *et al.*, silver nanoparticle-mediated excitation and singlet oxygen production are closely correlated with their shape, just like in the situations of gold nanoparticles. For example, using silver nanocubes produced either a little or absence of  $^1\text{O}_2$  phosphorescence signal, whereas stimulation of silver decahedrons as well as silver triangular nanoplates could generate singlet oxygen. A notable singlet oxygen production was seen during silver decahedrons photo-excitation (approximately 520 nm LSPR band) in NIR wavelength of 885 nm. Similarly, at 544 nm excitation, silver triangular plates (about 590 nm LSPR band) produced a robust  $^1\text{O}_2$  phosphorescence signal, whereas radiating silver nanocubes (about 500 nm LSPR band) in 525 nm produced only a faint singlet oxygen production.<sup>163</sup> Silver nanoparticles have a variety of shapes and compositions that can result in highly adjustable optical characteristics, which makes them appealing for use in photodynamic therapy. Furthermore, cancers can experience oxidative stress from silver nanoparticles, which triggers the death of tumor cells.<sup>164</sup>

In a work by Mahajan *et al.*, a new porphyrin derivative 5,10,15,20-tetrakis(2,4-dihydroxyphenyl) porphyrin (POR) was synthesized and loaded on the surface of readily manufactured

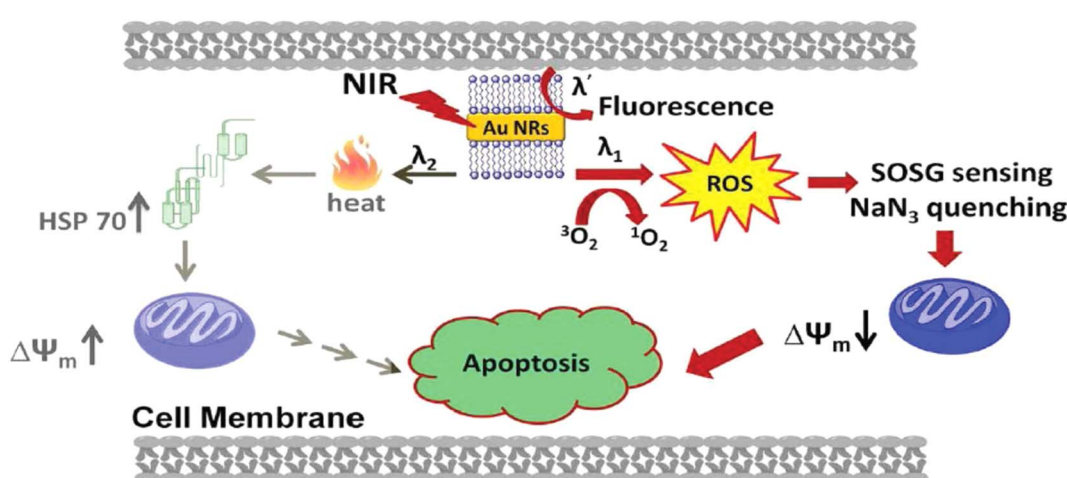


Fig. 8 Various cellular pathways involved in cellular death produced by PDT/PTT effects caused by gold nanorods after photoexcitation (Vankayala *et al.*, 2014).<sup>160</sup>



MSA-capped silver nanoparticles. The efficiency of singlet oxygen quantum yield was found to be greater when POR was integrated into MSA-AgNPs rather than in its free form. Furthermore, the produced nanocomposite might be a promising option for cell imaging applications against the cancer cell line A375, with non-toxic properties.<sup>165</sup> Khoza *et al.* evaluated the complex's *in vitro* photodynamic activity using a metastatic melanoma cancer cell line. When exposed to red light in the presence of varying amounts of phthalocyanine (complex 3) and silver nanoparticles, cell viability decreased proportionally. The photodynamic activity of complex 3 increased in the presence of AgNPs.<sup>166</sup>

Montaseri *et al.* studied the notion of photodynamic therapy (PDT) using silver-based nanohybrids to treat A375 melanoma cancer cells. Ag-PEG NPs and core/shell Ag@mSiO<sub>2</sub> NPs were synthesized and attached to zinc phthalocyanine tetrasulfonate (ZnPcS<sub>4</sub>) photosensitizers (PS). Folic acid (FA) was also used as a targeting moiety on the surface of nanohybrids to specifically target the overexpressed folate receptors in A375 cells. Cells subjected to 674 nm laser irradiation after incubation with ZnPcS<sub>4</sub>/Ag@mSiO<sub>2</sub>-FA had a strong PDT impact, with  $\sim 92\% \pm 1.1$  cell death compared to  $\sim 70\% \pm 2.9$  cell death for ZnPcS<sub>4</sub>/Ag-PEG-FA nanohybrids. This was due to the increased formation of ROS in the former nanohybrids. As the nanohybrids successfully localized in mitochondria, the bulk of cell death was caused by apoptosis rather than necrosis.<sup>167</sup>

**4.1.3. Silica and silicon nanoparticles.** Due to its reduced toxicity, chemical inactivity, and optical transparency, nanoparticles of silica can be utilized to encapsulate PSs in PDT even though silica doesn't seem active for PDT itself. Because silica has hydroxyl groups on its surface, chemical functionalization of the material is also possible. In these kinds of investigations, silica nanoparticles are typically employed for drug delivery.<sup>153</sup> Yan and colleagues used a modified Stöber sol-gel technique in 2007 to embed the PS *m*-THPC (*meta*-tetra(hydroxyphenyl)-chlorin) on matrix-based sol-gel silica nanoparticles.<sup>168</sup> The ability of organically manipulated silica (ORMOSIL) nanoparticles to effectively conjugate with hydrophilic and hydrophobic compounds makes them a viable vehicle for PS drug delivery.<sup>169</sup> When PS molecules were covalently bonded to ORMOSIL nanoparticles in 2007, Ohulchansky and colleagues observed that the molecules could produce singlet oxygen with stability upon excitation while maintaining their functional and spectroscopic characteristics.<sup>170</sup> The unique qualities of mesoporous silica nanoparticles (MSNs), such as a large surface area, pore volume, and chemical stability, make them a frequent choice for PS distribution. Hydrophobic PSs, such zinc picolinate (ZnPc), which have a tendency to self-aggregate in aqueous media, can be transported by MSNs Fig. 9.<sup>171,172</sup> In 2012, MSNs modified with galactose on their surface were reported for use as PDT agents and delivery vehicles.<sup>173,174</sup> Galactose functionalization can boost absorption by cancer cells *via* galactose receptor-mediated endocytosis, which leads to the aggregation of the nanomaterials in the lysosomal and endosomal compartments, according to confocal microscopy tests. As the synergistic anticancer effects of porphyrin (first generation PS) and camptothecin anti-cancer medication were evaluated on

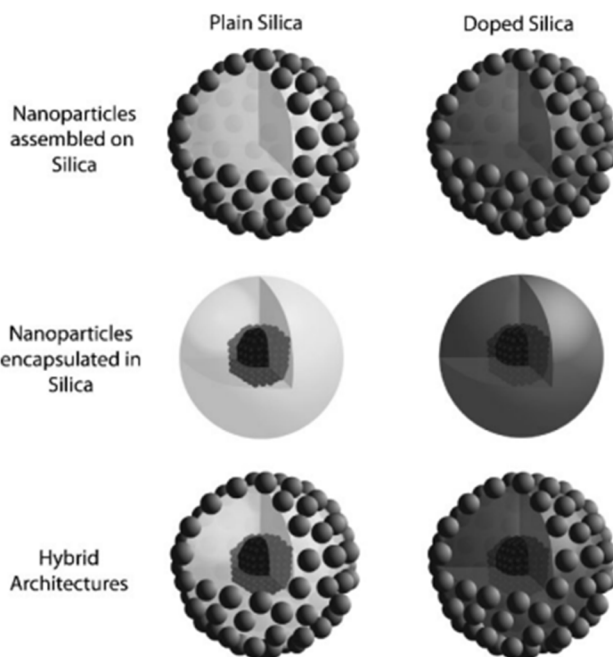


Fig. 9 Several topologies for generating multipurpose silica nanoparticles are demonstrated, including employing the silica matrix as a center, shell, or hybrid design, and adding components such as molecules and atoms (Piao *et al.*, 2008).<sup>171</sup>

MSNs, the results demonstrated a significant increase in cancer cell death under illumination at 650 nm as compared to individual treatments.<sup>175</sup> Different synthetic techniques may be used to create a range of silicon and silica nanoparticles with ideal sizes and porosities for PDT. Additionally, by surface functionalizing the silicon-based nanoparticles, cancer-specific medicines may be added, enhancing their capacity to target tumours. Furthermore, their potential applications in two-photon PDT and NIR for profound cancer treatment have been demonstrated by recent investigations.<sup>172</sup>

Li *et al.* used mesoporous silica nanoparticle (MSN) as a nanoplatform. SiNPs and the photosensitizer 5,10,15,20-tetrakis (1-methyl 4-pyridinio) porphyrin tetra (*p*-toluenesulfonate) (TlMPyP) were first embedded in the MSN and was further modified with folic acid (FA) to obtain the mesoporous silica nanocomposite (MSN@SiNPs@TlMPyP-FA) for targeted two-photon-excited fluorescence. The integrated TlMPyP could create singlet oxygen for PDT under light irradiation, and the anticancer medication doxorubicin (DOX) could be loaded for chemotherapy. Furthermore, due to SiNPs' two-photon stimulated fluorescence, the nanocomposite enabled targeted two-photon fluorescence cellular imaging at near-infrared (NIR) laser excitation, effectively avoiding interference from biological auto-fluorescence. *In vitro* cytotoxicity studies demonstrated that the combination treatment of PDT plus chemotherapy had a high therapeutic effectiveness against cancer cells.<sup>176</sup>

In another work, a new photo-responsive hollow silica nanoparticle (HNP)-based gene and photosensitizer (PS) co-delivery nanovehicle was developed for dual-wavelength light-triggered synergistic gene and PDT treatment. The resulting



HPN coupled with PDMAEMA polycation *via* a 405 nm light-cleavable Cou-linker, known as HPN-Cou-PD, has great gene condensation capacity, good biocompatibility, exceptional PS loading ability, and light-triggered gene release features. HPN-Cou-PD with Chlorin e6 (Ce6) loaded inside the silica cavity and a plasmid encoding caspase-8 gene (CSP8) attached to the PDMAEMA outside layer (Ce6-HPN-Cou-PD/CSP8) has been shown to have better antitumor effects under pre-405 nm and post-670 nm light irradiation both *in vitro* and *in vivo* due to light-triggered intracellular gene release and reactive oxygen species (ROS) generation.<sup>177</sup>

Dina Aggad *et al.* described ethylene-based periodic mesoporous organosilica nanoparticles (PMOs) for PDT and the autonomous administration of gemcitabine hydrochloride, an FDA-approved chemotherapeutic medication, in cancer cells. Depending on the nature of the photosensitizer (tetrasilylated or monosilylated porphyrin) and its aggregation state, they may create two-photon PDT. The synergistic impact of two-photon irradiation with gemcitabine increased the percentage of cell death by approximately 20% compared to the delivery procedure without irradiation.<sup>178</sup> Özge Er *et al.* developed mesoporous silica nanoparticles loaded with zinc(II) 2,3,9,10,16,17,23,24-octa (*tert*-butyl phenoxy phthalocyaninato (2-)-N29,N30,N31,N32 (ZnPcOBP) as a photosensitizer to determine the production of singlet oxygen and achieve *in vitro* PDT against pancreatic cancer cells. When ZnPcOBP was integrated into silica nanoparticles, it demonstrated a strong phototoxic impact, which was exacerbated by cetuximab. Cetuximab is a monoclonal antibody that primarily targets the epidermal growth factor receptor. Thus, the imidazole was a good carrier for the selective delivery of ZnPcOBP to pancreatic cancer cells (ASPC-1, PANC-1, MATpaca-2) *in vitro*.<sup>179</sup>

Qi Sun *et al.* were the first to disclose that gold (Au) nanorods were capped to chlorine e6-doped mesoporous silica nanorods for a single wavelength of NIR light-triggered combination phototherapy (PDT and PTT). This single wavelength of light, along with the rod form of the nanosystem for combination phototherapy, exhibited the following unique characteristics: (1) the impact of PDT and PTT could be realized under a single wavelength of near-infrared light (660 nm), making the therapeutic procedure viable and straightforward; (2) chlorin e6 is doped into a mesoporous nanorod but remains in the nanocarrier throughout delivery. AuNRs-Ce6-MSNRs are not only capable of producing single oxygen for PDT based on chlorin e6 after uncapping gold nanorods under single NIR irradiation, but they can also create heat to execute the PTT effect based on AuNRs.<sup>180</sup> In a separate investigation, the ICG was combined with doxorubicin hydrochloride to form hollow mesoporous silica nanoparticles and dopamine-modified hyaluronic acid (DA-HA) to serve as targeting agents and gatekeepers for HMSNPs *via* boronate ester linkages. *In vitro* cell culture investigations revealed that the ID@HMSNs-B-HA nanoplateform (where ID represents both DOX and ICG) may suppress murine mammary cancer cells (4T1) using a combination of PDT and chemotherapy.<sup>181</sup>

**4.1.4. Quantum dots (QDs).** QDs, a different kind of nanomaterial, have also been thoroughly researched for use in

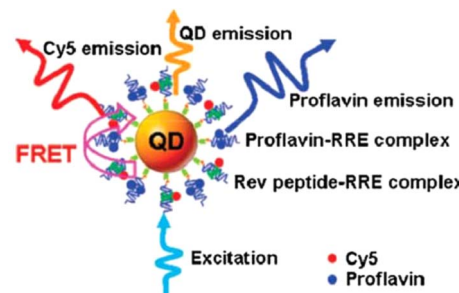


Fig. 10 A single-QD-based nanosensor can detect Rev peptide-RRE association and proflavin inhibitory efficacy using FRET between 605QD and Cy5 (Zhou *et al.* 2005).<sup>182</sup>

PDT. QDs are potential nanocarriers because of their unique optical features, which include high emission quantum yield, adjustable release based on size and composition, and easy surface modification Fig. 10.<sup>183,184</sup> QDs also contribute to fluorescence resonance energy transfer (FRET), a popular biomolecular dynamics approach.<sup>182</sup> In a study by Qi *et al.* (2010) where biocompatible CdSe QDs containing water-soluble porphyrin was produced for PDT using two-photon excitation. The results showed that the  $^1\text{O}_2$  quantum yield from porphyrin-conjugated QDs following two-photon stimulation was two times greater than from the porphyrin solution alone.<sup>185</sup> Shen and colleagues recently described a QD-based hybrid nanocomposite that targets tumors by encapsulating a QD-Zn-porphyrin (TMPPZn-QD) nanocomplex, an extremely fluorescent photosensitizer rhodamine 6G (R6G), and NIR775, an NIR fluorophores found in FA-decorated phospholipid polymers. These nanoparticles have a significant capacity to absorb light and may be significantly loaded with porphyrin. Consequently, an efficient dual energy transfer technique was used to generate an exceedingly high level of singlet oxygen quantum yield of around 0.91. Furthermore, the folate receptor may play a role in the highly targeted distribution of as-prepared nanoparticles to malignant tissues, enabling effective photodynamic tumor elimination *in vivo* and non-invasive fluorescent imaging without harming the nearby healthy cells.<sup>186</sup>

Murali *et al.* created hematoporphyrin (HP) photosensitizer-encapsulated carbon quantum dots (CQDs) (HP-CQDs) utilizing a well-controlled one-step microwave process with the HP monomer as a precursor. The HP-CQDs as synthesized preserved all of HP's fundamental optical and chemical features while demonstrating exceptional water solubility. Importantly, HP-CQDs' exceptional capacity to generate reactive oxygen species under deep red light suited its application in PDT-assisted effective eradication of human breast cancer cells (MCF-7). In comparison to HP, HP-CQDs displayed very significant phototoxicity and minimal dark toxicity towards MCF-7 cells.<sup>187</sup> Zeng *et al.* used microwave-assisted synthesis to create CQDs with green fluorescence as a targeted carrier for medication delivery in mice models to treat hepatocellular carcinoma. Researchers observed non-covalent coupling of DOX with CQDs. The CQD-DOX combination increased *in vivo* tumor stability and delivery efficacy.<sup>188</sup> Alaghmandfar *et al.*



demonstrated that CQDs work as a tool for gene delivery, conjugating with polyamidoamine (PAMAM) for the treatment of triple-negative breast cancer.<sup>189</sup>

**4.1.5. Carbon-based nanomaterials.** Carbon-based nanomaterials are popular in PDT research because to their unique optical and mechanical characteristics, tunable chemical functionalization, excellent biocompatibility, and low toxicity. Because carbon exists in so many allotropic forms, there are a wide variety of carbon-based nanomaterials. The ones that are most frequently used in PDT include graphene-based nanomaterials, fullerenes, and carbon nanotubes (CNTs).<sup>190</sup>

**4.1.5.1 Carbon nanotubes.** With an average inner diameter ranging from one to ten layers, carbon nanotubes (CNTs) are essentially rolled-up single or multilayered graphene in one dimension.<sup>33</sup> Murakami *et al.* demonstrated that with NIR light irradiation (808 nm), semi-conducting and metallic SWCNTs may produce ROS (singlet oxygen and  $O_2^-$ ). In this investigation, it was discovered that SWCNTs had more photodynamic aftermath than MWCNTs.<sup>191</sup> In another study, Wang and colleagues developed two modified SWCNTs by covalently functionalizing SWNTs with PEI or noncovalently functionalizing them with polyvinylpyrrolidone (PVPk30). The photodynamic ability was found to be influenced by the functionalization technique, and both of *in vivo* and *in vitro* the PEI functionalization demonstrated a greater photodynamic performance than the PVPk30 alteration.<sup>192</sup> Recently Zhang *et al.* described the usage of  $Fe_3O_4$ @CQDs coated on PEGylated SWCNTs to create a multifunctional nanoplateform. This nanoplateform may be employed concurrently for drug release, combined photodynamic/photothermal treatment, and magnetic resonance imaging (MRI) by loading the chemotherapeutic medication doxorubicin (DOX) and combining with sgc8c aptamer Fig. 11.<sup>193</sup>

**4.1.5.2 Fullerenes.** Fullerenes are all-carbon materials having 3D spherical, tubular or ellipsoidal structures; the best

researched example is  $C_{60}$ . While fullerenes on their own are intrinsically poisonous and poorly soluble in water, several surface modifications have been created to address these problems. Furthermore, it has been demonstrated that fullerenes are more biocompatible than other materials made from carbon like graphene and carbon nanotubes (CNTs) Fig. 12.<sup>195</sup> A multifunctional nanocomposite based on fullerene was described by Li *et al.* in 2015. Phenylalanine was used to modify  $C_{60}$ , and polylactic acid (PLA) was used to attach it. When exposed to visible light, this as-prepared nanoplateform may very specifically deliver the anticancer medication mitoxantrone into the tumors in C57BL mice, leading the combined effects of chemotherapy and photodynamic treatment with minimal harm to the normal, healthy organs.<sup>194</sup> Graphene oxide (GO) and  $C_{60}$  were conjugated, according to Li *et al.*, to create a GO- $C_{60}$  hybrid that demonstrated high stability in physiological settings. In addition to mediating the photothermal effects, GO may also transfer acquired light energy to  $C_{60}$ , causing  $C_{60}$  to produce ROS when exposed to near-infrared radiation. Consequently, HeLa cells can experience synergistic PDT/PTT effects from the prepared GO- $C_{60}$  hybrid *in vitro*.<sup>196</sup>

**4.1.5.3 Graphene-based nanomaterials.** PDT and other forms of cancer therapy have made graphene-based nanomaterials, including GO (graphene oxide) and GQDs (graphene quantum dots), and reduced graphene oxide (rGO) are widely used because of their excellent thermal and optical characteristics, large surface area, and good biocompatibility Fig. 13.<sup>197</sup> Ge *et al.* has shown that GQDs are an effective PDT agent, producing an outstanding quantum yield of  $^1O_2$  (up to 1.3). The graphene quantum dots were created utilizing the hydrothermal technique with polythiophenes serving as the carbon precursors. The killing of HeLa cells and breakdown of tumor in BALB/nu mice having breast cancer were seen during the *in vitro* and *in vivo* testing of the PDT effects of the graphene based QDs. Regretfully, photodynamic activity was only seen by the GQDs in

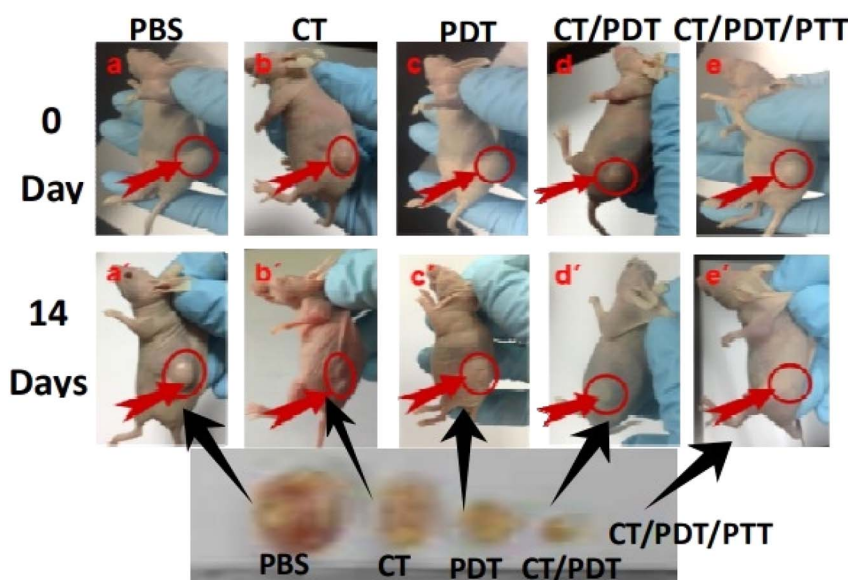


Fig. 11 Image of tumor-bearing mice following various treatments (Zhang *et al.*, 2018).<sup>193</sup>



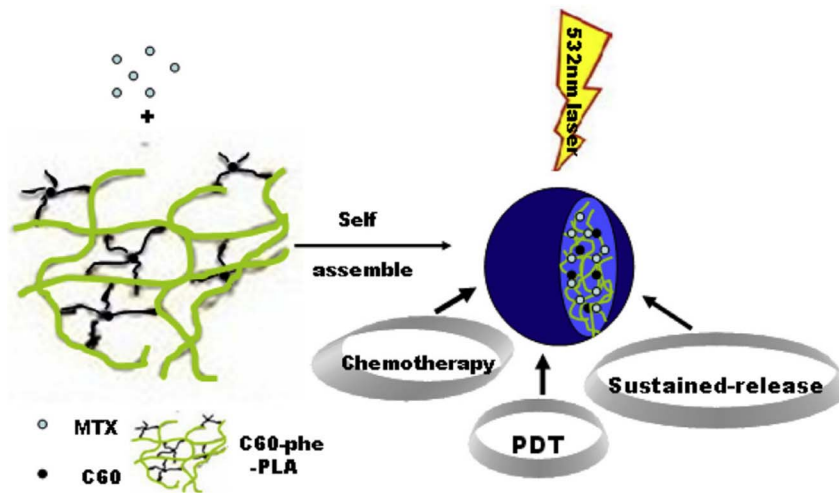


Fig. 12 Schematic of fullerene-based multifunctional sustained-release microsphere and its bio-functions (Li *et al.*, 2015).<sup>194</sup>

our investigation when they were stimulated by visible light.<sup>198</sup> When nitrogen as well as an amino group were added to the GQDs in 2018, Kuo *et al.* showed that the resulting amino-N-GQDs could produce exceptional amounts of singlet oxygen in the near-infrared (NIR) range (800 nm). Crucially, amino-N-GQDs were more potent PDT agents with better two-photon excitation than unmodified GQDs.<sup>199</sup> In order to create a light-sensitive medication delivery system, Ding and colleagues put PS hypocrellin A (HA) as well as  $TiO_2$  nanoparticles over the GO surface in 2016. A mutual sensitization process was used to achieve increased ROS generation capacity. The stable complex HA- $TiO_2$  was the source of the sensitization effect. Concurrently,

adding GO to  $TiO_2$  can potentially cause it to produce ROS when exposed to light. *In vitro* tests that demonstrated the obtained HA- $TiO_2$ -GO nanocomposite had significantly greater capacity to eliminate cancer cells compared to the  $TiO_2$ -GO or HA- $TiO_2$  complex validated the enhanced efficacy of PDT. Additionally, the produced ROS has the ability to degrade GO, suggesting that this drug delivery method may be used in clinical PDT with regard to metabolism.<sup>200</sup>

Apart from GO; rGO has been studied for theranostic application in cancer. Zhang *et al.* reported on a nanosystem consisting of a PEG infused Ru(II) complex (Ru-PEG) and rGO nanosheet, used in conjunction with photothermal/

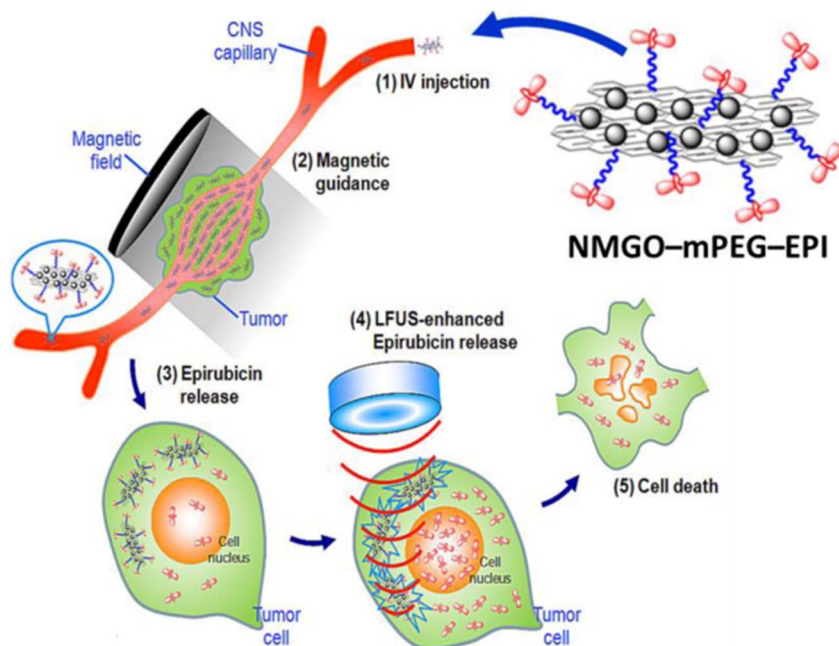


Fig. 13 The molecular mechanism of effect of NMGO-mPEG-EPI in cancer therapy and LFUS-induced hyperthermia. NMGO-mPEG-EPI functions as a heat-conducting basis, causing the local temperature to increase when LFUS is employed for deep targeting.<sup>197</sup>

photodynamic treatment and lysosome-targeted phosphorescent imaging. Using hydrophobic interactions as well as  $\pi$ - $\pi$  stacking, the Ru-PEG complex—which functions as both as an imaging agent and PS—was adhered to rGO. Ru-PEG produced a higher quantum yield of radicals (0.06 and 0.31, respectively) under 450 nm irradiation than rGO-Ru-PEG. This difference was most likely due to the quenching action of rGO. It was shown that A549 cells with particular localization to lysosomes could better absorb Ru-PEG when exposed to rGO. When rGO-Ru-PEG was used in conjunction with PTT and PDT, the anticancer effectiveness was greater than when each therapy was used alone. In addition to causing ROS, cathepsin-induced lysosomal damage by a combination photothermal and photodynamic action has also been discovered to aid in the death of cancer cells. Additionally, photothermal imaging of rGO-Ru-PEG under 808 nm light demonstrated the strong anticancer effectiveness of the constructed nanosystem *in vivo*.<sup>201</sup>

A team of scientists created a BODIPY-based phototheranostic nanoparticle with photo-chemo synergistic properties, and the nanoparticle MMC-Graphene@BODIPY-mPEG (MGBP) has excellent ROS production ability, high photothermal conversion efficiency (48%), and excellent therapy efficiency (HeLa cell viability was reduced to 17% after treatment) *in vitro*. Furthermore, because of the strong fluorescence and anti-photobleaching ability of BODIPY and the photothermal conversion capacity of graphene, MGBP demonstrated excellent fluorescence and photothermal imaging performance in the agar model.<sup>202</sup> Cheng *et al.* devised and manufactured the Fe<sub>3</sub>O<sub>4</sub>/g-C<sub>3</sub>N<sub>4</sub>@PPy-DOX nanocomposite, which contains magnetic iron oxide (Fe<sub>3</sub>O<sub>4</sub>) nanoparticles (NPs), a lamellar structure of graphite-like carbon nitride (g-C<sub>3</sub>N<sub>4</sub>), and a poly-pyrrole (PPy) shell with the anti-tumor medication doxorubicin hydrochloride (DOX). It is intriguing that Fe<sub>3</sub>O<sub>4</sub> NPs have photosensitizer properties for photodynamic treatment (PDT). The use of g-C<sub>3</sub>N<sub>4</sub> sheets in photocatalysis to degrade water and generate O<sub>2</sub> might successfully relieve solid tumor hypoxia and raise PDT efficiency. Furthermore, PPy has a high light-to-heat conversion efficiency, making it ideal for cancer photothermal treatment (PTT). Finally, an anticancer medication (DOX) was loaded onto the nanocomposite due to its mesoporous structure. Thus, the produced Fe<sub>3</sub>O<sub>4</sub>/g-C<sub>3</sub>N<sub>4</sub>@PPy-DOX nanocomposites have a synergistic chemotherapy/PTT/enhanced PDT anticancer activity.<sup>203</sup> Qin *et al.* (2018) created a nanocomposite composed of GO, magnetic nanoparticles (Fe<sub>3</sub>O<sub>4</sub>), chitosan, and a new photosensitizer HNPa (3-[1-hydroxyethyl]-3-divinyl-131-*b,b*-dicyano-methylene-131-deoxopyrroheophorbide-*a*). They demonstrated a higher singlet oxygen quantum yield than the single HNPa, at 62.9% and 42.6%, respectively. Furthermore, they found that the presence of GO-Fe<sub>3</sub>O<sub>4</sub> enhanced HNPa penetration into the nucleus of the human hepatocellular carcinoma cell line (HepG2). Furthermore, an MTT experiment conducted under 698 nm of irradiation confirmed that HNPa increased photodynamic cancer cell mortality.<sup>204</sup>

**4.1.6. Two-dimensional (2D) nanomaterials.** 2D nanomaterials have a huge surface area, extremely thin thickness, variable composition, and ease of surface modification, which

allow them to display certain distinct and chemical and physical characteristics.<sup>205</sup> These characteristics make them extremely desired for a wide range of possible uses, including energy storage, optoelectronics, catalysis, device manufacturing, sensing, and the detection and treatment of illness.<sup>206</sup>

**4.1.6.1 Manganese dioxide (MnO<sub>2</sub>) nanosheets.** One problem with PDT-based tumor therapy is that solid tumors, which are primarily hypoxic all the time, consume the ROS that are produced. Furthermore, the ROS generated by PDT drugs might also be consumed by the tumor cells attributed to the over-expression of glutathione (GSH).<sup>207</sup> It has been demonstrated that MnO<sub>2</sub> nanosheets may quickly raise the oxygen content of tumor tissues by interacting with H<sub>2</sub>O<sub>2</sub> in the surrounding tissue microenvironment to regenerate oxygen and reduce GSH.<sup>208</sup> Moreover, MnO<sub>2</sub> nanosheets have several desirable characteristics for PS transport, including significant PS adsorption capacity owing to electrostatic interaction as well as Mn-N coordinate bonds, that might facilitate PS endocytosis in the intracellular PDT.<sup>208</sup> Furthermore, MnO<sub>2</sub> nanosheets exhibit strong biocompatibility because nontoxic manganese plays a crucial role in physiological metabolism.<sup>209</sup>

MnO<sub>2</sub> nanosheets were employed as a PS Ce6 nanocarrier, whereas they also served as an oxidant to deplete intracellular GSH and increase photodynamic efficiency. This nanosystem, Ce6 has been effectively loaded onto the MnO<sub>2</sub> nanosheets also shielded from self-destruction by MnO<sub>2</sub> when exposed to light, facilitating the efficient delivery of PS to the cytoplasm. Surprisingly, the as-prepared Ce6-MnO<sub>2</sub> nanocomplex performed better in killing MCF-7 cells under the author's circumstances than other nanomaterial-based composites (such Ce6-GO and Ce6-MSN). Over 95% of cells were killed by the Ce6-MnO<sub>2</sub>-mediated PDT, compared to 36% and 21% for the Ce6-GO and Ce6-MSN nanosystems, respectively. These findings showed that MnO<sub>2</sub> nanosheets have a great deal of promise for raising PDT efficacy in a situation that is clinically relevant Fig. 14.<sup>208</sup> Recently, PEG-cyclic arginine-glycine-aspartic acid tripeptide (PEG-cRGD) was used to modify MnO<sub>2</sub> nanosheets in another work by Zeng and coauthors. PS Ce6 was then coupled with PEG-cRGD with high loading efficacy. Because of the cRGD-mediated tumor-targeting capacity, the produced MnO<sub>2</sub>-PEG-cRGD/Ce6 nanocomplex dramatically raise the concentration of oxygen and was particularly taken up by PC3 cells. This led to the achievement of good therapeutic results *in vitro* following irradiation at 660 nm.<sup>211</sup>

**4.1.6.2 2-Dimensional TMD nanosheets.** TMD nanosheets have a large specific surface area, excellent biocompatibility, ease of customization, and extremely light and heat conversion efficiencies, making them an effective tool for tumor treatment and drug administration.<sup>212</sup> In 2014, Liu *et al.* treated MoS<sub>2</sub> nanosheets with lipoic acid-terminated PEG (LA-PEG) to develop a PEGylated MoS<sub>2</sub>-PEG nanosystem, which exhibited remarkable stability in physiological conditions. When compared to cells incubated with free Ce6, the cells treated with MoS<sub>2</sub>-PEG/Ce6 exhibited much greater intracellular Ce6 fluorescence, indicating a considerably improved PS Ce6 delivery effectiveness. *In vitro* tests also showed that MoS<sub>2</sub>-PEG/Ce6 had significantly higher PDT efficacy than free Ce6 in eliminating



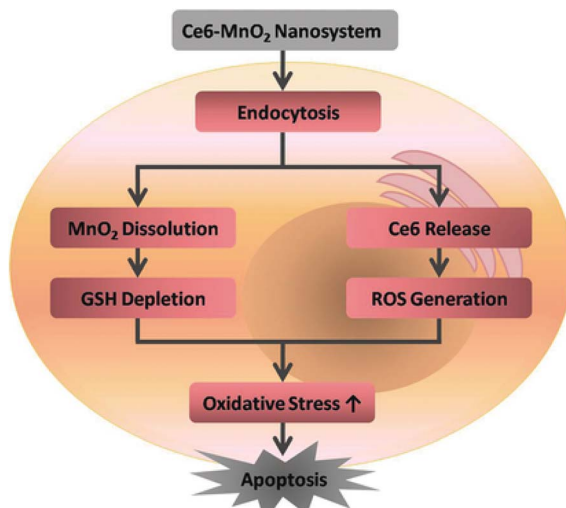


Fig. 14 The activation mechanism of the Ce6–MnO<sub>2</sub> nanosystem improves the photodynamic therapy efficiency (Fan *et al.*, 2016).<sup>210</sup>

4T1 cancer cells when exposed to 660 nm of light. This difference in efficacy may have resulted from the PS's enhanced cellular uptake, which increased the production of singlet oxygen inside the cells Fig. 15.<sup>213</sup> The p-MoS<sub>2</sub>/n-rGO-MnO<sub>2</sub>-PEG nanocomposite was created by Kapri and colleagues employing p–n heterojunction to incorporate p-type MoS<sub>2</sub> glycosheets onto n-type nitrogen-modified reduced GO. This was then organized using PEGylated modified MnO<sub>2</sub> nanoparticles. When subjected to NIR light, the p–n heterojunction found in this nanosystem promotes electron and hole mobility, resulting in improved separation of electron–hole pairs and increased ROS generation *via* photocatalysis. Furthermore, MnO<sub>2</sub> caused intracellular H<sub>2</sub>O<sub>2</sub> to disproportionate, producing additional O<sub>2</sub>, which enhanced ROS generation even further. Studies conducted *in vitro* demonstrated that this nanocomposite has a potent PDT impact on HeLa cell death.<sup>214</sup>

**4.1.6.3 Graphitic-phase carbon nitride nanosheets.** Due to its high biocompatibility, high stability, low toxicity, and high photoluminescence quantum yields, g-C<sub>3</sub>N<sub>4</sub> nanosheets, emerging 2D nanomaterials have been applied in a number of biomedical applications.<sup>212</sup> g-C<sub>3</sub>N<sub>4</sub> nanosheets have been used as PS to create singlet oxygen, effectively killing HeLa cells

following light revelation with a modest power density (20 mW cm<sup>-2</sup>) between 440–450 nm. Lin *et al.* published the first example of its application in PDT in 2014. Furthermore, because of their large surface-to-volume ratio, g-C<sub>3</sub>N<sub>4</sub> nanosheets may operate as a carrier with a significant loading capacity of 18 200 mg g<sup>-1</sup> when loaded with the anticancer medication DOX. Because DOX was more soluble and enhanced protonation in an acidic environment, its release was increased in an acidic pH environment. Furthermore, the g-C<sub>3</sub>N<sub>4</sub> nanosheet's strong photoluminescence quantum yield made it feasible to utilize them for imaging, which allowed researchers to follow the delivery process Fig. 16.<sup>215</sup>

Dai *et al.* recently used photo-excitation of the g-C<sub>3</sub>N<sub>4</sub> solutions having spherical gold nanoparticles to cover the g-C<sub>3</sub>N<sub>4</sub> nanosheets added to gold nanoparticles. Due to the improved electron/hole separation caused by the added gold nanoparticles, the absorption efficacy of 670 nm light may be improved, hence boosting the efficiency of <sup>1</sup>O<sub>2</sub> generation by photocatalytic water-splitting. The g-C<sub>3</sub>N<sub>4</sub>-AuNPs nanocomposites have shown good photodynamic therapy (PDT) results in inducing apoptosis or necrosis in three cancer cell



Fig. 16 g-C<sub>3</sub>N<sub>4</sub> nanosheets can function as photosensitizers as well as pH-responsive carriers of drugs for cancer therapy, as indicated in the schematic diagram (Lin *et al.*, 2014).<sup>215</sup>

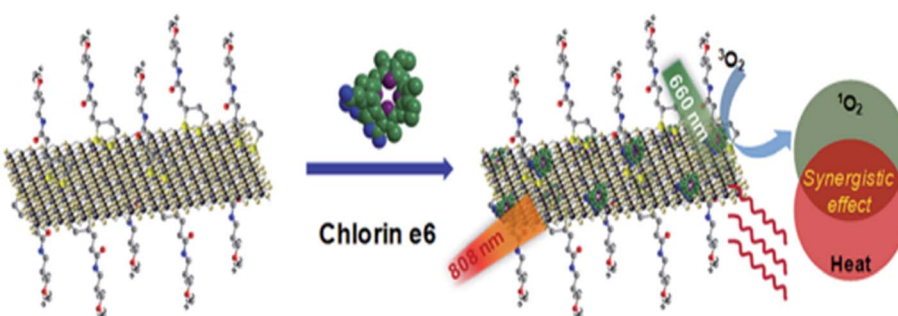


Fig. 15 A schematic of MoS<sub>2</sub>-PEG/Ce6 nanosheets that enable Ce6 loading and combined PTT and PDT (Liu *et al.*, 2014).<sup>213</sup>

lines (MCF-7, A549, and HeLa) that was test, when exposed to a 670 nm laser. Furthermore, in mice carrying MCF-7 tumors, efficient inhibition of tumor development has also been accomplished.<sup>216</sup>

**4.1.6.4 Black phosphorus (BP).** Because of its remarkable structural, optical, and chemical qualities, BP has developed as a unique kind of two-dimensional semiconductor that spurred a considerable lot of study in PDT after its first successful ablation from bulk to one or few layers of BP in 2014.<sup>216</sup> Gold nanoparticles and Iron oxide ( $\text{Fe}_3\text{O}_4$ ) were assembled on BP nanosheets using a standard electrostatic attraction technique to create a unique  $\text{BPs@Au@Fe}_3\text{O}_4$  nanocomposite. This nanosystem demonstrated better therapeutic impact with superior targeting abilities by combining the PTT response of gold nanoparticles, cancer localization and MRI targeting efficiency of  $\text{Fe}_3\text{O}_4$  nanoparticles, and the PDT effect of black phosphorus nanosheets. Moreover, the U14 tumor-bearing mice treated with  $\text{BPs@Au@Fe}_3\text{O}_4$  at 650 nm light demonstrated a notable inhibition of tumor development. The potential applications of BP nanosheets in biomedicine were unveiled by this work Fig. 17.<sup>217</sup>

In a different study, Liu and colleagues created a BP/ $\text{MnO}_2$  nanoplatform by electrostatically assembling fluorescein isothiocyanate (FITC)-designed FBP (BP with peptide modification) and Rhodamine B (RhB)-confined  $\text{MnO}_2$  ( $\text{R-MnO}_2$ ).  $\text{R-MnO}_2$  serves as the  $\text{O}_2$  supply and indicator in this  $\text{R-MnO}_2$ -FBP nanocomposite. Endocytosis mediated by the target FA receptor (FR) can cause the production of  $\text{O}_2$  in an acidic and  $\text{H}_2\text{O}_2$  rich

atmosphere. Additionally, due to the emitted dyes RhB and  $\text{Mn}^{2+}$ , fluorescence and magnetic resonance imaging (MRI) may be used to track the process of oxygen production. Both in, *in vitro* and *in vivo*, the FBP moiety could mediate very effective PDT in its capacity as the theranostic agent. Furthermore, by employing the activated caspase which is in the process of cell death brought on by oxygen-generating PDT, a self-feedback mechanism for the therapeutic response may be constructed.<sup>218</sup>

**4.1.7. Nanoscale metal-organic frameworks (MOFs).** Nanoscale metal-organic frameworks (NMOFs) have emerged as a potential delivery system for photodynamic therapy (PDT) owing to their diverse activities arising from their chemical compositions, unique crystalline structures, substantial porosity, and tunable framework stability. In a study by Meie He and his colleagues, they described a Mn-porphyrin based MOF made of biocompatible  $\text{Zr}^{4+}$  ions and Mn-porphyrin ligands. The Mn-porphyrin shown a strong catalytic capacity to convert  $\text{H}_2\text{O}_2$  to  $\text{O}_2$ , achieving oxygen self-supplementing PDT. Additionally, the special porous MOF frameworks may speed up the diffusion of produced  $\text{O}_2$  and  $\text{H}_2\text{O}_2$  and inhibit Mn-porphyrin from self-aggregating Fig. 18.<sup>219,220</sup>

**4.1.8. Organic nano-agents.** PDT has also made use of several newly created nano-agents, like porphysomes and nanostructured phthalocyanine self-assemblies Fig. 19.<sup>221</sup> Li *et al.* 2017 reported on nanostructured phthalocyanine self-assemblies made of zinc(II) phthalocyanine building blocks decorated with triethylene glycol (TEG) as target molecules. The unique noncovalent interactions among the targeting agents,

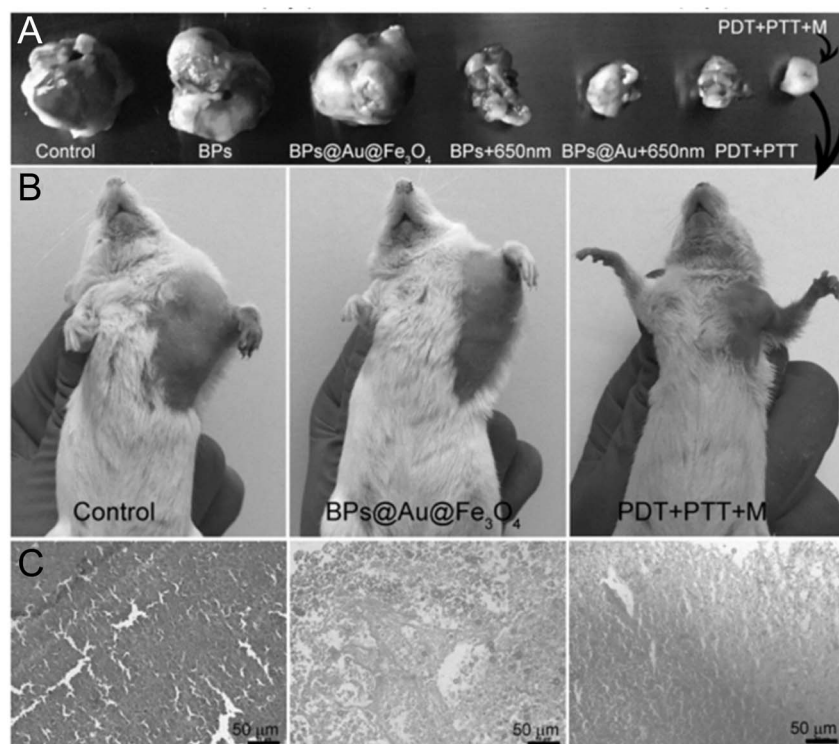


Fig. 17 On day 14, (A) tumor-bearing animals treated normal saline, BPs,  $\text{BPs@Au@Fe}_3\text{O}_4$ , BPs and BPs@Au in 650 nm irradiation,  $\text{BPs@Au@Fe}_3\text{O}_4$  with two stimuli, and  $\text{BPs@Au@Fe}_3\text{O}_4$ . (B) Photograph ordinary mice on day 14. (C) H&E-stained tumor slices from panel (C) groups (Yang *et al.*, 2017).<sup>217</sup>



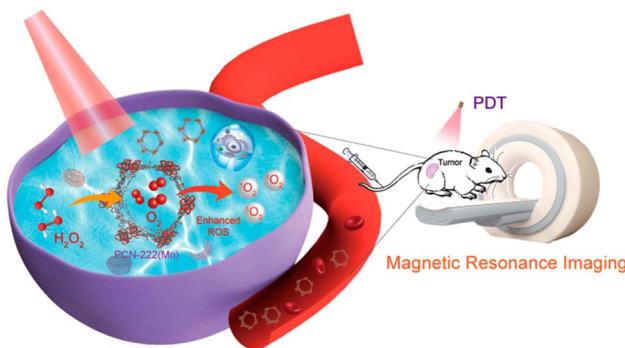


Fig. 18 Illustration of PCN-222(Mn) for MRI-guided oxygen self-supporting photodynamic therapy (He *et al.*, 2019).<sup>219</sup>

phthalocyanines, lead to the produced nanoassemblies demonstrating targeted protein-induced partial disintegration. The nano-phthalocyanine ensembles exhibit switchable photoactivity, facilitating the generation of reactive oxygen species (ROS) and enabling tumor-specific photodynamic treatment.<sup>222</sup> In summary, a growing number of novel nanomaterials are predicted to arise as a result of the biomedical field's tremendous advancement in nanoscience over the past several decades, presenting promise for the development of viable alternative cancer therapy techniques.<sup>197</sup>

**4.1.9. Nanofibers.** Localized cancer treatment is a very successful strategy for destroying solid tumors in early stages, minimizing adverse effects from cancer therapies. Electrospun nanofibers are a viable implantable platform for targeted cancer treatment. They allow for on-site delivery of therapeutic components while reducing negative effects on normal tissues. Paclitaxel was successfully loaded into electrospun PLGA nanofibers with over 90% efficiency. The study found that medication release can persist up to 60 days and kill up to 70% of C6 glioma cells within 72 hours.<sup>223</sup> Severyukhina *et al.* studied photosensitizer-loaded electrospun fibers for photodynamic cancer treatment. Electrospinning was used to produce chitosan/PEO nanofibers containing various photosens. The physically adsorbed photosens were released with the swelling of the nanofibers. The breakdown of the nanofiber complex caused a delay in release. 675 nm laser irradiation dramatically reduced metabolic activity in scaffold-treated human mammary gland T-47D cancer cells, with no recovery. In addition, limiting

the lighted region can reduce the phototoxic impact, leading to improved topical photodynamic cancer treatment.<sup>224</sup>

Wu *et al.* found that electrospun PLLA nanofibers containing purpurin-18 were biocompatible. Human esophageal cancer ECA109 and human hepatocellular carcinoma SMMC 7721 cells interacted and integrated well with the surrounding fibers. MTT experiments showed that cancer cells were killed promptly after PDT with a 702 nm laser light.<sup>225</sup> Costa *et al.* created core-shell electrospun nanofibers from biodegradable polymers such as poly(vinyl alcohol) (PVA) and gelatin (Gel) to function as a localized DDS for the treatment of cervical cancer with PDT. The synthesized porphyrin (Por) produced singlet oxygen ( $\Phi\Delta = 0.62$ ) and exhibited stronger phototoxicity against tumor cells than healthy cells (Table 1). The Por release profile from nanofibers demonstrated an initial rapid release phase, followed by continual release for at least 9 days. PVA-Gel + Por core-shell nanofibers inhibited cancer cell growth more effectively under light irradiation than under dark irradiation, and they had a greater phototoxic impact on tumor cells than non-tumor cells.<sup>226</sup>

#### 4.2. Photothermal agents in photothermal therapy

Stimulation-responsive nano-systems are being proposed as a method of precisely controlling nanomedicine expression. Because tumors can be deep-rooted, it is difficult to activate nano-systems in lesions while avoiding overexpression in healthy tissues. Because of this limitation, a suitable illumination source is required for efficient PTT. NIR light is regarded as a suitable excitation source as low-power NIR rays may enter tissues deeply while avoiding major harm or absorption by bodily fluids.<sup>227,228</sup> As a result, NIR-induced imaging and targeted therapy have lately received a great deal of interest. Because of its strong penetration through tissues, NIR fluorescence is currently used for diagnostics and labelling.<sup>229</sup> Nanomaterials have many distinct characteristics than their macroscopic analogue. It is vital to highlight that the effect of photothermal energy is linked to the nanoscale characteristics of agents. For example, gold nanoparticles (NPs) may transform excited state photon energy to heat *via* surface plasmon resonance (SPR).<sup>230</sup>

Nanomedicines also provide a benefit in cancer treatment for passive tumor targeting by the mechanism of nanoparticle produced endothelial leakage (NanoEL) or enhanced EPR of

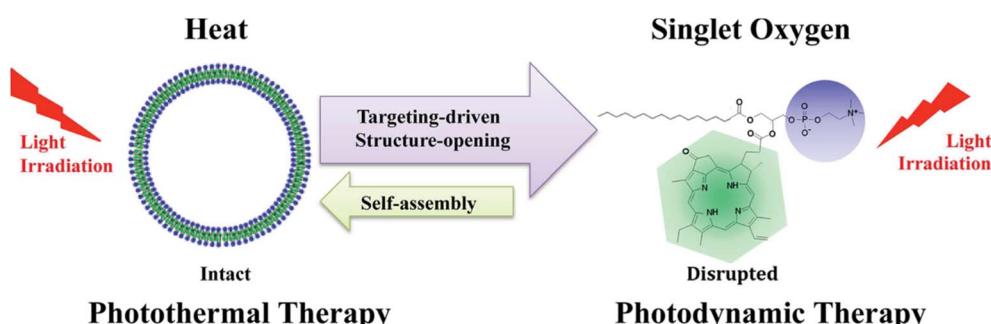


Fig. 19 Porphysomes are targeted for photodynamic activation in this illustration (Jin *et al.*, 2014).<sup>221</sup>





Table 1 Some of the nanoparticles studied for photodynamic therapy (PDT)

Type of nanoparticle	Material composition	In vivo and <i>in vitro</i> studies	Advantage	Reference
Gold nanoparticles	Gold nanorods	B16F0 melanoma tumor in mice	Single photon-induced fluorescence – for visualization in <i>in vivo</i> condition	160
	Gold and silver nanostructures	HeLa cells	Promising dual functional nanomaterials with capabilities of simultaneously serving as photodynamic therapy and photothermal therapy	163
Silver nanoparticles	Porphyrin-mercaptosuccinic acid-capped silver nanoparticles (POR-MSA-AgNPs) ZnPeS <sub>4</sub> /Ag-PEG-FA and ZnPeS <sub>4</sub> /Ag@mSiO <sub>2</sub> -F	Cancer cell line – A375	Significant singlet oxygen generation efficiency and cell imaging	165
Silica based nanomaterials	Mesoporous silica nanoparticle – SINPs – 5,10,15,20-tetrakis (1-methyl 4-pyridinio) porphyrin tetra ( <i>p</i> -toluenesulfonate) (TMPyP) (MSN@SINPs@TMPyP-FA)	A375 melanoma cancer cells	Cell death induced <i>via</i> apoptosis rather than necrosis	167
	Hollow silica nanoparticle (HNP) – with PDMAEMA polycation – chlorin e6 – caspase-8 gene (CSP8), (Ce6-HNP-Cou-PD/CSP8)	Human breast carcinoma cell lines (MCF-7) and human lung cancer cell lines (A549)	Targeted two-photon fluorescence cellular imaging at the near-infrared (NIR) laser excitation, this could effectively avoid the interference of biological auto-fluorescence	176
Quantum dots	Hematoporphyrin (HP)-encapsulated carbon quantum dots (CQDs)	Hepatocellular carcinoma cancer cell line (HepG2) and the human cervical cancer cell line (HeLa) MCF-7 cells	Relatively high sensitizing efficiency, remarkable singlet oxygen generation efficiency, and rapid elimination ability from the body	177
Carbon based nanomaterial	MMC-Graphene@BODIPY-mPEG (MGBP)	HeLa cell	Excellent ROS production ability, high photothermal conversion efficiency (48%), and excellent therapy efficiency <i>in vitro</i>	202
	Graphene oxide (GO) coupled with magnetic Fe <sub>3</sub> O <sub>4</sub> nanoparticles and chitosan (CS) (MCGO)	Human hepatoma cell lines HepG-2	High stability, good water solubility and biocompatibility, expected magnetic targetability, and good photostability for PDT	204
	PEG 2000N modified Fe <sub>3</sub> O <sub>4</sub> @carbon quantum dots (CQDs) coated single-walled carbon nanotubes (SWNTs), SWCNTs-PEG-Fe <sub>3</sub> O <sub>4</sub> @CQDs	HeLa cells	Imaging-guided collaborative treatment of cancer	193
	Fullerene (C60) <i>l</i> -phenylalanine derivative attached with poly (lactic acid) (C60-PLA) with mitoxantrone (MTX)	C57BL mice	High antitumor efficacy without toxic effects to normal organs, increased MTX tumor retention time, low MTX levels in normal organs and strong photodynamic activity	194
Two dimensional nanomaterials	MnO <sub>2</sub> nanosystem – chlorin e6 (Ce6)	MCF-7 breast cancer cells	Efficiently deliver it into cells, inhibits extracellular singlet oxygen generation by Ce6, leading to fewer side effects	210
	PEGylated MoS <sub>2</sub> (MoS2-PEG)	4T1 cells	Synergistic cancer killing with utilizing both PDT and PTT	213
	g-C <sub>3</sub> N <sub>4</sub> nanosheets	HeLa cells	Ultrahigh drug-loading capacity, pH-responsive release property, visualization of the delivery	215

nanoparticles for both immature and adult cancers, respectively. During leakage of endothelium, NPs of particular density and size react with the protein of adherens junction of endothelial cells, causing micro-sized gaps between them, boosting nanomedicine permeability and accumulation.<sup>231</sup> The size, surface chemistry and shape associated with nanoparticles have a significant impact on their biocompatibility and thermal performance.<sup>232</sup> Noble metal nanoparticles, being one of the earliest PTT ablation agents, have been extensively investigated in the past. Novel nanomaterials, including as nano-architected conducting polymers, have been developed for PTT usage in recent years.<sup>233</sup>

#### 4.3. Noble metal nanoparticles for photothermal treatment

Nanoparticles composed of noble metals, such as gold and platinum, have dominated research on PTT agents in the last few decades.<sup>234</sup> Unlike organic dyes, which often cause quick photobleaching when used as ablation agents, noble metal nanoparticles have a reasonable photothermal interaction efficiency and a considerable optical absorption capacity.<sup>235</sup> To convert light into heat, noble metal nanoparticles must have oscillations that resonantly match the practical frequency of the light.<sup>236</sup>

**4.3.1. Gold nanoparticles.** Noble metal nanomaterials have recently taken an attention in studies investigating the potential of gold nanoparticles for PTT. For instance, in the visible light spectrum, unaltered gold nanoparticles display SPR activity. It was illuminated by 20 ns bursts of 532 to 565 nm laser energy, according to Pitsillides *et al.* Short bursts of laser light were used to stop heat from diffusing, even though these wavelengths may not fall squarely inside the biological window.<sup>237</sup> If the gold nanoparticles are large and irregularly shaped, the Mie theory predicts, the SPR effect will be strong, and the SPR wavelength will be moved into the near-infrared spectrum.<sup>238</sup> To alter the SPR and enhance photothermal performance, many gold nanomaterials have been created, such as nanohexapods, nanorods (NRs), and nanoshells.<sup>239,240</sup>

The length and diameter of the rod determine the optical absorptions in gold NRs, which are transverse and longitudinal, respectively. Additionally, the SPR zone may be shifted to the near-infrared (NIR) area for PTT by adjusting the aspect ratio. Link *et al.* looked at how aspect ratio relates to longitudinal

plasmon resonance absorption maximum. Their research shows that whereas the transverse plasmon absorption of typical gold NP occurs in the visible light region, the longitudinal plasmon absorption moves to 740 nm when the average aspect ratio approaches 3.3.<sup>241</sup> The prospective uses of dendritic gold nanoparticles in photothermal therapy are also being explored, since their properties vary according to the hyperbranched structures they possess. A correlation between the degree of branching and the photothermal characteristics of gold nanodendrites has been studied. The optical characteristics of gold nanodendrites were found to be changeable. In the second near-infrared region (Fig. 20), photothermal treatment efficiency was better for gold nanodendrites with fewer branches.<sup>242</sup> Gold nanoparticles which have been created as drug transporters and image contrast agents, hinting that they might play a multifunctional role in medicine. A potential PTT ablation agent with further medical uses might be a hollow kind of gold nanomaterial, such a gold nanocage. In addition to their unique hollow nanostructure, which likely enables them to serve as drug carriers and contrast molecules for imaging, the hollow gold nanoparticles exhibit outstanding near-infrared absorption for photothermal therapy (PTT).<sup>243</sup> Yavuz *et al.* modified gold nanocages by coating them with a polymer blend of poly(*N*-isopropylacrylamide) and polyacrylamide. In order to facilitate the circulation of medications contained inside the gold nanocages, a polymer coating goes through a phase shift and produces open holes when exposed to the photothermal activity of the nanocages.<sup>244</sup> Nanoparticles of silica and iron oxide encased in gold have recently been suggested. These composites exhibited robust near-infrared optical absorption due to the nanostructure of the gold nanoshells.<sup>245</sup>

A group of scientists evaluated the effect of PEG-Cur-Au NPs on the C540 (B16/F10) cell line and implanted (bearing) melanoma tumors in inbred C57 mice after being exposed to an 808 nm laser. PEG-Cur-Au NPs exhibited dose-dependent cytotoxicity against the C540 (B16/F10) cell line at concentrations  $>25 \mu\text{g mL}^{-1}$ , with an IC<sub>50</sub> value of  $42.7 \mu\text{g mL}^{-1}$  in dark (and no toxicity at  $10 \mu\text{g mL}^{-1}$ ). For 10 minutes of 808 nm laser irradiation (without PEG-Cur-Au NPs), the C540 (B16/F10) cell line was killed in a laser power-dependent manner at power density  $>0.5 \text{ W cm}^{-2}$  (no toxicity at  $0.5 \text{ W cm}^{-2}$ ). However, PTT employing PEG-Cur-Au NPs was extremely visible following laser illumination. Even at a power intensity of  $0.5 \text{ W cm}^{-2}$  of PEG-Cur-Au NPs concentrations  $<10 \mu\text{g mL}^{-1}$ , the cells showed significant PTT.<sup>246</sup>

A group of scientists created hybrid albumin nanoparticles using AuNCs ( $\sim 88 \text{ nm}$ ) and AuNPs ( $\sim 4.5 \text{ nm}$ ). After 808 nm laser irradiation ( $1.5 \text{ W cm}^{-2}$ , 10 min), AuNCs/BSA-NPs significantly inhibited tumor development ( $17.8 \pm 16.9 \text{ mm}^3$  vs. PBS and AuNCs/BSA-NPs (formula E):  $\sim 1850$  and  $\sim 1250 \text{ mm}^3$ , respectively).<sup>247</sup> Wang *et al.* produced a multifunctional responsive drug carrier by loading resveratrol (Res) into chitosan (CTS) modified liposomes and coating them with gold nanoshells. The resulting GNS@CTS@Res-lips have a broad near-infrared (NIR) absorbance, high capability, stability, and photothermal conversion ability, making them suitable for effective photothermal treatment (PTT). In addition, the

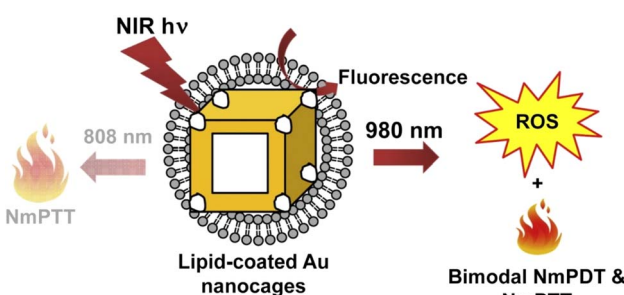


Fig. 20 Photo-induced lipid-coated gold nanocages' working mechanism is illustrated schematically (Vankayala *et al.*, 2014).<sup>240</sup>



GNS@CTS@Res-lips have on-demand pH/photothermal-sensitive drug release and a high-Res loading capacity. The drug delivery device might greatly improve drug uptake by cells when exposed to NIR laser irradiation. More notably, compared to single chemotherapy or PTT, carriers with NIR irradiation had a greater therapeutic impact on HeLa cells.<sup>248</sup>

Xia *et al.* reported a simple method for fabricating gold nanostars (GNS) attached with matrix metalloproteinases (MMP2) polypeptides (Ac-GPLGIAGQ) and IR-780 iodide *via* bovine serum albumin (BSA) for targeted dual-modal photo-acoustic (PA)/near-infrared (NIR) fluorescence imaging and enhanced photothermal therapy (PTT)/photodynamic therapy (PDT) for lung cancer. MMP2 polypeptides were used as a targeting ligand, IR-780 iodide as an NIR fluorescence imaging and PTT/PDT agent, and GNS as a carrier of IR-780 molecules for PA imaging and PTT. *In vitro* investigations confirmed that GNS@BSA/I-MMP2 nanoparticles (NPs) were successfully absorbed by A549 cancer cells, resulting in exceptional anti-cancer activity. GNS@BSA/I-MMP2 NPs could selectively target the tumor and greatly inhibit tumor development, and their anticancer effects were mostly due to the synergistic effects of PDT and PTT based on IR-780 and GNS.<sup>249</sup>

**4.3.2. Semiconductor nanomaterials used in PTT.** Due to their affordability and cytotoxicity, a number of semiconductor nanomaterials, including semiconductor copper chalcogenide nanomaterials, have drawn interest as PTT ablation agents in addition to noble metal nanoparticles.<sup>250</sup> Nevertheless, under standard NIR light at around 808 nm, the relatively poor photothermal interaction efficiency of certain copper-based nanomaterials may need increased NIR power to facilitate tumor ablation. To overcome this challenge, NIR light at 980 nm is frequently used as a replacement for certain Cu-based NPs. This light is a rather high threshold for exposure to human skin, with penetration across biological tissues potentially reaching several centimeters. With this regard, the strength of the NIR laser might be lowered while the treatment's effectiveness was maintained.<sup>251</sup> Hu's group successfully synthesized CuS nanoparticles exhibiting a consistent three-dimensional floral shape, enhancing photothermal efficiency. It was suggested that these superstructures may serve as laser-cavity mirrors for a 980 nm laser, enhancing reflectivity and hence photothermal efficiency. They also synthesized hydrophilic Cu9S5 plate-like nanocrystals with a photothermal efficiency of up to 25.7%, surpassing that of gold nanorods under analogous 980 nm light irradiation.<sup>252</sup>

CuS NPs are being employed in studies on the detrimental impact of PTT upon HeLa cells. The dependent impact of laser dosage and CuS concentration of particles was then investigated. In this study, an NIR laser (808 nm) with a power of up to  $24 \text{ W cm}^{-2}$  was used to accomplish relatively selective cancer treatment. The NIR laser as well as CuS NPs alone had a moderate effect on cell death. Furthermore, the minimal cytotoxicity of this NP was demonstrated individually in this study, meaning that copper sulfide NP-induced PTT was harmless to normal cells. Moreover, modified Cu7.2S4 nanocrystals with photothermal efficiencies as high as 56.7% were developed. These Cu7.2S4 nanocrystals effectively eradicated cancer cells using a low dose concentration and a diminished

power 980 nm laser. CuS nanoparticles has the potential to serve as an exceptional ablation agent for photothermal therapy due to their targeted ablation effect, low cytotoxicity, and cost-effectiveness.<sup>253</sup>

**4.3.3. Carbon-based nanomaterials used in PTT.** CNTs have recently been investigated in the medical area for application in thermal therapy due to their optical characteristics and outstanding thermal behavior. CNTs have been used in medical applications such as medication transporters and bioimaging probes. They can be covalently or noncovalently treated with various chemical groups. CNTs may readily be functionalized with other medicinal molecules, such as magnetic NPs and anti-cancer medicines, by binding or wrapping. This might increase the photothermal efficiency of CNTs and allow for the development of synergic medicines.<sup>254</sup> PEG coatings often enhance biocompatibility, inhibit aggregation, and prolong blood circulation duration, all of which are considered advantageous in nanoparticles used as ablation agents.<sup>255</sup> Burke *et al.* examined the response of BCSCs to hyperthermia by a water bath or the photothermal effect induced by MWNTs to elucidate the PTT mechanism mediated by CNTs. BCSCs exhibited resistance to hyperthermia throughout a broad temperature spectrum; yet, the photothermal action induced by MWCNTs may surmount this resistance by enhancing necrotic cell death. The hypothesis was formulated based on the interaction between cancer cell membranes and NIR-stimulated MWNTs exhibiting increased surface temperatures.<sup>256</sup>

Graphene-based nanomaterials, just like CNTs, have a substantial optical absorption in the near infrared area along with high surface activity, which makes them a prospective PTT ablation agent with synergic therapeutic applications Fig. 21.<sup>257</sup> Markovic *et al.* examined the sort of cell death caused by graphene-induced PTT. Based to their results, cells perished through combination of both necrosis and apoptosis. Though PTT causes necrosis, heat would increase oxidative stress/superoxide generation and, eventually, apoptosis.<sup>258</sup>

Lim *et al.* (2018) created a  $\sim 155 \text{ nm}$  nanocomposite containing GO, folic acid, and manganese dioxide ( $\text{MnO}_2$ ). In cancer,  $\text{MnO}_2$  decomposes hydrogen peroxide into oxygen, alleviating hypoxia. The results demonstrate that the composite has a higher heat capacity than a single GO. Under 808 nm laser illumination for 3.5 minutes, the nanocomposite reaches the target temperature of  $47^\circ\text{C}$ , whereas GO only reaches  $35^\circ\text{C}$ .<sup>259</sup>

Xie *et al.* (2019) created a composite with high stability and dispersibility using GO, magnetic nanoparticles ( $\text{Fe}_3\text{O}_4$ ), chitosan, sodium alginate, and doxorubicin hydrochloride. They tested the composite PTT qualities using an MTT assay using a human lung cancer cell line (A549) and 808 nm irradiation for 5 minutes, exhibiting good intracellular uptake characteristics and a temperature-dependent rise in concentration. The dosage of  $100 \text{ }\mu\text{g mL}^{-1}$  resulted in a 14.36% drop-in survival rate.<sup>260</sup> Gulzar *et al.* (2018) created a combination of GO, amino-modified upconversion nanoparticles ( $\text{NaGdF}_4:\text{Yb}^{3+}/\text{Er}^{3+}@\text{NaGdF}_4:\text{Nd}^{3+}/\text{Yb}^{3+}$ ), polyethylene glycol (PEG), and chlorin e6 (Ce6). Singlet oxygen production was confirmed using the DPBF (1,3-diphenyliso-benzofuran) chemical probe



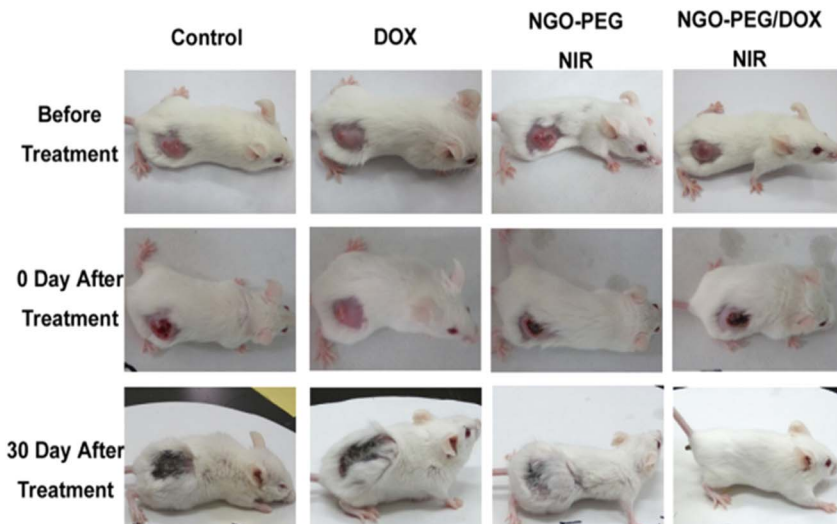


Fig. 21 Representative photographs of tumours on mice after different therapies are shown. The laser irradiated tumors on the NGO-PEG-DOX-injected mouse was fully destroyed (Zhang *et al.*, 2011).<sup>257</sup>

(PDT effect). In addition, an *in vivo* anticancer property was assessed in mice utilizing an U14 (murine hepatocarcinoma) cell line and 808 nm irradiation. As a result, the fluctuation in the relative volume of the tumor ( $V/V_0$ ) was decreased by half after 14 days as a result of the PTT effect, while this value in the control group rose by ninefold.<sup>261</sup>

De Paula *et al.* (2020) used red LED (640 nm) ablation to drastically reduce the tumor mass in mice (melanoma in B16F10 lineage cells) with a rGO-based therapy. The tumor volume was around  $70\text{ mm}^3$  on the first day, but decreased to around  $40\text{ mm}^3$  after 8 days of therapy. Furthermore, the immunological response was validated by measuring the development of  $\text{CD}^{8+}$  T cells.<sup>262</sup> Zhang *et al.* treated A549 lung cancer cells with two distinct light sources, 808 nm and 450 nm, to PTT and PDT, respectively. They employed an r-GO composite with a PEG-modified Ru(II) complex as the PS. This combination improved cytotoxicity and reduced tumor volume, as demonstrated by *in vivo* experiments. The PTT-PDT therapy slows tumor development, lowering the relative tumor volume value ( $V/V_0$ ) to near-zero. In contrast, PTT and PDT alone increased this value to around 1.5 and 2.5, respectively.<sup>201</sup>

Marangon *et al.* developed a nanosystem based on multi-walled carbon nanotubes (MWCNT) and the photosensitizer *m*-tetrahydroxyphenylchlorin (*m*THPC) for cancer treatment using photodynamic (PDT) and photothermal (PTT) therapy. The photothermal and photodynamic cytotoxicity of these *m*THPC/MWCNT on/off complexes was evaluated at the cell level using viability tests, imaging flow cytometry, confocal microscopy, and transmission electron microscopy, as well as at the molecular level using a proteomic analysis of apoptosis-related proteins and a genomic analysis of 84 oxidative stress genes. At the cell level, cytotoxicity was associated with *m*THPC/MWCNT absorption, whereas PDT and PTT treatment generated distinct signaling pathways that led to cell death. For the first time, the mechanisms of PDT/PTT synergy in cancer cell

eradication were investigated, indicating that different cell responses to PDT and PTT undermine the cell's oxidative stress defense.<sup>263</sup>

**4.3.4. Conducting polymers used in PTT.** PEG coatings often enhance biocompatibility, inhibit aggregation, and prolong blood circulation duration, all of which are considered advantageous for nanoparticles used as ablation agents.<sup>255</sup> Burke *et al.* examined the response of BCSCs to hyperthermia by a water bath or the photothermal effect induced by MWNTs to elucidate the PTT mechanism mediated by CNTs. BCSCs exhibited resistance to hyperthermia throughout a broad temperature spectrum; yet, the photothermal impact induced by MWCNTs might potentially surpass this resistance by enhancing necrotic cell death. The hypothesis was formulated based on the interaction between cancer cell membranes and NIR-stimulated MWNTs exhibiting increased surface temperatures.<sup>256</sup>

A multitude of nanoparticles has been included into photothermal therapy (PTT), signifying substantial promise for this focused and less deleterious cancer treatment. Although the experiments remain in preliminary phases, several biological investigations on PTT have shown encouraging outcomes. Despite the variability in the processes of various ablation agents, it was shown that the effects of photothermal radiation could generally be regulated by modifying the shape and dimensions of these PTT agents (Fig. 22). Given the multitude of potential alternatives and ablation chemicals for photothermal therapy (PTT), together with the use of nanotechnology, researchers may manufacture a molecule exhibiting enhanced photothermal effectiveness for PTT.<sup>33</sup>

**4.3.5. Tungsten based nanomaterial.** Zhou *et al.* developed a simple thermal decomposition method to produce tungsten oxide nanorods ( $\text{WO}_{2.9}$  NRs) measuring  $13.1 \pm 3.6\text{ nm}$  in length and  $4.4 \pm 1.5\text{ nm}$  in diameter for tumor theranostic applications. The generated  $\text{WO}_{2.9}$  NRs were treated with



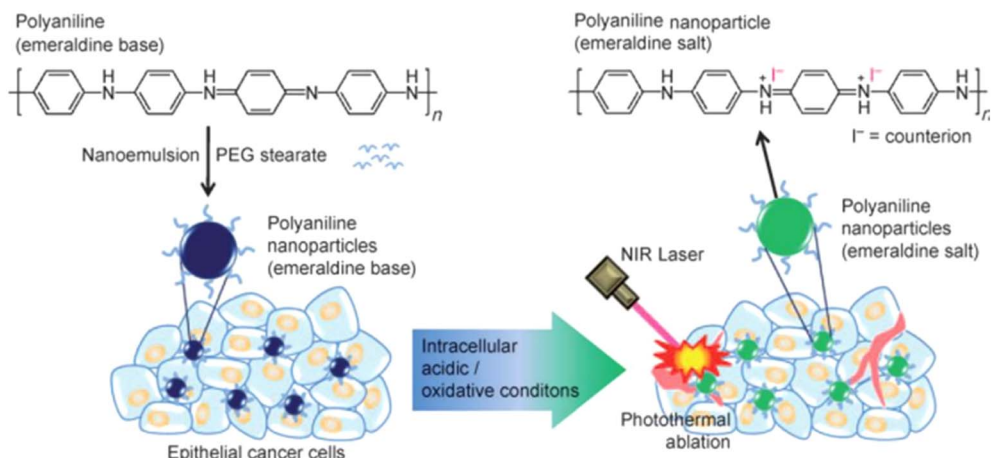


Fig. 22 Scheme for producing naturally occurring photothermal agents using polyaniline nanoparticles and using NIR laser irradiation to kill epithelial cancer cells (Yang *et al.*, 2011).<sup>264</sup>

methoxypoly(ethylene glycol) (PEG) carboxyl acid by ligand exchange to improve water dispersibility and biocompatibility. PEGylated  $\text{WO}_{2.9}$  NRs exhibit high photothermal conversion efficiency and superior X-ray attenuation compared to clinically used CT contrast agent Iohexol. They effectively inhibit cancer cell growth *in vitro* and tumor growth *in vivo*, allowing for effective CT imaging.<sup>265</sup>

Sharker and his colleagues reported a dopamine-conjugated hyaluronic acid (HA-D), a mussel-inspired simple capping material that can make tungsten oxide ( $\text{WO}_3$ ) nanoparticles biocompatible and targetable, enabling for precision delivery ( $\text{WO}_3\text{-HA}$ ) to a tumor location. Near-infrared (NIR) irradiation  $\text{WO}_3\text{-HA}$  demonstrated a quick and significant increase in photothermal heat, resulting in full *in vitro* thermolysis of malignant MDAMB and A549 cancer cells, but was shown to be less susceptible to normal MDCK cells. Long-term *in vivo* study of  $\text{WO}_3\text{-HA}$  nanoparticles with  $\sim 10$  nm HA thickness showed effective photo-thermal conversion and time-dependent tumor target accumulation. This long-term *in vivo* survival study of  $\text{WO}_3\text{-HA}$  demonstrated good biocompatibility, with full recovery from malignant tumors.<sup>266</sup>

**4.3.6. Nanofibers.** In recent years, life scientists have focused on precise spatiotemporal regulation of physiologically important species delivery. Light, particularly near-infrared (NIR) light, inside the “transparency window” for biological tissues, is an elegant on/off stimulus that meets these characteristics.<sup>267</sup> Cheng *et al.* introduced PEG-modified gold nanorods (PEGGNRs) into an electrospun PLGA/PLA-*b*-PEG membrane. This platform's polymer membrane provided both a physical barrier against surgical damage and a biocompatible carrier for PEG-GNRs. When incubated with cancer cells, the PEG-GNRs were released from the fibrous mat and eventually absorbed by the cells. PEG-GNRs released under 850 nm NIR irradiation generate heat. An *in vitro* investigation found that the PEG-GNR-incorporated mesh may selectively kill cancer cells and limit their growth.<sup>268</sup> In the work by Wang, doxorubicin (DOX) and indocyanine green (ICG) co-loaded mesoporous silica nanoparticles (DIMSN) were produced. The

nanoparticles were then electrospun into chitosan/poly(vinyl alcohol) (CS/PVA), resulting in multifunctional composite nanofibers (DIMSN/F). Under the mimic erosion of vaginal discharge, DIMSN/F demonstrated site-specific drug release, however local administration of a thermosensitive DIMSN-loaded gel (DIMSN/gel) did not. When compared to systematic DIMSN injection, vaginal implantation of DIMSN/F might optimize drug accumulation in mice's vaginas. DIMSN/F photothermalchemotherapy (PTCT) effects were investigated in both subcutaneous and orthotopic cervical cancer models in mice, although drug penetration in the hard nodular tumor offered a significant barrier. The tumor inhibition rate (TIR) for orthotopic cervical/vaginal cancer remained as high as 72.5%, indicating a good promise for cervical cancer therapy.<sup>269</sup> Paclitaxel, an anticancer medication, and graphene oxide/gold nanorods (GO/Au NRs) were loaded into poly (tetramethylene ether) glycol-based polyurethane (PTMG-PU) (core)/chitosan (shell) nanofibers generated by coaxial electrospinning. The potential of the produced nanofiber as a pH/temperature dual responsive carrier was examined for the controlled release of paclitaxel against A549 lung cancer using the PTT/CHT combination technique. The cell survival of manufactured nanofibers treated with A549 lung cancer cells was studied using the alone CHT, alone PTT, and PTT/CHT methods. *In vivo* investigations suggested that the PTT/CHT approach displayed an optimum therapeutic impact on tumor inhibition without changing body weight.<sup>270</sup>

## 5. Stimuli responsive nanomaterials

Although their clinical applications are still in the early stages, as compared to traditional chemotherapy, multiple significant pre-clinical investigations have indicated that stimuli responsive techniques provide superior therapeutic success with fewer adverse effects.<sup>271,272</sup> Specific triggers/stimuli can be roughly classed as intrinsic or external stimuli. Intrinsic stimuli are limited to the interior of the body/organism system, with the tumor microenvironment serving as an excellent example of





Table 2 Some of the nanoparticles studied for photothermal therapy (PTT)

Type of nanoparticle	Nanoparticle studied	Irradiation conditions	Temperature reached upon irradiation	Cancer studied <i>in vivo</i>	Advantage of nanocomposite	Study outcome	Ref
Gold nanosphere	Gold nanocluster-loaded hybrid albumin nanoparticles	808 nm, 1.5 W cm <sup>-2</sup> for 10 min	70 °C	HCT116 tumor	Facilitate an increase in temperature up	A decrease in size of tumor from 150 mm <sup>3</sup> to 17.8 mm <sup>3</sup>	247
	Gold nanoshell coated thermo-pH dual responsive liposomes for resveratrol delivery	808 nm, 2 W cm <sup>-2</sup> for 5 min	66.7 °C	HeLa cells	The photothermal effect created by such nanomaterials remained consistent over 5 cycles of irradiation under a NIR laser	HeLa cell viability is reduced by up to 57.3%	248
	Anti-EGFR antibody linked thiol chitosan-layered gold nanoshells	808, 1.2 W cm <sup>-2</sup> for 5 min	61.9 °C	MDA-MB-231 cells	The produced heat might be used to stimulate the release of paclitaxel from the chitosan layer on the outermost layer of the gold nanoshells	97.43% tumor inhibition rate	275
	DNA-conjugated gold nanorods	808 nm, 5 W cm <sup>-2</sup> for 30 min	45 °C	MCF-7/ADR cells	Strong photothermal effect. The gold nanorods have a pH and NIR sensitive drug release due to DOX intercalation alongside the DNA coated on the particles surface.	81% inhibition of MCF-7/ADR cell proliferation was observed	276
					When irradiated with an NIR laser, around 60% of the drug is released	93% reduction of the tumor volume	249
Gold nanorods				A549 cells	Strong absorption band		
				SMMC-7721	Targeted delivery	Reduced the growth of liver cancers and raised mice's median survival periods from 36 to 60 days	277
				SKOV3 cancer cells	The cytotoxic impact of nanotubes was enhanced by mixing them with <i>m</i> -tetrahydroxyphenylchlorin	Only 10% of the SKOV3 cells remained alive	263
Gold nanocages	Matrix metallopeptidase 2 targeted delivery of gold nanostars decorated with IR-780 Iodide	808 nm, 0.8 W cm <sup>-2</sup> for 5 min	63 °C		The capability of producing same level of increased temperature was maintained even after 5 cycles	Only around 20% of the cells remained alive	278
	Folic acid-functionalized gold nanocages for the targeted delivery of anti-miR-181b	808 nm, 1.25 W cm <sup>-2</sup> for 10 min	55 °C				
				MCF-7 cancer cells	The produced nanomaterial has a mean size of 108 nm and an NIR absorbance higher than that of graphene oxide	Cell viability to ≈ 6%	279
Graphene	Photosensitizer/carbon nanotube complexes	808 nm, 2.3 W cm <sup>-2</sup> , 200 seconds	50 °C		Broad absorption	6% of viable cells was observed	280
	Doxorubicin-loaded and folic acid-conjugated carbon nanotubes@ poly (N-vinyl pyrrole)	808 nm, 1.5 W cm <sup>-2</sup> for 6 min	45 °C	HeLa cells			
	Hyaluronic acid functionalized green reduced graphene oxide	808 nm, 1.7 W cm <sup>-2</sup> for 5 min	33 °C				
Tungsten	Poly (allylamine hydrochloride)-functionalized reduced graphene oxide	808 nm, 6 W cm <sup>-2</sup> for 6 min	45 °C	MCF-7 cells			
	PEGylated nonstoichiometric WO <sub>2.9</sub> nanorods	980 nm, 0.25 W cm <sup>-2</sup> for 10 min	20.1 °C	HeLa cells	Biocompatible	Less than 20% cell viability	265



Table 2 (Contd.)

Type of nanoparticle	Nanoparticle studied	Irradiation conditions	Temperature reached upon irradiation	Cancer studied <i>in vivo</i>	Advantage of nanocomposite	Study outcome	Ref
Dopamine-conjugated HA tungsten oxide nanoparticles	808 nm laser, 2 W cm <sup>-2</sup> for 5 min	44 °C	MDA-MB-231 and A549	Broad absorption	Less than 3% cell viability	266	
Molybdenum disulfide modified with hyperbranched polyglycidyl PEGylated plasmonic MoO <sub>3</sub> -x hollow nanospheres	808 nm, 2 W cm <sup>-2</sup> for 10 min	34 °C	B16 cells	Increased absorbance in NIR region	Cell viability to less than 30%	281	
Molybdenum oxide	808, 1 W cm <sup>-2</sup> for 10 min	48 °C	HeLa cells	Strong absorption band	Almost total tumor elimination with no recurrences by day 15	282	
Iron oxide	808 nm, 1 W cm <sup>-2</sup> for 9 min	18 °C	MDA-MB-231 cells	—	≈70% decrease of the cellular viability	283	
Copper sulfide	808 nm, 2 W cm <sup>-2</sup> for 5 min	40 °C	MCF-7 cells	Iron-dependent artesunate action	Death of 92.6% of cells	284	

creating local stimuli such as pH or interstitial pressure, among other things. A collection of characteristics known as 'external-stimuli' exist in addition to the host's internal system and include magnetic fields, ultrasound, light, and so on.<sup>273</sup> Light-responsive drug release systems have been developed using methods such as photoisomerization, photocrosslinking/decrosslinking, photosensitised oxidation, light-triggered polarity flipping, and photo- or photodegradation of the polymer backbone.<sup>274</sup> Cholesteryl succinyl silane (CSS) nanomicelles encapsulating DOX, Fe<sub>3</sub>O<sub>4</sub> magnetic NPs, and Au nanoshells were created as a multicomponent/functional drug delivery system. These composite nanomicelles show an 808 nm NIR laser-induced temperature rise, which causes progressive DOX release. These CSS nanomicelles have a high T<sub>m</sub> value, requiring a high temperature to destabilize them (Table 2). This is especially useful when considering the on-demand release of DOX only after NIR irradiation of the Au nanoshells, which raises the local temperature, loosens the micelles, and effects drug release, hence reducing undesirable drug leakage throughout circulation.<sup>285</sup>

Thermal ablation is becoming one of the most often reported forms of solid tumor treatment, and super paramagnetic iron oxide NPs (SPIONs) have been intensively studied in this area. HT treatment with iron oxide NPs (IONPs) entails administering an IONPs fluid to the tumor, followed by AMF application, which causes NPs heating and ablation. A temperature change of 41–46 °C can cause significant consequences on cells and tissues, including increased heat-shock protein production, protein denaturation/folding, and apoptosis. Specifically in tissues, the temperature surge stimulates pH alteration, perfusion, and oxygenation of the tumor microenvironment, with persistently elevated temperatures leading to necrosis.<sup>286–288</sup> Matsumine *et al.* used HT in patients with metastatic bone tumors. Following the first surgical surgery, a biocompatible bone replacement composed of 'Bare' magnetite NPs and calcium phosphate cement was implanted. Patients received a 15 minutes treatment every alternate day commencing on the eighth day after surgery. The results showed a 32% reduction in lesions with apparent bone growth, 64% without any progressing lesions for more than 3 months, and only 4% with a negative treatment response.<sup>289</sup>

Longer wavelength radiofrequency (10 kHz to 900 MHz) can also be used for cancer cell ablation *via* the HT effect. RF offers more tissue penetration than NIR light, allowing for the therapy of deep-seated cancers.<sup>290</sup> Elsherbini *et al.* used Au-coated magnetics for dual-mode HT against subcutaneous Ehrlich cancer in mice using laser and radiofrequency irradiation. Results analysis indicated that more than half of the tumors totally vanished after light/RF irradiation.<sup>291</sup>

## 6. Photodynamic combination therapy in cancer treatment

PDT includes activating a photosensitizer with a certain wavelength of light, resulting in transitory amounts of ROS. However, the use of PDT targeting deep tumors has been

severely limited due to inadequate luminous flux and possibility of peripheral damage to tissues. As a result, researchers have begun to investigate if combining PDT with other therapies might increase its efficacy.<sup>292</sup>

### 6.1. PDT in conjunction with chemotherapy

Chemotherapy, which is among the most common cancer treatment procedures, is used to manage a wide range of cancers. Chemotherapeutic medicines are thought to attach to tumor cell's DNA, inhibiting cell proliferation and replication, ultimately leading to cancer cell death.<sup>293</sup> Chemotherapy has the capacity to kill cancer cells, but its non-specific nature and susceptibility to resistance restrict its therapeutic usage. Several efforts have been undertaken to integrate PDT with chemotherapy in order to overcome the side effects and resistance and boost the therapeutic benefit. PDT coupled with chemotherapy may have a synergistic anti-tumor impact, reducing the therapeutic dosage of the chemotherapeutic medicines.<sup>292</sup> Numerous studies have shown that integrating PDT with chemotherapy may enhance treatment efficacy, while the reasons behind this augmentation are uncertain.<sup>294</sup> Xiaojun Wang discovered that employing the  $1O_2^-$  reactive nano-carrier NOP-DOX@BSA-FA as a delivery strategy in PDT combined chemotherapy allows DOX to swiftly reach tumor regions, successfully destroying cancer cells and decreasing chemotherapy's harmful effects on the body.<sup>295</sup>

Employing PDT along with chemotherapy may overcome multi-drug resistance (MDR) caused by tumor treatment. MDR is often caused by overexpression of *P*-glycoprotein on tumor cells, which can be triggered by short-term chemotherapy treatment.<sup>292</sup> Khdaire discovered that combining methylene blue mediated PDT with adriamycin resulted in substantial toxicity against MDR tumor cells. This was due to a high concentration of doxorubicin in the MDR following PDT. Drug-resistant tumor cells undergo necrosis or apoptosis as *P*-glycoprotein expression decreases and ROS levels increase in the tissue.<sup>296</sup> Bano found that coupling doxorubicin (DOX) along with nickel oxide nanoparticles (NOPs) with the form of NOP-DOX@BSA-FA, a potential PDT agent, resulted in a higher rate of cell death than utilizing NOPs alone Fig. 23.<sup>297</sup>

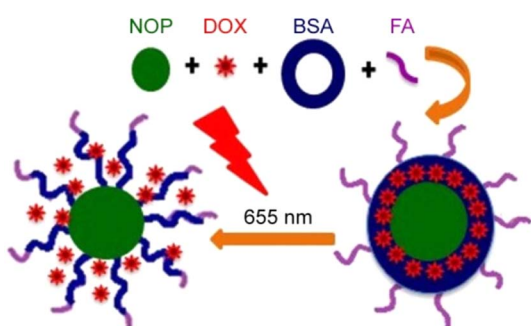


Fig. 23 Mechanism of NOP-DOX@BSA-FA in PDT (Bano *et al.*, 2016).<sup>297</sup>

### 6.2. PDT in conjunction with radiotherapy

Local tumor irradiation using X-rays constitutes one of the most effective anti-tumor treatments. Approximately 60–70% of individuals with malignant malignancies require radiation therapy. Radiotherapy for advanced cancer patients can improve symptoms, reduce discomfort, and boost survival rates.<sup>292</sup> Non-specific radiotherapy can cause harm to normal tissue in the radiation field. Furthermore, hypoxic cells in tumor tissues may be resistant to radiation. For individuals with advanced cancers, PDT coupled radiation can considerably enhance quality of life, reduce symptoms, decrease pain, and increase survival.<sup>298</sup> Yi-shan Wang studied the effectiveness of PDT in combination with radiation therapy in 90 incidents of gastric cancer, 12 incidents of esophageal cancer, 24 incidents of rectal cancer, 8 incidents of bladder cancer, 6 incidents of cervical cancer, and 8 incidents of superficial tumors. The study found that combining PDT with intensity-modulated radiation (IMRT) improved the quality of life for patients with advanced malignant tumors, particularly those with cavity viscera. Combination treatment promotes palliative care for individuals with malignant tumors who have failed radiation and chemotherapy due to obstructive symptoms. Studies have indicated that combining PDT with radiotherapy might increase tumor susceptibility to irradiation and improve therapeutic efficacy. At the identical time, it can cut the exposure period or lower the radiation dosage.<sup>299</sup>

### 6.3. PDT in conjunction with immunotherapy

PDT-induced immune response is critical for avoiding tumor spread and recurrence. Designing PDT drugs specific to the immunological target can improve its anti-tumor impact while minimizing immune response suppression.<sup>292</sup> Yuanhong Zheng discovered that tumor cells adjust to immunological pressure and demonstrate improved tumorigenic and stemlike characteristics following PDT immunization.<sup>292</sup> Hisataka Kobayashi employed a photosensitizer coupled to MAbs binding epidermal growth factor receptors (EGFRs) for deeper tissue infiltration and selective targeting, resulting in tumor

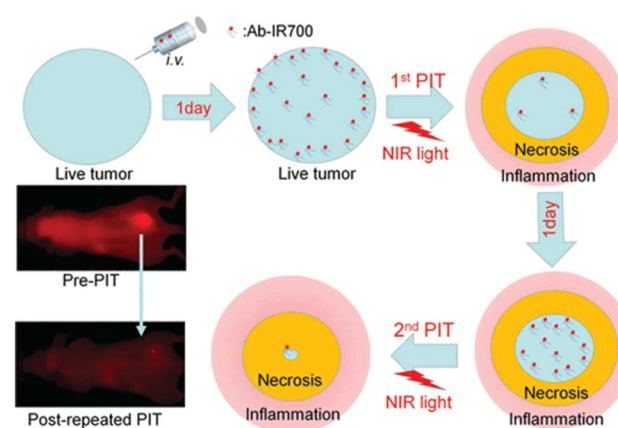


Fig. 24 Fractionated dosing of mAb-IR700 conjugate and NIR light (Mitsunaga *et al.*, 2012).<sup>300</sup>

elimination Fig. 24.<sup>300</sup> When paired with checkpoint inhibitors (PD-L1/PD1), PDT induces a robust tumor-specific immune response, this results in a reduction of both light-irradiated original tumors and non-irradiated distant malignancies.<sup>301</sup> Laser immunotherapy (LIT) is a new approach that combines PDT with an immunological adjuvant. Recent research has shown that indocyanine green and glycated chitosan, when combined with PDT, have superior therapeutic results than PDT alone. Furthermore, GC has a better immune stimulating power than some other commonly used immune adjuvants.<sup>302,303</sup> Utilizing PDT along with an immunological adjuvant can boost its efficiency. Korbelik discovered that combining PDT with mycobacterium extract (MCWE) significantly improves immune cell activation.<sup>304</sup>

## 7. Photothermal combination therapy in cancer treatment

PTT offers several advantages, including good temporospatial control, cheap cost, and little invasiveness. This can also be employed alone to eliminate the underlying tumor or lymph metastases in superficial tissues. But illumination has a limit on penetrating depth. Even while NIR light are able to penetrate deep than UV as well as visible light, but can reach only a depth of around 3 cm in tissue.<sup>305</sup> Due to the limited penetration into tissue at NIR light in deep layers of tissues, it is difficult for PTT alone to eliminate metastatic cancer cells and metastatic nodules in organs that are far away. As a result, in order to achieve the desired effectiveness against cancer metastasis, PTT must be combined with already known medicines.<sup>7</sup>

### 7.1. PTT in conjunction with chemotherapy

Multiple studies have revealed that CHT causes medication resistance, intrinsic cytotoxicity to normal cells, and distinct patient behavioral problems.<sup>32</sup> Synergistic treatment with PTT may address these issues. When combined with nanocarriers, these agents may deliver CHT drugs to tumors without exposing normal cells, reducing drug dosage and perhaps reducing side

effects and chemotherapy-resistant cancer cell growth. It takes less medicine to have the intended effect since drug release is slow without NIR irradiation and fast when photothermal agents are activated.<sup>306</sup> If the dispensing mechanism is sufficient, turning off NIR laser may halt smart drug-releasing nanoparticles. Meng *et al.* created a smart G-CuS-DOX MEO<sub>2</sub>-MA@MEO<sub>2</sub> MA-*co*-OEGMA composite. PTT agents were CuS nanoparticles, CHT medications were DOX, and thermosensitive nanogel was MEO<sub>2</sub>MA@MEO<sub>2</sub>MA-*co*-OEGMA (G). Nano-capsule hyperthermia shrank nanogels and released DOX under NIR irradiation. Turning off NIR irradiation eliminated PTT and CHT effects. Combined PTT and CHT showed controllable and efficient advantages *in vivo* Fig. 25.<sup>307</sup> Liu and Wang created hydrogel-based nanoplatforms for PTT and CHT tumor therapy. The chemical was injected into malignant tissue at room temperature, and the hydrogel formed instantly at 37 °C. Hydrogel matrix controlled chemotherapeutic drug release and had photothermal effects. They found that the composite hydrogel was an efficient tumor therapeutic platform.<sup>308,309</sup>

### 7.2. PTT in conjunction with radiotherapy

Anticancer medications are unable to reach tumors because of the abnormal microenvironment that surrounds them. Nanoparticles face many obstacles on their way to the tumor site, such as growth-induced solid stress, complex tumor vascular networks, increased interstitial fluid pressure, and tangled interstitial structures.<sup>310</sup> Arterial perfusion, vascular permeability, and interstitial fluid pressure are all positively impacted by malignancies that have had radiation treatment.<sup>311</sup> Increased tumor perfusion, vascular permeability, and nanoparticle absorption are equivalent outcomes of mild hyperthermia produced by PTT.<sup>312</sup> The penetrating depth of NIR light is limited, but X-ray and  $\gamma$ -ray irradiation do not have such limitations. However, PTT successfully kills hypoxic cancer cells due to hyperthermia and may improve oxygenation situation in the tumor, but RT has poor therapeutic efficacy for these cells.<sup>313</sup> Accordingly, the therapeutic efficacy of both PTT and RT may be enhanced when administered together.<sup>36</sup> In order to provide

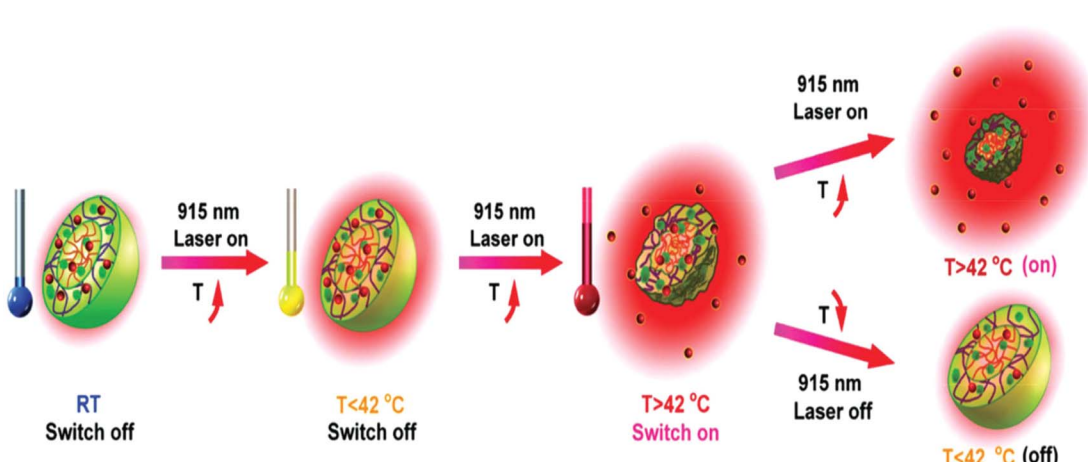


Fig. 25 An ex vivo NIR laser switches the intelligent DOX release "on" or "off" (Meng *et al.*, 2016).<sup>307</sup>



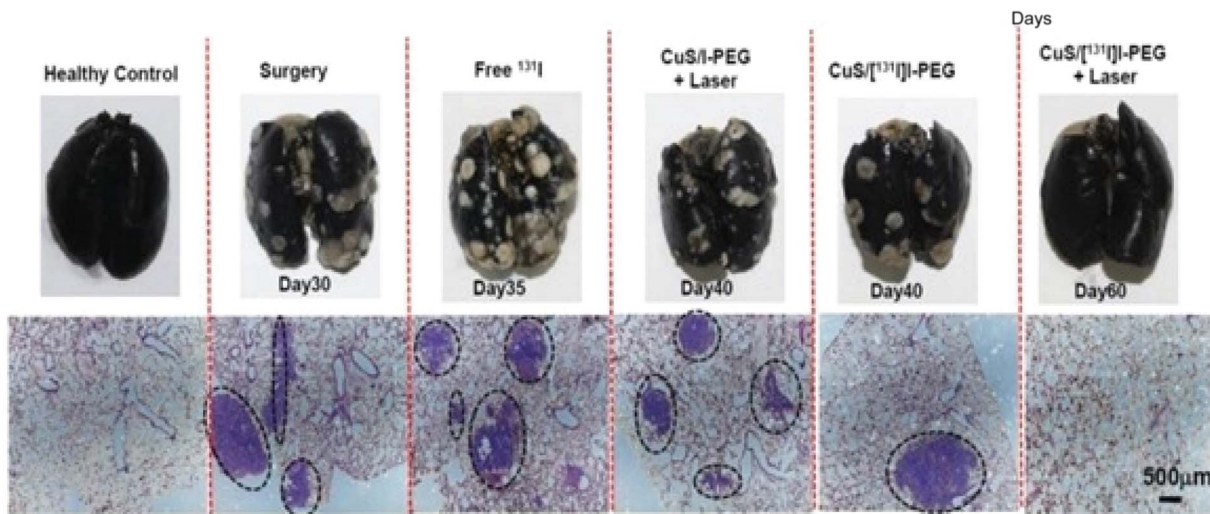


Fig. 26 Photographs of complete lungs stained with India ink and micrographs of H&E-stained lung slices from various mouse groups. Dashed circles highlight tumor metastatic locations (Yi *et al.*, 2015).<sup>315</sup>

both PTT and RT treatments at the same time, Cheng *et al.* modified FeSe<sub>2</sub>/Bi<sub>2</sub>Se<sub>3</sub> nanosheets with PEG. Important for RT and PTT, respectively, are the intrinsic properties of FeSe<sub>2</sub>/Bi<sub>2</sub>Se<sub>3</sub>-PEG, such as high NIR absorption and substantial X-ray attenuation. In addition, the composite nanostructure might be used as a contrast agent for *in vivo* computer tomography, photoacoustic (PA), positron emission tomography (PET) tetra-modal imaging, magnetic resonance (MR), and radioisotope <sup>64</sup>Cu tagging. According to a study,<sup>314</sup> FeSe<sub>2</sub>/Bi<sub>2</sub>Se<sub>3</sub>-PEG effectively killed tumors and inhibited their development. Yi *et al.* created PEG-improvised, iodine-131-doped CS (CuS/[<sup>131</sup>I]-PEG) nanomaterials for PTT and RT. This nanomaterial employed high NIR absorption for PTT, but doped <sup>131</sup>I-radioactivity in internal CT, which differed from the exterior CT used by previous two nanomaterials. Yi's research found that CuS/[<sup>131</sup>I]-PEG had excellent synergistic therapeutic effectiveness in both *in vitro* as well as in *in vivo* trials. Importantly, when combined PTT and RT are administered to lymph nodes to aid in the surgical excision of primary tumors, they can limit cancer spread and prolong animal survival Fig. 26.<sup>315</sup>

### 7.3. PTT in conjunction with immunotherapy

In comparison with gold-standard cancer therapies such as surgery, chemotherapy and radiotherapy, immunotherapy is a newer treatment that trains or stimulates the host's immune systems to eliminate tumor cells.<sup>316</sup> IT has demonstrated amazing potential, but it still has significant limitations, including expensive, immunotoxicity, and wide individual variance.<sup>314</sup> PTT-induced hyperthermia can kill cancer cells directly while also inducing the liberation of tumor-associated antigens, that are required for antigen processing and presentation. If immunotherapy and PTT are conjugated into a single therapy, IT may have a higher therapeutic efficacy against tumors due to the released antigens and immune adjuvants.<sup>317</sup> Tao *et al.* used PEG and polyethyleneimine (PEI) dual polymer-

operationalized graphene oxide (GO) as a carrier to transport CpG. GOPEG-PEI-CpG nanocomplexes have been shown to significantly increase proinflammatory cytokine production and immunostimulatory activity when exposed to NIR light. Furthermore, immunological responses are significantly boosted because GO's photothermal action promotes intracellular transport of CpG ODNs Fig. 27.<sup>318</sup>

### 7.4. PTT in conjunction with PDT

PTT and PDT are both light responsive nanomaterial-based therapies, however PTT kills cancer cells by hyperthermia, whilst PDT kills tumor cells through reactive oxygen species (ROS). Despite their distinct treatment processes, PTT and PDT share comparable light triggering circumstances. Thus, photothermal and photodynamic therapy can function separately and in tandem under identical NIR laser irradiation.<sup>319</sup> Tham *et al.* described a new nanomaterial zinc phthalocyanine (ZnPc) embedded silica-coated gold nanorods (AuNRs) for combinations of PDT and PTT. Imbedded ZnPc acts as a PDT precursor that produces singlet oxygen. AuNR is a PTT agent with LSPR, which means that hyperthermia caused by AuNRs can increase oxygenation within the tumor and blood flow, hence increasing PDT. In Tham's work, NIR light stimulated both ZnPc and AuNR, causing hyperthermia and ROS near the tumor location, resulting in synergistic PTT and PDT Fig. 28.<sup>320</sup>

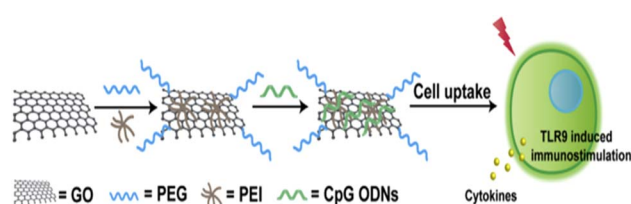


Fig. 27 Schematic depicting the production of GGIC and its immunostimulatory function (Tao *et al.*, 2014).<sup>318</sup>



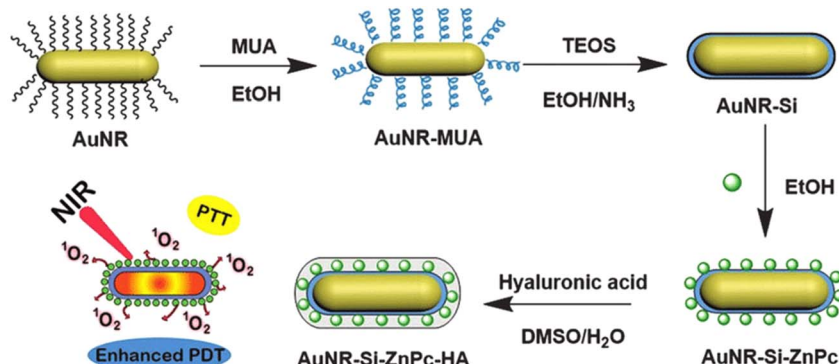


Fig. 28 Schematic representation of AuNR-Si-ZnPc-HA (Tham *et al.*, 2016).<sup>320</sup>

Kalluru *et al.* created a GO-PEG-folate nanocomposite with PTT and PDT therapeutic effects on tumors. The nanomaterial's core, GO, has inherent photothermal characteristics and can produce a singlet oxygen for PDT. *In vitro* experiments showed that PDT and PTT both caused cellular death, and *in vivo* experiments supported that the combinatorial therapy was more efficient and powerful than PDT or PTT alone.<sup>321</sup> Wang *et al.* created a multifunctional nanoplateform by covalently introduced upconversion nanoparticles (UCNPs) using nanographene oxide (NGO) and loading ZnPc on its surface. In UCNPs-NGO/ZnPc, ZnPc were employed as a PS for PDT, while UCNPs served as PTT agents for PTT. NGO then served as a carrier of ZnPc and UCNPs owing to its strong NIR absorption and huge surface area. Based on the results of this research, the combination treatment performed much better in cancer therapy.<sup>322</sup> A combinatorial therapy by synergistic work of PTT along with PDT will be advantageous for killing cancer cell with minimal side effects to healthy cells and tissues.

## 8. Barriers and challenges in clinical translation of nanomaterials for PDT and PTT

Current investigations on nanotechnology-driven photodynamic therapy (PDT) and photothermal therapy (PTT) for cancer treatment have significant limitations that prevent its clinical use. One significant constraint is that most research is limited to preclinical phases, with just a few nanomaterials progressing to human clinical trials. This disparity is mostly owing to obstacles such as possible toxicity, uncertain immunological responses, and rigorous regulatory procedures. Furthermore, the variability of tumor microenvironments is a difficulty, since these medicines frequently show uneven effectiveness across cancer kinds and stages. Another major concern is the lack of real-time monitoring tools that allow for exact management of therapeutic effects while minimizing injury to adjacent healthy tissues. Furthermore, scalability and reproducibility in nanomaterial fabrication remain a challenge, resulting in heterogeneity in performance.<sup>323,324</sup>

To address these concerns, additional extensive *in vivo* studies on long-term safety, pharmacokinetics, and

biodistribution are required. Standardizing techniques for nanomaterial fabrication and functionalization would increase repeatability and ease regulatory approval. Integrating real-time imaging tools might improve therapeutic precision, but creating patient-specific approaches could assist overcome tumor heterogeneity. Furthermore, combining PDT and PTT with other treatment methods, including as immunotherapy and chemotherapy, has the potential to improve therapeutic results and widen these techniques' clinical application.

Despite substantial advances in nanotechnology-driven photodynamic treatment (PDT) and photothermal therapy (PTT), only a few nanomaterials, including liposomal photosensitizers and gold-based nanoparticles, have made it to clinical trials. However, most nanomaterials are still in the preclinical stage due to a variety of obstacles. One major concern is their possible toxicity and long-term biocompatibility, since many nanomaterials can persist in healthy tissues, causing undesirable side effects or immunological reactions. Regulatory barriers also play an important role, with high safety and effectiveness standards that are difficult to achieve due to unpredictability in nanomaterial manufacturing and performance. Furthermore, the variability of tumor microenvironments hinders their efficacy, because different malignancies respond differently to various medicines. Another impediment is the absence of standardized testing methodologies, which makes it difficult to compare preclinical data and construct a strong case for clinical trials. Finally, exorbitant development costs and limited financing keep many promising nanomaterials from moving forward. To address these problems, more predictive preclinical models, standardized evaluation methodologies, better nanomaterial designs for increased safety, and greater coordination among researchers, industry, and regulatory authorities will be required to shorten the approval process.<sup>324,325</sup>

## 9. Conclusion

To summarize, the use of nanomaterials into photodynamic therapy (PDT) and photothermal therapy (PTT) is a potential area in cancer treatment. Nanomaterials such as gold, silver, silica, quantum dots, carbon-based nanomaterials, and



manganese dioxide nanosheets have demonstrated remarkable therapeutic efficacy in PDT and PTT by improving photosensitizer and photothermal agent targeting, stability, and bioavailability, respectively. These advancements make cancer therapy more accurate and effective, with fewer side effects.

However, there are still obstacles in improving the design of nanomaterial-based delivery vehicles for cancer treatment. One major concern is the possible toxicity of several nanoparticles, especially at high concentrations or after extended exposure, which may restrict their therapeutic utility. Furthermore, the complicated biological milieu of tumors, including hypoxia and diverse vascularization, frequently impairs the efficiency of these treatments. Furthermore, the possibility of nanomaterial degradation and the immune system's reaction to these materials are major challenges that must be addressed for their effective clinical translation.

Future methods should concentrate on creating more biocompatible and biodegradable nanomaterials, increasing the specificity and selectivity of nanoparticle distribution to tumor locations, and improving the controlled release of therapeutic chemicals. Combining PDT and PTT with other modalities, such as chemotherapy, radiation, and immunotherapy, has considerable potential for synergistic benefits, allowing for more complete cancer treatment. Furthermore, advances in nanomaterial functionalization, real-time imaging, and personalised treatment regimens will be critical to improve the overall clinical results of nanomaterial-based cancer treatments. Finally, more study into molecular interactions, nanoparticle formulation optimization, and integration with multimodal therapy will pave the way for more effective and safer cancer treatments.

## Data availability

No new data sets were generated during the study.

## Conflicts of interest

The authors declare no conflict of interests regarding the publication of this paper.

## Acknowledgements

The authors are thankful to the management of Saveetha school of engineering, SIMATS, Chennai, Tamil Nadu, India.

## References

- 1 D. W. Felsher and J. M. Bishop, Reversible tumorigenesis by MYC in hematopoietic lineages, *Mol. Cell*, 1999, **4**(2), 199–207.
- 2 P. Agostinis, K. Berg, K. A. Cengel, T. H. Foster, A. W. Girotti, S. O. Gollnick, S. M. Hahn, M. R. Hamblin, A. Juzeniene, D. Kessel and M. Korbelik, Photodynamic therapy of cancer: an update, *Ca-Cancer J. Clin.*, 2011, **61**(4), 250–281.
- 3 R. Bhole, C. Bonde, P. Kadam and R. Wavwale, A comprehensive review on photodynamic therapy (PDT) and photothermal therapy (PTT) for cancer treatment, *Turk. J. Oncol.*, 2021, **36**(1), 125.
- 4 V. I. Group1A, Verteporfin therapy of subfoveal choroidal neovascularization in age-related macular degeneration: two-year results of a randomized clinical trial including lesions with occult with no classic choroidal neovascularization—verteporfin in photodynamic therapy report 2, *Am. J. Ophthalmol.*, 2001, **131**(5), 541–560.
- 5 C. J. Gomer and N. J. Razum, Acute skin response in albino mice following porphyrin photosensitization under oxic and anoxic conditions, *Photochem. Photobiol.*, 1984, **40**(4), 435–439.
- 6 W. R. Chen, R. L. Adams, S. Heaton, D. T. Dickey, K. E. Bartels and R. E. Nordquist, Chromophore-enhanced laser-tumor tissue photothermal interaction using an 808-nm diode laser, *Cancer Lett.*, 1995, **88**(1), 15–19.
- 7 L. Zou, H. Wang, B. He, L. Zeng, T. Tan, H. Cao, X. He, Z. Zhang, S. Guo and Y. Li, Current approaches of photothermal therapy in treating cancer metastasis with nanotherapeutics, *Theranostics*, 2016, **6**(6), 762.
- 8 U. Anand, A. Dey, A. K. Chandel, R. Sanyal, A. Mishra, D. K. Pandey, V. De Falco, A. Upadhyay, R. Kandimalla and A. Chaudhary, JK Dhanjal, Cancer chemotherapy and beyond: Current status, drug candidates, associated risks and progress in targeted therapeutics, *Genes Dis.*, 2023, **10**(4), 1367–1401.
- 9 G. Mohan, A. H. TP, J. AJ, S. D. KM, A. Narayanasamy and B. Vellingiri, Recent advances in radiotherapy and its associated side effects in cancer—a review, *J. Basic Appl. Zool.*, 2019, **80**(1), 1.
- 10 S. Tan, D. Li and X. Zhu, Cancer immunotherapy: Pros, cons and beyond, *Biomed. Pharmacother.*, 2020, **124**, 109821.
- 11 B. Nasseri, E. Alizadeh, F. Bani, S. Davaran, A. Akbarzadeh, N. Rabiee, A. Bahadori, M. Ziae, M. Bagherzadeh, M. R. Saeb and M. Mozafari, Nanomaterials for photothermal and photodynamic cancer therapy, *Appl. Phys. Rev.*, 2022, **9**(1), 011317.
- 12 S. L. Li, P. Jiang, F. L. Jiang and Y. Liu, Recent advances in nanomaterial-based nanoplates for chemodynamic cancer therapy, *Adv. Funct. Mater.*, 2021, **31**(22), 2100243.
- 13 S. Liu, X. Pan and H. Liu, Two-dimensional nanomaterials for photothermal therapy, *Angew. Chem.*, 2020, **132**(15), 5943–5953.
- 14 R. A. Petros and J. M. DeSimone, Strategies in the design of nanoparticles for therapeutic applications, *Nat. Rev. Drug Discovery*, 2010, **9**(8), 615–627.
- 15 W. K. Shin, J. Cho, A. G. Kannan, Y. S. Lee and D. W. Kim, Cross-linked composite gel polymer electrolyte using mesoporous methacrylate-functionalized SiO<sub>2</sub> nanoparticles for lithium-ion polymer batteries, *Sci. Rep.*, 2016, **6**(1), 26332.
- 16 A. Prokop and J. M. Davidson, Nanovehicular intracellular delivery systems, *J. Pharm. Sci.*, 2008, **97**(9), 3518–3590.
- 17 J. K. Patel and A. P. Patel, Passive targeting of nanoparticles to cancer, *Surface Modification of Nanoparticles for Targeted Drug Delivery*, 2019, pp. 125–143.



18 Z. Chen, R. K. Kankala, L. Long, S. Xie, A. Chen and L. Zou, Current understanding of passive and active targeting nanomedicines to enhance tumor accumulation, *Coord. Chem. Rev.*, 2023, **481**, 215051.

19 R. P. Das, V. V. Gandhi, B. G. Singh and A. Kunwar, Passive and active drug targeting: role of nanocarriers in rational design of anticancer formulations, *Curr. Pharm. Des.*, 2019, **25**(28), 3034–3056.

20 B. Dutta, K. C. Barick and P. A. Hassan, Recent advances in active targeting of nanomaterials for anticancer drug delivery, *Adv. Colloid Interface Sci.*, 2021, **296**, 102509.

21 M. H. Akhter, M. Rizwanullah, J. Ahmad, M. J. Ahsan, M. A. Mujtaba and S. Amin, Nanocarriers in advanced drug targeting: setting novel paradigm in cancer therapeutics, *Artif. Cells, Nanomed., Biotechnol.*, 2018, **46**(5), 873–884.

22 M. Alavi and M. Hamidi, Passive and active targeting in cancer therapy by liposomes and lipid nanoparticles, *Drug Metab. Pers. Ther.*, 2019, **34**(1), 20180032.

23 S. M. Narum, T. Le, D. P. Le, J. C. Lee, N. D. Donahue and W. Yang, S. Wilhelm, Passive targeting in nanomedicine: fundamental concepts, body interactions, and clinical potential. In *Nanoparticles for Biomedical Applications*, Elsevier, 2020, pp. 37–53.

24 F. S. Anarjan, Active targeting drug delivery nanocarriers: Ligands, *Nano-Struct. Nano-Objects*, 2019, **19**, 100370.

25 A. K. Pearce and R. K. O'Reilly, Insights into active targeting of nanoparticles in drug delivery: advances in clinical studies and design considerations for cancer nanomedicine, *Bioconjugate Chem.*, 2019, **30**(9), 2300–2311.

26 T. D. Clemons, R. Singh, A. Sorolla, N. Chaudhari, A. Hubbard and K. S. Iyer, Distinction between active and passive targeting of nanoparticles dictate their overall therapeutic efficacy, *Langmuir*, 2018, **34**(50), 15343–15349.

27 M. F. Attia, N. Anton, J. Wallyn, Z. Omran and T. F. Vandamme, An overview of active and passive targeting strategies to improve the nanocarriers efficiency to tumour sites, *J. Pharm. Pharmacol.*, 2019, **71**(8), 1185–1198.

28 Y. Yao, Y. Zhou, L. Liu, Y. Xu, Q. Chen, Y. Wang, S. Wu, Y. Deng, J. Zhang and A. Shao, Nanoparticle-based drug delivery in cancer therapy and its role in overcoming drug resistance, *Front. Mol. Biosci.*, 2020, **7**, 193.

29 Y. Dang and J. Guan, Nanoparticle-based drug delivery systems for cancer therapy, *Smart Mater. Med.*, 2020, **1**, 10–19.

30 D. Mundekkad and W. C. Cho, Nanoparticles in clinical translation for cancer therapy, *Int. J. Mol. Sci.*, 2022, **23**(3), 1685.

31 Y. Gao, K. Wang, J. Zhang, X. Duan, Q. Sun and K. Men, Multifunctional nanoparticle for cancer therapy, *MedComm*, 2023, **4**(1), e187.

32 D. Peer, J. M. Karp, S. Hong, O. C. Farokhzad, R. Margalit and R. Langer, Nanocarriers as an emerging platform for cancer therapy, *Nano-Enabled Med. Appl.*, 2020, **23**, 61–91.

33 J. Chen, T. Fan, Z. Xie, Q. Zeng, P. Xue, T. Zheng, Y. Chen, X. Luo and H. Zhang, Advances in nanomaterials for photodynamic therapy applications: Status and challenges, *Biomaterials*, 2020, **237**, 119827.

34 Z. Yang, Z. Sun, Y. Ren, X. Chen, W. Zhang, X. Zhu, Z. Mao, J. Shen and S. Nie, Advances in nanomaterials for use in photothermal and photodynamic therapeutics, *Mol. Med. Rep.*, 2019, **20**(1), 5–15.

35 Z. Cheng, M. Li, R. Dey and Y. Chen, Nanomaterials for cancer therapy: current progress and perspectives, *J. Hematol. Oncol.*, 2021, **14**, 1–27.

36 J. Wang, X. Wu, P. Shen, J. Wang, Y. Shen, Y. Shen, T. J. Webster and J. Deng, Applications of inorganic nanomaterials in photothermal therapy based on combinational cancer treatment, *Int. J. Nanomed.*, 2020, **19**, 1903–1914.

37 G. Chen, Y. Qian, H. Zhang, A. Ullah, X. He, Z. Zhou, H. Fenniri and J. Shen, Advances in cancer theranostics using organic-inorganic hybrid nanotechnology, *Appl. Mater. Today*, 2021, **23**, 101003.

38 A. A. Ali, W. H. Abuwatfa, M. H. Al-Sayah and G. A. Husseini, Gold-nanoparticle hybrid nanostructures for multimodal cancer therapy, *Nanomaterials*, 2022, **12**(20), 3706.

39 P. G. Calavia, G. Bruce, L. Pérez-García and D. A. Russell, Photosensitiser-gold nanoparticle conjugates for photodynamic therapy of cancer, *Photochem. Photobiol. Sci.*, 2018, **17**(11), 1534–1552.

40 Y. Zheng, Z. Li, H. Chen and Y. Gao, Nanoparticle-based drug delivery systems for controllable photodynamic cancer therapy, *Eur. J. Pharm. Sci.*, 2020, **144**, 105213.

41 J. Li, J. Li, Y. Pu, S. Li, W. Gao and B. He, PDT-enhanced ferroptosis by a polymer nanoparticle with pH-activated singlet oxygen generation and superb biocompatibility for cancer therapy, *Biomacromolecules*, 2021, **22**(3), 1167–1176.

42 G. M. Calixto, J. Bernegossi, L. M. De Freitas, C. R. Fontana and M. Chorilli, Nanotechnology-based drug delivery systems for photodynamic therapy of cancer: a review, *Molecules*, 2016, **21**(3), 342.

43 M. S. Baptista, J. Cadet, P. Di Mascio, A. A. Ghogare, A. Greer, M. R. Hamblin, C. Lorente, S. C. Nunez, M. S. Ribeiro, A. H. Thomas and M. Vignoni, Type I and type II photosensitized oxidation reactions: guidelines and mechanistic pathways, *Photochem. Photobiol. Sci.*, 2017, **93**(4), 912–919.

44 U. Chitgupi, Y. Qin and J. F. Lovell, Targeted nanomaterials for phototherapy, *Nano-theranostics*, 2017, **1**(1), 38.

45 H. Barr, C. J. Tralau, P. B. Boulos, A. J. MacRobert, R. Tilly and S. G. Bown, The contrasting mechanisms of colonic collagen damage between photodynamic therapy and thermal injury, *Photochem. Photobiol.*, 1987, **46**(5), 795–800.

46 F. J. Civantos, B. Karakullukcu, M. Biel, C. E. Silver, A. Rinaldo, N. F. Saba, R. P. Takes, V. Vander Poorten and A. Ferlito, A review of photodynamic therapy for neoplasms of the head and neck, *Adv. Ther.*, 2018, **35**, 324–340.

47 V. P. Pattani, J. Shah, A. Atalis, A. Sharma and J. W. Tunnell, Role of apoptosis and necrosis in cell death induced by nanoparticle-mediated photothermal therapy, *J. Nanopart. Res.*, 2015, **17**, 1.



48 S. Stapleton, M. Dunne, M. Milosevic, C. W. Tran, M. J. Gold, A. Vedadi, T. D. McKee, P. S. Ohashi, C. Allen and D. A. Jaffray, Radiation and heat improve the delivery and efficacy of nanotherapeutics by modulating intratumoral fluid dynamics, *ACS Nano*, 2018, **12**(8), 7583–7600.

49 D. Kessel, Y. Luo, Y. Deng and C. K. Chang, The role of subcellular localization in initiation of apoptosis by photodynamic therapy, *Photochem. Photobiol.*, 1997, **65**(3), 422.

50 I. Rizvi, G. Obaid, S. Bano, T. Hasan and D. Kessel, Photodynamic therapy: Promoting in vitro efficacy of photodynamic therapy by liposomal formulations of a photosensitizing agent, *Lasers Surg. Med.*, 2018, **50**(5), 499–505.

51 H. R. Choi Kim, Y. Luo, G. Li and D. Kessel, Enhanced apoptotic response to photodynamic therapy after bcl-2 transfection, *Cancer Res.*, 1999, **59**(14), 3429–3432.

52 S. Nath, G. Obaid and T. Hasan, The course of immune stimulation by photodynamic therapy: bridging fundamentals of photochemically induced immunogenic cell death to the enrichment of T-cell repertoire, *Photochem. Photobiol.*, 2019, **95**(6), 1288–1305.

53 Y. Xiong, Y. Rao, J. Hu, Z. Luo and C. Chen, Nanoparticle-Based Photothermal Therapy for Breast Cancer Noninvasive Treatment, *Adv. Mater.*, 2023, **10**, 2305140.

54 B. Chen, Y. Xu, P. Agostinis and P. A. De Witte, Synergistic effect of photodynamic therapy with hypericin in combination with hyperthermia on loss of clonogenicity of RIF-1 cells, *Int. J. Oncol.*, 2001, **18**(6), 1279–1285.

55 L. O. Svaasand, D. R. Doiron and T. J. Dougherty, Temperature rise during photoradiation therapy of malignant tumors, *Med. Phys.*, 1983, **10**(1), 10–17.

56 Y. Zhang, X. Zhan, J. Xiong, S. Peng, W. Huang, R. Joshi, Y. Cai, Y. Liu, R. Li, K. Yuan and N. Zhou, Temperature-dependent cell death patterns induced by functionalized gold nanoparticle photothermal therapy in melanoma cells, *Sci. Rep.*, 2018, **8**(1), 8720.

57 R. Geoghegan, G. Ter Haar, K. Nightingale, L. Marks and S. Natarajan, Methods of monitoring thermal ablation of soft tissue tumors—A comprehensive review, *Med. Phys.*, 2022, **49**(2), 769–791.

58 G. Gunaydin, M. E. Gedik and S. Ayan, Photodynamic therapy—current limitations and novel approaches, *Front. Chem.*, 2021, **9**, 691697.

59 C. M. Moore, D. Pendse and M. Emberton, Photodynamic therapy for prostate cancer—a review of current status and future promise, *Nat. Clin. Pract. Urol.*, 2009, **6**(1), 18–30.

60 A. P. Castano, P. Mroz and M. R. Hamblin, Photodynamic therapy and anti-tumour immunity, *Nat. Rev. Cancer*, 2006, **6**(7), 535–545.

61 N. L. Oleinick, R. L. Morris and I. Belichenko, The role of apoptosis in response to photodynamic therapy: what, where, why, and how, *Photochem. Photobiol. Sci.*, 2002, **1**(1), 1–21.

62 B. Krammer, Vascular effects of photodynamic therapy, *Anticancer Res.*, 2001, **21**(6B), 4271–4277.

63 D. E. Dolmans, A. Kadambi, J. S. Hill, C. A. Waters, B. C. Robinson, J. P. Walker, D. Fukumura and R. K. Jain, Vascular accumulation of a novel photosensitizer, MV6401, causes selective thrombosis in tumor vessels after photodynamic therapy, *Cancer Res.*, 2002, **62**(7), 2151–2156.

64 G. Canti, A. De Simone and M. Korbelik, Photodynamic therapy and the immune system in experimental oncology, *Photochem. Photobiol. Sci.*, 2002, **1**(1), 79–80.

65 S. G. Bown, A. Z. Rogowska, D. E. Whitelaw, W. R. Lees, L. B. Lovat, P. Ripley, L. Jones, P. Wyld, A. Gillams and A. W. Hatfield, Photodynamic therapy for cancer of the pancreas, *Gut*, 2002, **50**(4), 549–557.

66 T. J. Dougherty, C. J. Gomer, B. W. Henderson, G. Jori, D. Kessel, M. Korbelik, J. Moan and Q. Peng, Photodynamic therapy, *J. Natl. Cancer Inst.*, 1998, **90**(12), 889–905.

67 T. M. Busch, E. P. Wileyto, M. J. Emanuele, F. Del Piero, L. Marconato, E. Glatstein and C. J. Koch, Photodynamic therapy creates fluence rate-dependent gradients in the intratumoral spatial distribution of oxygen, *Cancer Res.*, 2002, **62**(24), 7273–7279.

68 Q. Peng and J. M. Nesland, Effects of photodynamic therapy on tumor stroma, *Ultrastruct. Pathol.*, 2004, **28**(5–6), 333–340.

69 B. W. Henderson, S. M. Waldow, T. S. Mang, W. R. Potter, P. B. Malone and T. J. Dougherty, Tumor destruction and kinetics of tumor cell death in two experimental mouse tumors following photodynamic therapy, *Cancer Res.*, 1985, **45**(2), 572–576.

70 D. Kessel, M. G. Vicente and J. J. Reiners Jr, Initiation of apoptosis and autophagy by photodynamic therapy, *Lasers Surg. Med.*, 2006, **38**(5), 482–488.

71 J. O. Yoo and K. S. Ha, New insights into the mechanisms for photodynamic therapy-induced cancer cell death, *Int. Rev. Cell Mol. Biol.*, 2012, **295**, 139–174.

72 M. L. Agarwal, M. E. Clay, E. J. Harvey, H. H. Evans, A. R. Antunez and N. L. Oleinick, Photodynamic therapy induces rapid cell death by apoptosis in L5178Y mouse lymphoma cells, *Cancer Res.*, 1991, **51**(21), 5993–5996.

73 D. R. Mokoena, B. P. George and H. Abrahamse, Photodynamic therapy induced cell death mechanisms in breast cancer, *Int. J. Mol. Sci.*, 2021, **22**(19), 10506.

74 H. E. Yoon, M. Y. Ahn, Y. C. Kim and J. H. Yoon, Involvement of endoplasmic reticulum stress and cell death by synthesized Pa-PDT in oral squamous cell carcinoma cells, *J. Dent. Sci.*, 2022, **17**(4), 1722–1730.

75 A. F. Dos Santos, A. Inague, G. S. Arini, L. F. Terra, R. A. Wailemann, A. C. Pimentel, M. Y. Yoshinaga, R. R. Silva, D. Severino, D. R. de Almeida and V. M. Gomes, Distinct photo-oxidation-induced cell death pathways lead to selective killing of human breast cancer cells, *Cell Death Dis.*, 2020, **11**(12), 1070.

76 Y. Y. Wang, Y. K. Chen, C. S. Hu, L. Y. Xiao, W. L. Huang, T. C. Chi, K. H. Cheng, Y. M. Wang and S. S. Yuan,



MAL-PDT inhibits oral precancerous cells and lesions via autophagic cell death, *Oral Dis.*, 2019, **25**(3), 758–771.

77 Z. Sun, M. Zhao, W. Wang, L. Hong, Z. Wu, G. Luo, S. Lu, Y. Tang, J. Li, J. Wang and Y. Zhang, 5-ALA mediated photodynamic therapy with combined treatment improves anti-tumor efficacy of immunotherapy through boosting immunogenic cell death, *Cancer Lett.*, 2023, **554**, 216032.

78 J. Zhang, L. Liu, X. Li, X. Shen, G. Yang, Y. Deng, Z. Hu, J. Zhang and Y. Lu, 5-ALA-PDT induced ferroptosis in keloid fibroblasts via ROS, accompanied by downregulation of xCT, GPX4, *Photodiagn. Photodyn. Ther.*, 2023, **42**, 103612.

79 A. A. Abdelrahim, S. Hong and J. M. Song, Integrative in situ photodynamic therapy-induced cell death measurement of 3D-bioprinted MCF-7 tumor spheroids, *Anal. Chem.*, 2022, **94**(40), 13936–13943.

80 Y. Huang, Z. Xiao, Z. Guan, Y. Shen, Y. Jiang, X. Xu, Z. Huang and C. Zhao, A light-triggered self-reinforced nanoagent for targeted chemo-photodynamic therapy of breast cancer bone metastases via ER stress and mitochondria mediated apoptotic pathways, *J. Controlled Release*, 2020, **319**, 119–134.

81 D. Kessel, Photodynamic therapy: apoptosis, paraptosis and beyond, *Apoptosis*, 2020, **25**(9), 611–615.

82 G. C. Lamarque, D. A. Méndez, A. A. Matos, T. J. Dionísio, M. A. Machado, A. C. Magalhães, R. C. Oliveira and T. Cruvinel, Cytotoxic effect and apoptosis pathways activated by methylene blue-mediated photodynamic therapy in fibroblasts, *Photodiagn. Photodyn. Ther.*, 2020, **29**, 101654.

83 C. Song, W. Xu, H. Wu, X. Wang, Q. Gong, C. Liu, J. Liu and L. Zhou, Photodynamic therapy induces autophagy-mediated cell death in human colorectal cancer cells via activation of the ROS/JNK signaling pathway, *Cell Death Dis.*, 2020, **11**(10), 938.

84 F. Valli, M. C. Vior, L. P. Roguin and J. Marino, Crosstalk between oxidative stress-induced apoptotic and autophagic signaling pathways in Zn (II) phthalocyanine photodynamic therapy of melanoma, *Free Radicals Biol. Med.*, 2020, **152**, 743–754.

85 L. Ke, F. Wei, L. Xie, J. Karges, Y. Chen, L. Ji and H. Chao, A Biodegradable Iridium (III) Coordination Polymer for Enhanced Two-Photon Photodynamic Therapy Using an Apoptosis–Ferroptosis Hybrid Pathway, *Angew. Chem., Int. Ed.*, 2022, **61**(28), e202205429.

86 X. Wang, Q. Gong, C. Song, J. Fang, Y. Yang, X. Liang, X. Huang and J. Liu, Berberine-photodynamic therapy sensitizes melanoma cells to cisplatin-induced apoptosis through ROS-mediated P38 MAPK pathways, *Toxicol. Appl. Pharmacol.*, 2021, **418**, 115484.

87 B. Ortel, C. R. Shea and P. Calzavara-Pinton, Molecular mechanisms of photodynamic therapy, *Front. Biosci.*, 2009, **14**(14), 4157–4172.

88 K. Plaetzer, T. Kiesslich, C. B. Oberdanner and B. Krammer, Apoptosis following photodynamic tumor therapy: induction, mechanisms and detection, *Curr. Pharm. Des.*, 2005, **11**(9), 1151–1165.

89 T. Kaneko, H. Chiba, T. Yasuda and K. Kusama, Detection of photodynamic therapy-induced early apoptosis in human salivary gland tumor cells in vitro and in a mouse tumor model, *Oral Oncol.*, 2004, **40**(8), 787–792.

90 R. Chaloupka, T. Obšil, J. Plášek and F. Sureau, The effect of hypericin and hypocrellin-A on lipid membranes and membrane potential of 3T3 fibroblasts, *Biochim. Biophys. Acta, Biomembr.*, 1999, **1418**(1), 39–47.

91 D. Kessel and Y. Luo, Photodynamic therapy: a mitochondrial inducer of apoptosis, *Cell Death Differ.*, 1999, **6**(1), 28–35.

92 A. J. Kowaltowski, J. Turin, G. L. Indig and A. E. Vercesi, Mitochondrial effects of triarylmethane dyes, *J. Bioenerg. Biomembr.*, 1999, **31**, 581–590.

93 E. Ucar, O. Seven, D. Lee, G. Kim, J. Yoon and E. U. Akkaya, Selectivity in photodynamic action: higher activity of mitochondria targeting photosensitizers in cancer cells, *ChemPhotoChem*, 2019, **3**(3), 129–132.

94 R. Wang, X. Li and J. Yoon, Organelle-targeted photosensitizers for precision photodynamic therapy, *ACS Appl. Mater. Interfaces*, 2021, **13**(17), 19543–19571.

95 I. F. Mariz, S. N. Pinto, A. M. Santiago, J. M. Martinho, J. Recio, J. J. Vaquero, A. M. Cuadro and E. Maçôas, Two-photon activated precision molecular photosensitizer targeting mitochondria, *Commun. Chem.*, 2021, **4**(1), 142.

96 M. Yang, J. Deng, D. Guo, Q. Sun, Z. Wang, K. Wang and F. Wu, Mitochondria-targeting Pt/Mn porphyrins as efficient photosensitizers for magnetic resonance imaging and photodynamic therapy, *Dyes Pigm.*, 2019, **166**, 189–195.

97 Y. Ni, H. Zhang, C. Chai, B. Peng, A. Zhao, J. Zhang, L. Li, C. Zhang, B. Ma, H. Bai and K. L. Lim, Mitochondria-Targeted Two-Photon Fluorescent Photosensitizers for Cancer Cell Apoptosis via Spatial Selectability, *Adv. Healthcare Mater.*, 2019, **8**(14), 1900212.

98 B. Wang, H. Zhou, L. Chen, Y. Ding, X. Zhang, H. Chen, H. Liu, P. Li, Y. Chen, C. Yin and Q. Fan, A Mitochondria-Targeted Photosensitizer for Combined Pyroptosis and Apoptosis with NIR-II Imaging/Photoacoustic Imaging-Guided Phototherapy, *Angew. Chem., Int. Ed.*, 2024, **23**, e202408874.

99 X. Zhao, Y. Huang, G. Yuan, K. Zuo, Y. Huang, J. Chen, J. Li and J. Xue, A novel tumor and mitochondria dual-targeted photosensitizer showing ultra-efficient photodynamic anticancer activities, *Chem. Commun.*, 2019, **55**(6), 866–869.

100 D. J. Granville, C. M. Carthy, H. Jiang, J. G. Levy, B. M. McManus, J. Y. Matroule, J. Piette and D. W. Hunt, Nuclear factor- $\kappa$ B activation by the photochemotherapeutic agent verteporfin, *Blood*, 2000, **95**(1), 256–262.

101 L. Y. Xue, S. M. Chiu and N. L. Oleinick, Photodynamic therapy-induced death of MCF-7 human breast cancer cells: a role for caspase-3 in the late steps of apoptosis but not for the critical lethal event, *Exp. Cell Res.*, 2001, **263**(1), 145–155.



102 D. J. Granville, J. G. Levy and D. W. Hunt, Photodynamic therapy induces caspase-3 activation in HL-60 cells, *Cell Death Differ.*, 1997, **4**(7), 623–628.

103 A. C. Moor, Signaling pathways in cell death and survival after photodynamic therapy, *J. Photochem. Photobiol. B*, 2000, **57**(1), 1–3.

104 M. Korbelik and G. Krosł, Cellular levels of photosensitisers in tumours: the role of proximity to the blood supply, *Br. J. Cancer*, 1994, **70**(4), 604–610.

105 B. J. Tromberg, A. Orenstein, S. Kimel, S. J. Barker, J. Hyatt, J. S. Nelson and M. W. Berns, In vivo tumor oxygen tension measurements for the evaluation of the efficiency of photodynamic therapy, *Photochem. Photobiol.*, 1990, **52**(2), 375–385.

106 B. W. Pogue, R. D. Braun, J. L. Lanzen, C. Erickson and M. W. Dewhirst, Analysis of the Heterogeneity of pO<sub>2</sub> Dynamics During Photodynamic Therapy with Verteporfin, *Photochem. Photobiol.*, 2001, **74**(5), 700–706.

107 I. S. Turan, D. Yıldız, A. Turksoy, G. Gunaydin and E. U. Akkaya, A bifunctional photosensitizer for enhanced fractional photodynamic therapy: singlet oxygen generation in the presence and absence of light, *Angew. Chem., Int. Ed.*, 2016, **55**(8), 2875–2878.

108 R. K. Jain and T. Stylianopoulos, Delivering nanomedicine to solid tumors, *Nat. Rev. Clin. Oncol.*, 2010, **7**(11), 653–664.

109 S. J. Martin, C. M. Henry and S. P. Cullen, A perspective on mammalian caspases as positive and negative regulators of inflammation, *Mol. Cell*, 2012, **46**(4), 387–397.

110 J. L. Li and M. Gu, Surface plasmonic gold nanorods for enhanced two-photon microscopic imaging and apoptosis induction of cancer cells, *Biomaterials*, 2010, **31**(36), 9492–9498.

111 M. Pérez-Hernández, P. Del Pino, S. G. Mitchell, M. Moros, G. Stepien, B. Pelaz, W. J. Parak, E. M. Galvez, J. Pardo and J. M. de la Fuente, Dissecting the molecular mechanism of apoptosis during photothermal therapy using gold nanoprisms, *ACS Nano*, 2015, **9**(1), 52–61.

112 T. Cirman, K. Oresić, G. D. Mazovec, V. Turk, J. C. Reed, R. M. Myers, G. S. Salvesen and B. Turk, Selective disruption of lysosomes in HeLa cells triggers apoptosis mediated by cleavage of Bid by multiple papain-like lysosomal cathepsins, *J. Biol. Chem.*, 2004, **279**(5), 3578–3587.

113 J. M. Stern, V. V. Kabanov Solomonov, E. Sazykina, J. A. Schwartz, S. C. Gad and G. P. Goodrich, Initial evaluation of the safety of nanoshell-directed photothermal therapy in the treatment of prostate disease, *Int. J. Toxicol.*, 2016, **35**(1), 38–46.

114 G. Alfranca and D. Cui, The true complexity of photothermal therapy: A brief perspective, *Nano Biomed. Eng.*, 2017, **9**(2), 129–134.

115 C. Ayala-Orozco, C. Urban, M. W. Knight, A. S. Urban, O. Neumann, S. W. Bishnoi, S. Mukherjee, A. M. Goodman, H. Charron, T. Mitchell and M. Shea, Au nanomtryoshkas as efficient near-infrared photothermal transducers for cancer treatment: benchmarking against nanoshells, *ACS Nano*, 2014, **8**(6), 6372–6381.

116 L. O. Svaasand, C. J. Gomer and E. Morinelli, On the physical rationale of laser induced hyperthermia, *Lasers Med. Sci.*, 1990, **5**, 121–128.

117 V. P. Nguyen, S. W. Kim, H. Kim, H. Kim, K. H. Seok, M. J. Jung, Y. C. Ahn and H. W. Kang, Biocompatible astaxanthin as a novel marine-oriented agent for dual chemo-photothermal therapy, *PLoS one*, 2017, **12**(4), e0174687.

118 Z. Qin and J. C. Bischof, Thermophysical and biological responses of gold nanoparticle laser heating, *Chem. Soc. Rev.*, 2012, **41**(3), 1191–1217.

119 B. E. Smith, P. B. Roder, X. Zhou and P. J. Pauzauskie, Nanoscale materials for hyperthermal theranostics, *Nanoscale*, 2015, **7**(16), 7115–7126.

120 M. Pérez-Hernández, Mechanisms of cell death induced by optical hyperthermia, In *Nanomaterials for Magnetic and Optical Hyperthermia Applications*, Elsevier, 2019, pp. 201–228.

121 S. Lal, S. E. Clare and N. J. Halas, Nanoshell-enabled photothermal cancer therapy: impending clinical impact, *Acc. Chem. Res.*, 2008, **41**(12), 1842–1851.

122 M. Aioub, S. R. Panikkanvalappil and M. A. El-Sayed, Platinum-coated gold nanorods: efficient reactive oxygen scavengers that prevent oxidative damage toward healthy, untreated cells during plasmonic photothermal therapy, *ACS Nano*, 2017, **11**(1), 579–586.

123 L. Minai, D. Yeheskely-Hayon and D. Yelin, High levels of reactive oxygen species in gold nanoparticle-targeted cancer cells following femtosecond pulse irradiation, *Sci. Rep.*, 2013, **3**(1), 2146.

124 M. R. Ali, Y. Wu, T. Han, X. Zang, H. Xiao, Y. Tang, R. Wu, F. M. Fernández and M. A. El-Sayed, Simultaneous time-dependent surface-enhanced Raman spectroscopy, metabolomics, and proteomics reveal cancer cell death mechanisms associated with gold nanorod photothermal therapy, *J. Am. Chem. Soc.*, 2016, **138**(47), 15434–15442.

125 J. J. Li, D. Hartono, C. N. Ong, B. H. Bay and L. Y. Yung, Autophagy and oxidative stress associated with gold nanoparticles, *Biomaterials*, 2010, **31**(23), 5996–6003.

126 X. Ma, Y. Wu, S. Jin, Y. Tian, X. Zhang, Y. Zhao, L. Yu and X. J. Liang, Gold nanoparticles induce autophagosome accumulation through size-dependent nanoparticle uptake and lysosome impairment, *ACS Nano*, 2011, **5**(11), 8629–8639.

127 Z. Zhou, Y. Yan, K. Hu, Y. Zou, Y. Li, R. Ma, Q. Zhang and Y. Cheng, Autophagy inhibition enabled efficient photothermal therapy at a mild temperature, *Biomaterials*, 2017, **141**, 116–124.

128 V. L. Crotzer and J. S. Blum, Autophagy and adaptive immunity, *Immunology*, 2010, **131**(1), 9–17.

129 D. M. Katschinski, On heat and cells and proteins, *Physiology*, 2004, **19**(1), 11–15.

130 J. W. Fisher, S. Sarkar, C. F. Buchanan, C. S. Szot, J. Whitney, H. C. Hatcher, S. V. Torti, C. G. Rylander and M. N. Rylander, Photothermal response of human and murine cancer cells to multiwalled carbon nanotubes after laser irradiation, *Cancer Res.*, 2010, **70**(23), 9855–9864.



131 S. K. Calderwood, M. A. Khaleque, D. B. Sawyer and D. R. Ciocca, Heat shock proteins in cancer: chaperones of tumorigenesis, *Trends Biochem. Sci.*, 2006, **31**(3), 164–172.

132 X. F. Huang, W. Ren, L. Rollins, P. Pittman, M. Shah, L. Shen, Q. Gu, R. Strube, F. Hu, S. Y. Chen and A. broadly applicable, personalized heat shock protein-mediated oncolytic tumor vaccine, *Cancer Res.*, 2003, **63**(21), 7321–7329.

133 K. F. Chu and D. E. Dupuy, Thermal ablation of tumours: biological mechanisms and advances in therapy, *Nat. Rev. Cancer*, 2014, **14**(3), 199–208.

134 Q. Chen, L. Xu, C. Liang, C. Wang, R. Peng and Z. Liu, Photothermal therapy with immune-adjuvant nanoparticles together with checkpoint blockade for effective cancer immunotherapy, *Nat. Commun.*, 2016, **7**(1), 13193.

135 S. Basu, R. J. Binder, R. Suto, K. M. Anderson and P. K. Srivastava, Necrotic but not apoptotic cell death releases heat shock proteins, which deliver a partial maturation signal to dendritic cells and activate the NF- $\kappa$ B pathway, *Int. Immunol.*, 2000, **12**(11), 1539–1546.

136 M. Wei, N. Chen, J. Li, M. Yin, L. Liang, Y. He, H. Song, C. Fan and Q. Huang, Polyvalent immunostimulatory nanoagents with self-assembled CpG oligonucleotide-conjugated gold nanoparticles, *Angew. Chem.*, 2012, **5**(124), 1228–1232.

137 L. A. Dykman and N. G. Khlebtsov, Immunological properties of gold nanoparticles, *Chem. Sci.*, 2017, **8**(3), 1719–1735.

138 M. A. Curran, W. Montalvo, H. Yagita and J. P. Allison, PD-1 and CTLA-4 combination blockade expands infiltrating T cells and reduces regulatory T and myeloid cells within B16 melanoma tumors, *Proc. Natl. Acad. Sci. U. S. A.*, 2010, **107**(9), 4275–4280.

139 J. Fornalski, Photodynamic therapy mechanism of action and adhibition in dermatology, *Nowa Medycyna*, 2006, 71–74.

140 R. R. Allison and C. H. Sibata, Oncologic photodynamic therapy photosensitizers: a clinical review, *Photodiagn. Photodyn. Ther.*, 2010, **7**(2), 61–75.

141 A. F. Taub, Photodynamic therapy in dermatology: history and horizons, *J. Drugs Dermatol.*, 2004, **3**(1 Suppl), S8–S25.

142 M. H. Gold, History of photodynamic therapy. In *Photodynamic Therapy in Dermatology*, Springer New York, New York, NY, 2011, pp. 1–4.

143 H. Abrahamse and M. R. Hamblin, New photosensitizers for photodynamic therapy, *Biochem. J.*, 2016, **473**(4), 347–364.

144 D. K. Chatterjee, L. S. Fong and Y. Zhang, Nanoparticles in photodynamic therapy: an emerging paradigm, *Adv. Drug Delivery Rev.*, 2008, **60**(15), 1627–1637.

145 S. Kwiatkowski, B. Knap, D. Przystupski, J. Saczko, E. Kędzierska, K. Knap-Czop, J. Kotlińska, O. Michel, K. Kotowski and J. Kulbacka, Photodynamic therapy-mechanisms, photosensitizers and combinations, *Biomed. Pharmacother.*, 2018, **106**, 1098–1107.

146 I. Yoon, J. Z. Li and Y. K. Shim, Advance in photosensitizers and light delivery for photodynamic therapy, *Clin. Endosc.*, 2013, **46**(1), 7–23.

147 C. A. Morton, The emerging role of 5-ALA-PDT in dermatology: is PDT superior to standard treatments?, *J. Dermatol. Treat.*, 2002, **13**(sup1), s25–s29.

148 A. Nowak-Stepniowska, P. Pergoł and A. Padzik-Graczyk, Photodynamic method of cancer diagnosis and therapy-mechanisms and applications, *Postepy Biochem.*, 2013, **59**(1), 53–63.

149 L. B. Josefson and R. W. Boyle, Photodynamic therapy: novel third-generation photosensitizers one step closer?, *Br. J. Pharmacol.*, 2008, **154**(1), 1–3.

150 P. P. Lee, P. C. Lo, E. Y. Chan, W. P. Fong, W. H. Ko and D. K. Ng, Synthesis and in vitro photodynamic activity of novel galactose-containing phthalocyanines, *Tetrahedron Lett.*, 2005, **46**(9), 1551–1554.

151 H. Kataoka, H. Nishie, N. Hayashi, M. Tanaka, A. Nomoto, S. Yano and T. Joh, New photodynamic therapy with next-generation photosensitizers, *Ann. Transl. Med.*, 2017, **5**(8).

152 M. R. Hamblin, L. Y. Chiang, S. Lakshmanan, Y. Y. Huang, M. Garcia-Diaz, M. Karimi, A. N. de Souza Rastelli and R. Chandran, Nanotechnology for photodynamic therapy: A perspective from the laboratory of Dr Michael R. Hamblin in the Wellman Center for Photomedicine at Massachusetts General Hospital and Harvard Medical School, *Nanotechnol. Rev.*, 2015, **4**(4), 359–372.

153 J. Krajczewski, K. Rucińska, H. E. Townley and A. Kudelski, Role of various nanoparticles in photodynamic therapy and detection methods of singlet oxygen, *Photodiagn. Photodyn. Ther.*, 2019, **26**, 162–178.

154 T. Kato, C. S. Jin, H. Ujiie, D. Lee, K. Fujino, H. Wada, H. P. Hu, R. A. Weersink, J. Chen, M. Kaji and K. Kaga, Nanoparticle targeted folate receptor 1-enhanced photodynamic therapy for lung cancer, *Lung Cancer*, 2017, **113**, 59–68.

155 W. H. Tsai, K. H. Yu, Y. C. Huang and C. I. Lee, EGFR-targeted photodynamic therapy by curcumin-encapsulated chitosan/TPP nanoparticles, *Int. J. Nanomed.*, 2018, **9**, 903–916.

156 S. Wang, R. Gao, F. Zhou and M. Selke, Nanomaterials and singlet oxygen photosensitizers: potential applications in photodynamic therapy, *J. Mater. Chem.*, 2004, **14**(4), 487–493.

157 S. S. Lucky, K. C. Soo and Y. Zhang, Nanoparticles in photodynamic therapy, *Chem. Rev.*, 2015, **115**(4), 1990–2042.

158 C. J. Ackerson, P. D. Jazdzinsky and R. D. Kornberg, Thiolate ligands for synthesis of water-soluble gold clusters, *J. Am. Chem. Soc.*, 2005, **127**(18), 6550–6551.

159 P. Ghosh, G. Han, M. De, C. K. Kim and V. M. Rotello, Gold nanoparticles in delivery applications, *Adv. Drug Delivery Rev.*, 2008, **60**(11), 1307–1315.

160 R. Vankayala, Y. K. Huang, P. Kalluru, C. S. Chiang and K. C. Hwang, First demonstration of gold nanorods-mediated photodynamic therapeutic



destruction of tumors via near infra-red light activation, *Small*, 2014, **10**(8), 1612–1622.

161 G. Pasparakis, Light-induced generation of singlet oxygen by naked gold nanoparticles and its implications to cancer cell phototherapy, *Small*, 2013, **9**(24), 4130–4134.

162 C. Jiang, T. Zhao, P. Yuan, N. Gao, Y. Pan, Z. Guan, N. Zhou and Q. H. Xu, Two-photon induced photoluminescence and singlet oxygen generation from aggregated gold nanoparticles, *ACS Appl. Mater. Interfaces*, 2013, **5**(11), 4972–4977.

163 R. Vankayala, C. L. Kuo, A. Sagadevan, P. H. Chen, C. S. Chiang and K. C. Hwang, Morphology dependent photosensitization and formation of singlet oxygen ( $1\Delta g$ ) by gold and silver nanoparticles and its application in cancer treatment, *J. Mater. Chem. B*, 2013, **1**(35), 4379–4387.

164 A. Sharma, A. K. Goyal and G. Rath, Recent advances in metal nanoparticles in cancer therapy, *J. Drug Targeting*, 2018, **26**(8), 617–632.

165 P. G. Mahajan, N. C. Dige, B. D. Vanjare, S. H. Eo, S. Y. Seo, S. J. Kim, S. K. Hong, C. S. Choi and K. H. Lee, A potential mediator for photodynamic therapy based on silver nanoparticles functionalized with porphyrin, *J. Photochem. Photobiol. A*, 2019, **377**, 26–35.

166 P. Khoza, I. Ndhundhuma, A. Karsten and T. Nyokong, Photodynamic therapy activity of phthalocyanine-silver nanoparticles on melanoma cancer cells, *J. Nanosci. Nanotechnol.*, 2020, **20**(5), 3097–3104.

167 H. Montaseri, N. W. Nkune and H. Abrahamse, Active targeted photodynamic therapeutic effect of silver-based nanohybrids on melanoma cancer cells, *J. Photochem. Photobiol.*, 2022, **11**, 100136.

168 F. Yan and R. Kopelman, The Embedding of Meta-tetra (Hydroxyphenyl)-Chlorin into Silica Nanoparticle Platforms for Photodynamic Therapy and Their Singlet Oxygen Production and pH-dependent Optical Properties, *Photochem. Photobiol.*, 2003, **78**(6), 587–591.

169 J. Lin, S. Wang, P. Huang, Z. Wang, S. Chen, G. Niu, W. Li, J. He, D. Cui, G. Lu and X. Chen, Photosensitizer-loaded gold vesicles with strong plasmonic coupling effect for imaging-guided photothermal/photodynamic therapy, *ACS Nano*, 2013, **7**(6), 5320–5329.

170 T. Y. Ohulchanskyy, I. Roy, L. N. Goswami, Y. Chen, E. J. Bergey, R. K. Pandey, A. R. Oseroff and P. N. Prasad, Organically modified silica nanoparticles with covalently incorporated photosensitizer for photodynamic therapy of cancer, *Nano Lett.*, 2007, **7**(9), 2835–2842.

171 Y. Piao, A. Burns, J. Kim, U. Wiesner and T. Hyeon, Designed fabrication of silica-based nanostructured particle systems for nanomedicine applications, *Adv. Funct. Mater.*, 2008, **18**(23), 3745–3758.

172 P. Couleaud, V. Morosini, C. Frochot, S. Richeter, L. Raehm and J. O. Durand, Silica-based nanoparticles for photodynamic therapy applications, *Nanoscale*, 2010, **2**(7), 1083–1095.

173 D. S. Nady, A. Hassan, M. U. Amin, U. Bakowsky and S. A. Fahmy, Recent Innovations of Mesoporous Silica Nanoparticles Combined with Photodynamic Therapy for Improving Cancer Treatment, *Pharmaceutics*, 2023, **16**(1), 14.

174 S. Bayir, A. Barras, R. Boukherroub, S. Szunerits, L. Raehm, S. Richeter and J. O. Durand, Mesoporous silica nanoparticles in recent photodynamic therapy applications, *Photochem. Photobiol. Sci.*, 2018, **17**, 1651–1674.

175 M. Gary-Bobo, O. Hocine, D. Brevet, M. Maynadier, L. Raehm, S. Richeter, V. Charasson, B. Loock, A. Morère, P. Maillard and M. Garcia, Cancer therapy improvement with mesoporous silica nanoparticles combining targeting, drug delivery and PDT, *Int. J. Pharm.*, 2012, **423**(2), 509–515.

176 S. Li, Y. Zhang, X. W. He, W. Y. Li and Y. K. Zhang, Multifunctional mesoporous silica nanoplatform based on silicon nanoparticles for targeted two-photon-excited fluorescence imaging-guided chemo/photodynamic synergistic therapy in vitro, *Talanta*, 2020, **209**, 120552.

177 X. Lin, M. Wu, M. Li, Z. Cai, H. Sun, X. Tan, J. Li, Y. Zeng, X. Liu and J. Liu, Photo-responsive hollow silica nanoparticles for light-triggered genetic and photodynamic synergistic therapy, *Acta Biomater.*, 2018, **76**, 178–192.

178 D. Aggar, C. M. Jimenez, S. Dib, J. G. Croissant, L. Lichon, D. Laurencin, S. Richeter, M. Maynadier, S. K. Alsaiari, M. Bouafat and L. Raehm, Gemcitabine delivery and photodynamic therapy in cancer cells via porphyrin-ethylene-based periodic mesoporous organosilica nanoparticles, *ChemNanoMat*, 2018, **4**(1), 46–51.

179 Ö. Er, S. G. Colak, K. Ocakoglu, M. Ince, R. Bresolí-Obach, M. Mora, M. L. Sagristá, F. Yurt and S. Nonell, Selective photokilling of human pancreatic cancer cells using cetuximab-targeted mesoporous silica nanoparticles for delivery of zinc phthalocyanine, *Molecules*, 2018, **23**(11), 2749.

180 Q. Sun, Q. You, X. Pang, X. Tan, J. Wang, L. Liu, F. Guo, F. Tan and N. Li, A photoresponsive and rod-shape nanocarrier: Single wavelength of light triggered photothermal and photodynamic therapy based on AuNRs-capped & Ce6-doped mesoporous silica nanorods, *Biomaterials*, 2017, **122**, 188–200.

181 Y. Zhou, C. Chang, Z. Liu, Q. Zhao, Q. Xu, C. Li, Y. Chen, Y. Zhang and B. Lu, Hyaluronic acid-functionalized hollow mesoporous silica nanoparticles as pH-sensitive nanocarriers for cancer chemo-photodynamic therapy, *Langmuir*, 2021, **37**(8), 2619–2628.

182 D. Zhou, J. D. Piper, C. Abell, D. Klenerman, D. J. Kang and L. Ying, Fluorescence resonance energy transfer between a quantum dot donor and a dye acceptor attached to DNA, *Chem. Commun.*, 2005, (38), 4807–4809.

183 A. C. Samia, S. Dayal and C. Burda, Quantum dot-based energy transfer: perspectives and potential for applications in photodynamic therapy, *Photochem. Photobiol.*, 2006, **82**(3), 617–625.

184 A. R. Clapp, T. Pons, I. L. Medintz, J. B. Delehanty, J. S. Melinger, T. Tiefenbrunn, P. E. Dawson, B. R. Fisher,



B. O'Rourke and H. Mattoussi, Two-photon excitation of quantum-dot-based fluorescence resonance energy transfer and its applications, *Adv. Mater.*, 2007, **19**(15), 1921–1926.

185 Z. D. Qi, D. W. Li, P. Jiang, F. L. Jiang, Y. S. Li, Y. Liu, W. K. Wong and K. W. Cheah, Biocompatible CdSe quantum dot-based photosensitizer under two-photon excitation for photodynamic therapy, *J. Mater. Chem.*, 2011, **21**(8), 2455–2458.

186 Y. Shen, Y. Sun, R. Yan, E. Chen, H. Wang, D. Ye, J. J. Xu and H. Y. Chen, Rational engineering of semiconductor QDs enabling remarkable  $1\text{O}_2$  production for tumor-targeted photodynamic therapy, *Biomaterials*, 2017, **148**, 31–40.

187 G. Murali, B. Kwon, H. Kang, J. K. Modigunta, S. Park, S. Lee, H. Lee, Y. H. Park, J. Kim, S. Y. Park and Y. J. Kim, Hematoporphyrin photosensitizer-linked carbon quantum dots for photodynamic therapy of cancer cells, *ACS Appl. Nano Mater.*, 2022, **5**(3), 4376–4385.

188 Q. Zeng, D. Shao, X. He, Z. Ren, W. Ji, C. Shan, S. Qu, J. Li, L. Chen and Q. Li, Carbon dots as a trackable drug delivery carrier for localized cancer therapy *in vivo*, *J. Mater. Chem. B*, 2016, **4**(30), 5119–5126.

189 A. Alaghmandfar, O. Sedighi, N. T. Rezaei, A. A. Abedini, A. M. Khachatourian, M. S. Toprak and A. Seifalian, Recent advances in the modification of carbon-based quantum dots for biomedical applications, *Mater. Sci. Eng. C*, 2021, **120**, 111756.

190 J. Saleem, L. Wang and C. Chen, Carbon-based nanomaterials for cancer therapy via targeting tumor microenvironment, *Adv. Healthcare Mater.*, 2018, **7**(20), 1800525.

191 T. Murakami, H. Nakatsuji, M. Inada, Y. Matoba, T. Umeyama, M. Tsujimoto, S. Isoda, M. Hashida and H. Imahori, Photodynamic and photothermal effects of semiconducting and metallic-enriched single-walled carbon nanotubes, *J. Am. Chem. Soc.*, 2012, **134**(43), 17862–17865.

192 L. Wang, J. Shi, R. Liu, Y. Liu, J. Zhang, X. Yu, J. Gao, C. Zhang and Z. Zhang, Photodynamic effect of functionalized single-walled carbon nanotubes: a potential sensitizer for photodynamic therapy, *Nanoscale*, 2014, **6**(9), 4642–4651.

193 M. Zhang, W. Wang, Y. Cui, X. Chu, B. Sun, N. Zhou and J. Shen, Magnetofluorescent  $\text{Fe}_3\text{O}_4$ /carbon quantum dots coated single-walled carbon nanotubes as dual-modal targeted imaging and chemo/photodynamic/photothermal triple-modal therapeutic agents, *Chem. Eng. J.*, 2018, **338**, 526–538.

194 Z. Li, F. L. Zhang, L. L. Pan, X. L. Zhu and Z. Z. Zhang, Preparation and characterization of injectable Mitoxantrone poly (lactic acid)/fullerene implants for *in vivo* chemo-photodynamic therapy, *J. Photochem. Photobiol. B*, 2015, **149**, 51–57.

195 C. M. Lin and T. Y. Lu, C60 fullerene derivatized nanoparticles and their application to therapeutics, *Recent Pat. Nanotechnol.*, 2012, **6**(2), 105–113.

196 Q. Li, L. Hong, H. Li and C. Liu, Graphene oxide-fullerene C60 (GO-C60) hybrid for photodynamic and photothermal therapy triggered by near-infrared light, *Biosens. Bioelectron.*, 2017, **89**, 477–482.

197 Y. W. Chen, Y. L. Su, S. H. Hu and S. Y. Chen, Functionalized graphene nanocomposites for enhancing photothermal therapy in tumor treatment, *Adv. Drug Delivery Rev.*, 2016, **105**, 190–204.

198 J. Ge, M. Lan, B. Zhou, W. Liu, L. Guo, H. Wang, Q. Jia, G. Niu, X. Huang, H. Zhou and X. Meng, A graphene quantum dot photodynamic therapy agent with high singlet oxygen generation, *Nat. Commun.*, 2014, **5**(1), 4596.

199 W. S. Kuo, Y. T. Shao, K. S. Huang, T. M. Chou and C. H. Yang, Antimicrobial amino-functionalized nitrogen-doped graphene quantum dots for eliminating multidrug-resistant species in dual-modality photodynamic therapy and bioimaging under two-photon excitation, *ACS Appl. Mater. Interfaces*, 2018, **10**(17), 14438–14446.

200 Y. Ding, L. Zhou, X. Chen, Q. Wu, Z. Song, S. Wei, J. Zhou and J. Shen, Mutual sensitization mechanism and self-degradation property of drug delivery system for *in vitro* photodynamic therapy, *Int. J. Pharm.*, 2016, **498**(1–2), 335–346.

201 D. Y. Zhang, Y. Zheng, C. P. Tan, J. H. Sun, W. Zhang, L. N. Ji and Z. W. Mao, Graphene oxide decorated with Ru (II)-polyethylene glycol complex for lysosome-targeted imaging and photodynamic/photothermal therapy, *ACS Appl. Mater. Interfaces*, 2017, **9**(8), 6761–6771.

202 Y. Su, N. Wang, B. Liu, Y. Du, R. Li, Y. Meng, Y. Feng, Z. Shan and S. Meng, A phototheranostic nanoparticle for cancer therapy fabricated by BODIPY and graphene to realize photo-chemo synergistic therapy and fluorescence/photothermal imaging, *Dyes Pigm.*, 2020, **177**, 108262.

203 H. L. Cheng, H. L. Guo, A. J. Xie, Y. H. Shen and M. Z. Zhu, 4-in-1  $\text{Fe}_3\text{O}_4/\text{g-C}_3\text{N}_4$ @PPy-DOX nanocomposites: magnetic targeting guided trimode combinatorial chemotherapy/PDT/PTT for cancer, *J. Inorg. Biochem.*, 2021, **215**, 111329.

204 X. Qin, H. Zhang, Z. Wang and Y. Jin, Magnetic chitosan/graphene oxide composite loaded with novel photosensitizer for enhanced photodynamic therapy, *RSC Adv.*, 2018, **8**(19), 10376–10388.

205 C. Murugan, V. Sharma, R. K. Murugan, G. Malaimedu and A. Sundaramurthy, Two-dimensional cancer theranostic nanomaterials: Synthesis, surface functionalization and applications in photothermal therapy, *J. Controlled Release*, 2019, **299**, 1–20.

206 T. Fan, Z. Xie, W. Huang, Z. Li and H. Zhang, Two-dimensional non-layered selenium nanoflakes: facile fabrications and applications for self-powered photodetector, *Nanotechnology*, 2019, **30**(11), 114002.

207 J. N. Liu, W. Bu and J. Shi, Chemical design and synthesis of functionalized probes for imaging and treating tumor hypoxia, *Chem. Rev.*, 2017, **117**(9), 6160–6224.

208 Y. Chen, D. Ye, M. Wu, H. Chen, L. Zhang, J. Shi and L. Wang, Break-up of two-dimensional  $\text{MnO}_2$  nanosheets



promotes ultrasensitive pH-triggered theranostics of cancer, *Adv. Mater.*, 2014, **26**(41), 7019–7026.

209 Y. Chen, H. Chen, S. Zhang, F. Chen, S. Sun, Q. He, M. Ma, X. Wang, H. Wu, L. Zhang and L. Zhang, Structure-property relationships in manganese oxide-mesoporous silica nanoparticles used for T1-weighted MRI and simultaneous anti-cancer drug delivery, *Biomaterials*, 2012, **33**(7), 2388–2398.

210 H. Fan, G. Yan, Z. Zhao, X. Hu, W. Zhang, H. Liu, X. Fu, T. Fu, X. B. Zhang and W. Tan, A smart photosensitizer-manganese dioxide nanosystem for enhanced photodynamic therapy by reducing glutathione levels in cancer cells, *Angew. Chem., Int. Ed.*, 2016, **55**(18), 5477–5482.

211 D. Zeng, L. Wang, L. Tian, S. Zhao, X. Zhang and H. Li, Synergistic photothermal/photodynamic suppression of prostatic carcinoma by targeted biodegradable MnO<sub>2</sub> nanosheets, *Drug Delivery*, 2019, **26**(1), 661–672.

212 H. Chen, T. Liu, Z. Su, L. Shang and G. Wei, 2D transition metal dichalcogenide nanosheets for photo/thermo-based tumor imaging and therapy, *Nanoscale Horiz.*, 2018, **3**(2), 74–89.

213 T. Liu, C. Wang, W. Cui, H. Gong, C. Liang, X. Shi, Z. Li, B. Sun and Z. Liu, Combined photothermal and photodynamic therapy delivered by PEGylated MoS<sub>2</sub> nanosheets, *Nanoscale*, 2014, **6**(19), 11219–11225.

214 S. Kapri and S. Bhattacharyya, Molybdenum sulfide-reduced graphene oxide p–n heterojunction nanosheets with anchored oxygen generating manganese dioxide nanoparticles for enhanced photodynamic therapy, *Chem. Sci.*, 2018, **9**(48), 8982–8989.

215 L. S. Lin, Z. X. Cong, J. Li, K. M. Ke, S. S. Guo, H. H. Yang and G. N. Chen, Graphitic-phase C 3 N 4 nanosheets as efficient photosensitizers and pH-responsive drug nanocarriers for cancer imaging and therapy, *J. Mater. Chem. B*, 2014, **2**(8), 1031–1037.

216 Z. Chu, J. Liu, Z. Guo and H. Zhang, 2 μm passively Q-switched laser based on black phosphorus, *Opt. Mater. Express*, 2016, **6**(7), 2374–2379.

217 D. Yang, G. Yang, P. Yang, R. Lv, S. Gai, C. Li, F. He and J. Lin, Assembly of Au plasmonic photothermal agent and iron oxide nanoparticles on ultrathin black phosphorus for targeted photothermal and photodynamic cancer therapy, *Adv. Funct. Mater.*, 2017, **27**(18), 1700371.

218 J. Liu, P. Du, T. Liu, B. J. Wong, W. Wang, H. Ju and J. Lei, A black phosphorus/manganese dioxide nanoplatform: oxygen self-supply monitoring, photodynamic therapy enhancement and feedback, *Biomaterials*, 2019, **192**, 179–188.

219 M. He, Y. Chen, C. Tao, Q. Tian, L. An, J. Lin, Q. Tian, H. Yang and S. Yang, Mn-porphyrin-based metal-organic framework with high longitudinal relaxivity for magnetic resonance imaging guidance and oxygen self-supplementing photodynamic therapy, *ACS Appl. Mater. Interfaces*, 2019, **11**(45), 41946–41956.

220 K. Lu, T. Aung, N. Guo, R. Weichselbaum and W. Lin, Nanoscale metal-organic frameworks for therapeutic, imaging, and sensing applications, *Adv. Mater.*, 2018, **30**(37), 1707634.

221 C. S. Jin, L. Cui, F. Wang, J. Chen and G. Zheng, Targeting-triggered porphysome nanostructure disruption for activatable photodynamic therapy, *Adv. Healthcare Mater.*, 2014, **3**(8), 1240–1249.

222 X. Li, C. Y. Kim, S. Lee, D. Lee, H. M. Chung, G. Kim, S. H. Heo, C. Kim, K. S. Hong and J. Yoon, Nanostructured phthalocyanine assemblies with protein-driven switchable photoactivities for biophotonic imaging and therapy, *J. Am. Chem. Soc.*, 2017, **139**(31), 10880–10886.

223 Y. Fu, X. Li, Z. Ren, C. Mao and G. Han, Multifunctional electrospun nanofibers for enhancing localized cancer treatment, *Small*, 2018, **14**(33), 1801183.

224 A. N. Severyukhina, N. V. Petrova, K. Smuda, G. S. Terentyuk, B. N. Klebtsov, R. Georgieva, H. Bäumler and D. A. Gorin, Photosensitizer-loaded electrospun chitosan-based scaffolds for photodynamic therapy and tissue engineering, *Colloids Surf., B*, 2016, **144**, 57–64.

225 H. M. Wu, N. Chen, Z. M. Wu, Z. L. Chen and Y. J. Yan, Preparation of photosensitizer-loaded PLLA nanofibers and its anti-tumor effect for photodynamic therapy in vitro, *J. Biomater. Appl.*, 2013, **27**(6), 773–779.

226 S. M. Costa, L. M. Lourenço, R. C. Calhelha, I. Calejo, C. C. Barrias, R. Fangueiro and D. P. Ferreira, Localized cancer photodynamic therapy approach based on core-shell electrospun nanofibers, *Mater. Adv.*, 2024, **5**(16), 6489–6500.

227 L. M. Maestro, J. E. Ramirez-Hernandez, N. Bogdan, J. A. Capobianco, F. Vetrone, J. G. Solé and D. Jaque, Deep tissue bio-imaging using two-photon excited CdTe fluorescent quantum dots working within the biological window, *Nanoscale*, 2012, **4**(1), 298–302.

228 Q. Ju, X. Chen, F. Ai, D. Peng, X. Lin, W. Kong, P. Shi, G. Zhu and F. Wang, An upconversion nanoprobe operating in the first biological window, *J. Mater. Chem. B*, 2015, **3**(17), 3548–3555.

229 Y. A. Povrozin, L. I. Markova, A. L. Tatarets, V. I. Sidorov, E. A. Terpetschnig and L. D. Patsenker, Near-infrared, dual-ratiometric fluorescent label for measurement of pH, *Anal. Biochem.*, 2009, **390**(2), 136–140.

230 L. R. Hirsch, R. J. Stafford, J. A. Bankson, S. R. Sershen, B. Rivera, R. E. Price, J. D. Hazle, N. J. Halas and J. L. West, Nanoshell-mediated near-infrared thermal therapy of tumors under magnetic resonance guidance, *Proc. Natl. Acad. Sci. U. S. A.*, 2003, **100**(23), 13549–13554.

231 M. I. Setyawati, C. Y. Tay, B. H. Bay and D. T. Leong, Gold nanoparticles induced endothelial leakiness depends on particle size and endothelial cell origin, *ACS Nano*, 2017, **11**(5), 5020–5030.

232 P. K. Jain, K. S. Lee, I. H. El-Sayed and M. A. El-Sayed, Calculated absorption and scattering properties of gold nanoparticles of different size, shape, and composition: applications in biological imaging and biomedicine, *J. Phys. Chem. B*, 2006, **110**(14), 7238–7248.

233 H. H. Richardson, Z. N. Hickman, A. O. Govorov, A. C. Thomas, W. Zhang and M. E. Kordesch,



Thermo-optical properties of gold nanoparticles embedded in ice: characterization of heat generation and melting, *Nano Lett.*, 2006, **6**(4), 783–788.

234 M. Manikandan, N. Hasan and H. F. Wu, Platinum nanoparticles for the photothermal treatment of Neuro 2A cancer cells, *Biomaterials*, 2013, **34**(23), 5833–5842.

235 R. Jiang, S. Cheng, L. Shao, Q. Ruan and J. Wang, Mass-based photothermal comparison among gold nanocrystals, PbS nanocrystals, organic dyes, and carbon black, *J. Phys. Chem. C*, 2013, **117**(17), 8909–8915.

236 S. Link and M. A. El-Sayed, Spectral properties and relaxation dynamics of surface plasmon electronic oscillations in gold and silver nanodots and nanorods, *J. Phys. Chem. B*, 1999, **103**(40), 8410–8426.

237 C. M. Pitsillides, E. K. Joe, X. Wei, R. R. Anderson and C. P. Lin, Selective cell targeting with light-absorbing microparticles and nanoparticles, *Biophys. J.*, 2003, **84**(6), 4023–4032.

238 G. Mie, Beiträge zur Optik trüber Medien, speziell kolloidaler Metallösungen, *Ann. Phys.*, 1908, **330**(3), 377–445.

239 M. F. Tsai, S. H. Chang, F. Y. Cheng, V. Shanmugam, Y. S. Cheng, C. H. Su and C. S. Yeh, Au nanorod design as light-absorber in the first and second biological near-infrared windows for in vivo photothermal therapy, *ACS Nano*, 2013, **7**(6), 5330–5342.

240 R. Vankayala, C. C. Lin, P. Kalluru, C. S. Chiang and K. C. Hwang, Gold nanoshells-mediated bimodal photodynamic and photothermal cancer treatment using ultra-low doses of near infra-red light, *Biomaterials*, 2014, **35**(21), 5527–5538.

241 S. Link, M. B. Mohamed and M. A. El-Sayed, Simulation of the optical absorption spectra of gold nanorods as a function of their aspect ratio and the effect of the medium dielectric constant, *J. Phys. Chem. B*, 1999, **103**(16), 3073–3077.

242 P. Qiu, M. Yang, X. Qu, Y. Huai, Y. Zhu and C. Mao, Tuning photothermal properties of gold nanodendrites for in vivo cancer therapy within a wide near infrared range by simply controlling their degree of branching, *Biomaterials*, 2016, **104**, 138–144.

243 K. Niikura, T. Matsunaga, T. Suzuki, S. Kobayashi, H. Yamaguchi, Y. Orba, A. Kawaguchi, H. Hasegawa, K. Kajino, T. Ninomiya and K. Ijiro, Gold nanoparticles as a vaccine platform: influence of size and shape on immunological responses in vitro and in vivo, *ACS Nano*, 2013, **7**(5), 3926–3938.

244 M. S. Yavuz, Y. Cheng, J. Chen, C. M. Cobley, Q. Zhang, M. Rycenga, J. Xie, C. Kim, K. H. Song, A. G. Schwartz and L. V. Wang, Gold nanocages covered by smart polymers for controlled release with near-infrared light, *Nat. Mater.*, 2009, **8**(12), 935–939.

245 H. Liu, D. Chen, L. Li, T. Liu, L. Tan, X. Wu and F. Tang, Multifunctional gold nanoshells on silica nanorattles: a platform for the combination of photothermal therapy and chemotherapy with low systemic toxicity, *Angew. Chem., Int. Ed.*, 2011, **4**(50), 891–895.

246 F. Rahimi-Moghaddam, N. Azarpira and N. Sattarahmady, Evaluation of a nanocomposite of PEG-curcumin-gold nanoparticles as a near-infrared photothermal agent: An in vitro and animal model investigation, *Lasers Med. Sci.*, 2018, **33**, 1769–1779.

247 S. Park, H. Kim, S. C. Lim, K. Lim, E. S. Lee, K. T. Oh, H. G. Choi and Y. S. Youn, Gold nanocluster-loaded hybrid albumin nanoparticles with fluorescence-based optical visualization and photothermal conversion for tumor detection/ablation, *J. Controlled Release*, 2019, **304**, 7–18.

248 M. Wang, Y. Liu, X. Zhang, L. Luo, L. Li, S. Xing, Y. He, W. Cao, R. Zhu and D. Gao, Gold nanoshell coated thermo-pH dual responsive liposomes for resveratrol delivery and chemo-photothermal synergistic cancer therapy, *J. Mater. Chem. B*, 2017, **5**(11), 2161–2171.

249 F. Xia, J. Niu, Y. Hong, C. Li, W. Cao, L. Wang, W. Hou, Y. Liu and D. Cui, Matrix metallopeptidase 2 targeted delivery of gold nanostars decorated with IR-780 iodide for dual-modal imaging and enhanced photothermal/photodynamic therapy, *Acta Biomater.*, 2019, **89**, 289–299.

250 Y. Li, W. Lu, Q. Huang, C. Li and W. Chen, Copper sulfide nanoparticles for photothermal ablation of tumor cells, *Nanomedicine*, 2010, **5**(8), 1161–1171.

251 J. T. Robinson, K. Welsher, S. M. Tabakman, S. P. Sherlock, H. Wang, R. Luong and H. Dai, High performance in vivo near-IR ( $> 1 \mu\text{m}$ ) imaging and photothermal cancer therapy with carbon nanotubes, *Nano Res.*, 2010, **3**, 779–793.

252 Q. Tian, F. Jiang, R. Zou, Q. Liu, Z. Chen, M. Zhu, S. Yang, J. Wang, J. Wang and J. Hu, Hydrophilic Cu9S5 nanocrystals: a photothermal agent with a 25.7% heat conversion efficiency for photothermal ablation of cancer cells in vivo, *ACS Nano*, 2011, **5**(12), 9761–9771.

253 B. Li, Q. Wang, R. Zou, X. Liu, K. Xu, W. Li and J. Hu, Cu 7.2 S 4 nanocrystals: a novel photothermal agent with a 56.7% photothermal conversion efficiency for photothermal therapy of cancer cells, *Nanoscale*, 2014, **6**(6), 3274–3282.

254 L. M. Peng, Z. Zhang, S. Wang and Y. Li, Carbon Nanotube (CNT)-Based High-Performance Electronic and Optoelectronic Devices. *One-Dimensional Nanostructures: Principles and Applications*, 2012, pp. 321–338.

255 X. Liu, N. Huang, H. Wang, H. Li, Q. Jin and J. Ji, The effect of ligand composition on the in vivo fate of multidentate poly (ethylene glycol) modified gold nanoparticles, *Biomaterials*, 2013, **34**(33), 8370–8381.

256 A. R. Burke, R. N. Singh, D. L. Carroll, J. C. Wood, R. B. D'Agostino Jr, P. M. Ajayan, F. M. Torti and S. V. Torti, The resistance of breast cancer stem cells to conventional hyperthermia and their sensitivity to nanoparticle-mediated photothermal therapy, *Biomaterials*, 2012, **33**(10), 2961–2970.

257 W. Zhang, Z. Guo, D. Huang, Z. Liu, X. Guo and H. Zhong, Synergistic effect of chemo-photothermal therapy using PEGylated graphene oxide, *Biomaterials*, 2011, **32**(33), 8555–8561.



258 Z. M. Markovic, L. M. Harhaji-Trajkovic, B. M. Todorovic-Markovic, D. P. Kepić, K. M. Arsikin, S. P. Jovanović, A. C. Pantovic, M. D. Dramićanin and V. S. Trajkovic, In vitro comparison of the photothermal anticancer activity of graphene nanoparticles and carbon nanotubes, *Biomaterials*, 2011, **32**(4), 1121–1129.

259 J. H. Lim, D. E. Kim, E. J. Kim, C. D. Ahrberg and B. G. Chung, Functional graphene oxide-based nanosheets for photothermal therapy, *Macromol. Res.*, 2018, **26**(6), 557–565.

260 M. Xie, F. Zhang, H. Peng, Y. Zhang, Y. Li, Y. Xu and J. Xie, Layer-by-layer modification of magnetic graphene oxide by chitosan and sodium alginate with enhanced dispersibility for targeted drug delivery and photothermal therapy, *Colloids Surf., B*, 2019, **176**, 462–470.

261 A. Gulzar, J. Xu, D. Yang, L. Xu, F. He, S. Gai and P. Yang, Nano-graphene oxide-UCNP-Ce6 covalently constructed nanocomposites for NIR-mediated bioimaging and PTT/PDT combinatorial therapy, *Dalton Trans.*, 2018, **47**(11), 3931–3939.

262 R. F. de Paula, I. A. Rosa, I. F. Gafanhão, J. L. Fachí, A. M. Melero, A. O. Roque, V. O. Boldrini, L. A. Ferreira, S. P. Irazusta, H. J. Ceragioli and E. C. de Oliveira, Reduced graphene oxide, but not carbon nanotubes, slows murine melanoma after thermal ablation using LED light in B16F10 lineage cells. *Nanomedicine, Nanomedicine*, 2020, **28**, 102231.

263 I. Marangon, C. Ménard-Moyon, A. K. Silva, A. Bianco, N. Luciani and F. Gazeau, Synergic mechanisms of photothermal and photodynamic therapies mediated by photosensitizer/carbon nanotube complexes, *Carbon*, 2016, **97**, 110–123.

264 J. Yang, J. Choi, D. Bang, E. Kim, E. K. Lim, H. Park, J. S. Suh, K. Lee, K. H. Yoo, E. K. Kim and Y. M. Huh, Convertible organic nanoparticles for near-infrared photothermal ablation of cancer cells, *Angew. Chem., Int. Ed.*, 2011, **50**(2), 441–444.

265 Z. Zhou, B. Kong, C. Yu, X. Shi, M. Wang, W. Liu, Y. Sun, Y. Zhang, H. Yang and S. Yang, Tungsten oxide nanorods: an efficient nanoplatform for tumor CT imaging and photothermal therapy, *Sci. Rep.*, 2014, **4**(1), 3653.

266 S. M. Sharker, S. M. Kim, J. E. Lee, K. H. Choi, G. Shin, S. Lee, K. D. Lee, J. H. Jeong, H. Lee and S. Y. Park, Functionalized biocompatible WO<sub>3</sub> nanoparticles for triggered and targeted in vitro and in vivo photothermal therapy, *J. Controlled Release*, 2015, **217**, 211–220.

267 E. Vittorino, M. T. Sciortino, G. Siracusano and S. Sortino, Light-Activated Release of Nitric Oxide with Fluorescence Reporting in Living Cells, *ChemMedChem*, 2011, **6**(9), 1551–1554.

268 M. Cheng, H. Wang, Z. Zhang, N. Li, X. Fang and S. Xu, Gold nanorod-embedded electrospun fibrous membrane as a photothermal therapy platform, *ACS Appl. Mater. Interfaces*, 2014, **6**(3), 1569–1575.

269 X. Wang, L. Wang, S. Zong, R. Qiu and S. Liu, Use of multifunctional composite nanofibers for photothermal chemotherapy to treat cervical cancer in mice, *Biomater. Sci.*, 2019, **7**(9), 3846–3854.

270 M. H. Azerbaijan, E. Bahmani, M. H. Jouybari, A. Hassaniazardaryani, P. Goleij, M. Akrami and M. Irani, Electrospun gold nanorods/graphene oxide loaded-core-shell nanofibers for local delivery of paclitaxel against lung cancer during photo-chemotherapy method, *Eur. J. Pharm. Sci.*, 2021, **164**, 105914.

271 S. Veeranarayanan and T. Maekawa, External stimulus responsive inorganic nanomaterials for cancer theranostics, *Adv. Drug Delivery Rev.*, 2019, **138**, 18–40.

272 A. Sneider, D. VanDyke, S. Paliwal and P. Rai, Remotely triggered nano-theranostics for cancer applications, *Nanotheranostics*, 2017, **1**(1), 1.

273 Q. Chen, H. Ke, Z. Dai and Z. Liu, Nanoscale theranostics for physical stimulus-responsive cancer therapies, *Biomaterials*, 2015, **73**, 214–230.

274 Y. Chen, H. Li, Y. Deng, H. Sun, X. Ke and T. Ci, Near-infrared light triggered drug delivery system for higher efficacy of combined chemo-photothermal treatment, *Acta Biomater.*, 2017, **51**, 374–392.

275 P. Manivasagan, S. W. Jun, G. Hoang, S. Mondal, H. Kim, V. H. Doan, J. Kim, C. S. Kim and J. Oh, Anti-EGFR antibody conjugated thiol chitosan-layered gold nanoshells for dual-modal imaging-guided cancer combination therapy, *J. Controlled Release*, 2019, **311**, 26–42.

276 W. Zhang, F. Wang, Y. Wang, J. Wang, Y. Yu, S. Guo, R. Chen and D. Zhou, pH and near-infrared light dual-stimuli responsive drug delivery using DNA-conjugated gold nanorods for effective treatment of multidrug resistant cancer cells, *J. Controlled Release*, 2016, **232**, 9–19.

277 S. Huang, S. Duan, J. Wang, S. Bao, X. Qiu, C. Li, Y. Liu, L. Yan, Z. Zhang and Y. Hu, Folic-acid-mediated functionalized gold nanocages for targeted delivery of anti-miR-181b in combination of gene therapy and photothermal therapy against hepatocellular carcinoma, *Adv. Funct. Mater.*, 2016, **26**(15), 2532–2544.

278 D. Wang, Y. Ren, Y. Shao, D. Yu and L. Meng, Facile preparation of doxorubicin-loaded and folic acid-conjugated carbon nanotubes@ poly (N-vinyl pyrrole) for targeted synergistic chemo-Photothermal Cancer treatment, *Bioconjugate Chem.*, 2017, **28**(11), 2815–2822.

279 R. Lima-Sousa, D. de Melo-Diogo, C. G. Alves, E. C. Costa, P. Ferreira, R. O. Louro and I. J. Correia, Hyaluronic acid functionalized green reduced graphene oxide for targeted cancer photothermal therapy, *Carbohydr. Polym.*, 2018, **200**, 93–99.

280 S. Roy, A. Sarkar and A. Jaiswal, Poly (allylamine hydrochloride)-functionalized reduced graphene oxide for synergistic chemo-photothermal therapy, *Nanomedicine*, 2019, **14**(3), 255–274.

281 K. Wang, Q. Chen, W. Xue, S. Li and Z. Liu, Combined chemo-photothermal antitumor therapy using molybdenum disulfide modified with hyperbranched polyglycidyl, *ACS Biomater. Sci. Eng.*, 2017, **3**(10), 2325–2335.



282 T. Bao, W. Yin, X. Zheng, X. Zhang, J. Yu, X. Dong, Y. Yong, F. Gao, L. Yan, Z. Gu and Y. Zhao, One-pot synthesis of PEGylated plasmonic  $\text{MoO}_3\text{-x}$  hollow nanospheres for photoacoustic imaging guided chemo-photothermal combinational therapy of cancer, *Biomaterials*, 2016, **76**, 11–24.

283 R. M. Yang, C. P. Fu, J. Z. Fang, X. D. Xu, X. H. Wei, W. J. Tang, X. Q. Jiang and L. M. Zhang, Hyaluronan-modified superparamagnetic iron oxide nanoparticles for bimodal breast cancer imaging and photothermal therapy, *Int. J. Nanomed.*, 2017, **23**, 197–206.

284 L. Hou, X. Shan, L. Hao, Q. Feng and Z. Zhang, Copper sulfide nanoparticle-based localized drug delivery system as an effective cancer synergistic treatment and theranostic platform, *Acta Biomater.*, 2017, **54**, 307–320.

285 Y. Ma, X. Liang, S. Tong, G. Bao, Q. Ren and Z. Dai, Gold nanoshell nanomicelles for potential magnetic resonance imaging, light-triggered drug release, and photothermal therapy, *Adv. Funct. Mater.*, 2013, **23**(7), 815–822.

286 M. Bañobre-López, A. Teijeiro and J. Rivas, Magnetic nanoparticle-based hyperthermia for cancer treatment, *Rep. Pract. Oncol. Radiother.*, 2013, **18**(6), 397–400.

287 Z. Hedayatnasab, F. Abnisa and W. M. Daud, Review on magnetic nanoparticles for magnetic nanofluid hyperthermia application, *Mater. Des.*, 2017, **123**, 174–196.

288 M. Angelakeris, Magnetic nanoparticles: A multifunctional vehicle for modern theranostics, *Biochim. Biophys. Acta - Gen. Subj.*, 2017, **1861**(6), 1642–1651.

289 A. Matsumine, K. Takegami, K. Asanuma, T. Matsubara, T. Nakamura, A. Uchida and A. Sudo, A novel hyperthermia treatment for bone metastases using magnetic materials, *Int. J. Clin. Oncol.*, 2011, **16**, 101–108.

290 Y. Ni, S. Mulier, Y. Miao, L. Michel and G. Marchal, A review of the general aspects of radiofrequency ablation, *Abdom. Imaging*, 2005, **30**, 381–400.

291 A. A. Elsherbini, M. Saber, M. Aggag, A. El-Shahawy and H. A. Shokier, Laser and radiofrequency-induced hyperthermia treatment via gold-coated magnetic nanocomposites, *Int. J. Nanomed.*, 2011, **28**, 2155–2165.

292 Q. Zhang and L. Li, Photodynamic combinational therapy in cancer treatment, *J. BUON.*, 2018, **23**(3), 561–567.

293 M. Faber, C. Coudray, H. Hida, M. Mousseau and A. Favier, Lipid peroxidation products, and vitamin and trace element status in patients with cancer before and after chemotherapy, including adriamycin: a preliminary study, *Biol. Trace Elem. Res.*, 1995, **47**, 117–123.

294 G. Canti, A. Nicolin, R. Cubeddu, P. Taroni, G. Bandieramonte and G. Valentini, Antitumor efficacy of the combination of photodynamic therapy and chemotherapy in murine tumors, *Cancer Lett.*, 1998, **125**(1–2), 39–44.

295 X. Wang, G. Meng, S. Zhang and X. Liu, A reactive  $\text{1O}_2$ -responsive combined treatment system of photodynamic and chemotherapy for cancer, *Sci. Rep.*, 2016, **6**(1), 1–9.

296 A. Khair, D. Chen, Y. Patil, L. Ma, Q. P. Dou, M. P. Shekhar and J. Panyam, Nanoparticle-mediated combination chemotherapy and photodynamic therapy overcomes tumor drug resistance, *J. Controlled Release*, 2010, **141**(2), 137–144.

297 S. Bano, S. Nazir, S. Munir, M. F. AlAjmi, M. Afzal and K. Mazhar, “Smart” nickel oxide based core-shell nanoparticles for combined chemo and photodynamic cancer therapy, *Int. J. Nanomed.*, 2016, **12**, 3159–3166.

298 A. Nakano, D. Watanabe, Y. Akita, T. Kawamura, Y. Tamada and Y. Matsumoto, Treatment efficiency of combining photodynamic therapy and ionizing radiation for Bowen's disease, *J. Eur. Acad. Dermatol. Venereol.*, 2011, **25**(4), 475–478.

299 J. Takahashi, M. Misawa and H. Iwahashi, Transcriptome analysis of porphyrin-accumulated and X-ray-irradiated cell cultures under limited proliferation and non-lethal conditions, *Microarrays*, 2015, **4**(1), 25–40.

300 M. Mitsunaga, T. Nakajima, K. Sano, P. L. Choyke and H. Kobayashi, Near-infrared theranostic photoimmunotherapy (PIT): repeated exposure of light enhances the effect of immunoconjugate, *Bioconjugate Chem.*, 2012, **23**(3), 604–609.

301 C. He, X. Duan, N. Guo, C. Chan, C. Poon, R. R. Weichselbaum and W. Lin, Core-shell nanoscale coordination polymers combine chemotherapy and photodynamic therapy to potentiate checkpoint blockade cancer immunotherapy, *Nat. Commun.*, 2016, **7**(1), 12499.

302 X. Zheng, D. Xing, F. Zhou, B. Wu and W. R. Chen, Indocyanine green-containing nanostructure as near infrared dual-functional targeting probes for optical imaging and photothermal therapy, *Mol. Pharmaceutics*, 2011, **8**(2), 447–456.

303 X. Zheng, F. Zhou, B. Wu, W. R. Chen and D. Xing, Enhanced tumor treatment using biofunctional indocyanine green-containing nanostructure by intratumoral or intravenous injection, *Mol. Pharmaceutics*, 2012, **9**(3), 514–522.

304 M. Korbelik and I. Cecic, Enhancement of tumour response to photodynamic therapy by adjuvant mycobacterium cell-wall treatment, *J. Photochem. Photobiol. B*, 1998, **44**(2), 151–158.

305 S. Wu and H. J. Butt, Near-infrared photochemistry at interfaces based on upconverting nanoparticles, *Phys. Chem. Chem. Phys.*, 2017, **19**(35), 23585–23596.

306 Y. Li, D. He, J. Tu, R. Wang, C. Zu, Y. Chen, W. Yang, D. Shi, T. J. Webster and Y. Shen, The comparative effect of wrapping solid gold nanoparticles and hollow gold nanoparticles with doxorubicin-loaded thermosensitive liposomes for cancer thermo-chemotherapy, *Nanoscale*, 2018, **10**(18), 8628–8641.

307 Z. Meng, F. Wei, R. Wang, M. Xia, Z. Chen, H. Wang and M. Zhu, NIR-laser-switched in vivo smart nanocapsules for synergic photothermal and chemotherapy of tumors, *Adv. Mater.*, 2016, **28**(2), 245–253.

308 Y. Liu, Y. Xi, J. Zhao, J. Li, G. Huang, J. Li, F. Fang, L. Gu and S. Wang, Preparation of therapeutic-laden konjac hydrogel for tumor combination therapy, *Chem. Eng. J.*, 2019, **375**, 122048.



309 Y. Zheng, W. Wang, J. Zhao, C. Wu, C. Ye, M. Huang and S. Wang, Preparation of injectable temperature-sensitive chitosan-based hydrogel for combined hyperthermia and chemotherapy of colon cancer, *Carbohydr. Polym.*, 2019, **222**, 115039.

310 V. P. Chauhan, T. Stylianopoulos, Y. Boucher and R. K. Jain, Delivery of molecular and nanoscale medicine to tumors: transport barriers and strategies, *Annu. Rev. Chem. Biomol. Eng.*, 2011, **2**(1), 281–298.

311 R. K. Jain, J. D. Martin and T. Stylianopoulos, The role of mechanical forces in tumor growth and therapy, *Annu. Rev. Biomed. Eng.*, 2014, **16**(1), 321–346.

312 Y. Zheng, F. Zou, J. Wang, G. Yin, V. Le, Z. Fei and J. Liu, Photodynamic therapy-mediated cancer vaccination enhances stem-like phenotype and immune escape, which can be blocked by thrombospondin-1 signaling through CD47 receptor protein, *J. Biol. Chem.*, 2015, **290**(14), 8975–8986.

313 Y. Liu, Y. Liu, W. Bu, Q. Xiao, Y. Sun, K. Zhao, W. Fan, J. Liu and J. Shi, Radiation-/hypoxia-induced solid tumor metastasis and regrowth inhibited by hypoxia-specific upconversion nanoradiosensitizer, *Biomaterials*, 2015, **49**, 1–8.

314 L. Cheng, S. Shen, S. Shi, Y. Yi, X. Wang, G. Song, K. Yang, G. Liu, T. E. Barnhart, W. Cai and Z. Liu, FeSe<sub>2</sub>-decorated Bi<sub>2</sub>Se<sub>3</sub> nanosheets fabricated via cation exchange for chelator-free <sup>64</sup>Cu-labeling and multimodal image-guided photothermal-radiation therapy, *Adv. Funct. Mater.*, 2016, **26**(13), 2185–2197.

315 X. Yi, K. Yang, C. Liang, X. Zhong, P. Ning, G. Song, D. Wang, C. Ge, C. Chen, Z. Chai and Z. Liu, Imaging-guided combined photothermal and radiotherapy to treat subcutaneous and metastatic tumors using iodine-131-doped copper sulfide nanoparticles, *Adv. Funct. Mater.*, 2015, **25**(29), 4689–4699.

316 W. Y. Sheng and L. Huang, Cancer immunotherapy and nanomedicine, *Pharm. Res.*, 2011, **28**, 200–214.

317 X. Dong, J. Liang, A. Yang, Z. Qian, D. Kong and F. Lv, Fluorescence imaging guided CpG nanoparticles-loaded IR820-hydrogel for synergistic photothermal immunotherapy, *Biomaterials*, 2019, **209**, 111–125.

318 Y. Tao, E. Ju, J. Ren and X. Qu, Immunostimulatory oligonucleotides-loaded cationic graphene oxide with photothermally enhanced immunogenicity for photothermal/immune cancer therapy, *Biomaterials*, 2014, **35**(37), 9963–9971.

319 S. Wang, P. Huang, L. Nie, R. Xing, D. Liu, Z. Wang, J. Lin, S. Chen, G. Niu, G. Lu and X. Chen, Single continuous wave laser induced photodynamic/plasmonic photothermal therapy using photosensitizer-functionalized gold nanostars, *Adv. Mater.*, 2013, **25**(22), 3055.

320 H. P. Tham, H. Chen, Y. H. Tan, Q. Qu, S. Sreejith, L. Zhao, S. S. Venkatraman and Y. Zhao, Photosensitizer anchored gold nanorods for targeted combinational photothermal and photodynamic therapy, *Chem. Commun.*, 2016, **52**(57), 8854–8857.

321 P. Kalluru, R. Vankayala, C. S. Chiang and K. C. Hwang, Nano-graphene oxide-mediated *In vivo* fluorescence imaging and bimodal photodynamic and photothermal destruction of tumors, *Biomaterials*, 2016, **95**, 1.

322 Y. Wang, H. Wang, D. Liu, S. Song, X. Wang and H. Zhang, Graphene oxide covalently grafted upconversion nanoparticles for combined NIR mediated imaging and photothermal/photodynamic cancer therapy, *Biomaterials*, 2013, **34**(31), 7715–7724.

323 M. Overchuk, R. A. Weersink, B. C. Wilson and G. Zheng, Photodynamic and photothermal therapies: synergy opportunities for nanomedicine, *ACS Nano*, 2023, **17**(9), 7979–8003.

324 J. Kadkhoda, A. Tarighatnia, J. Barar, A. Aghanejad and S. Davaran, Recent advances and trends in nanoparticles based photothermal and photodynamic therapy, *Photodiagn. Photodyn. Ther.*, 2022, **37**, 102697.

325 I. Rizvi, S. Nath, G. Obaid, M. K. Ruhi, K. Moore, S. Bano, D. Kessel and T. Hasan, A combination of visudyne and a lipid-anchored liposomal formulation of benzoporphyrin derivative enhances photodynamic therapy efficacy in a 3D model for ovarian cancer, *Photochem. Photobiol.*, 2019, **95**(1), 419–429.

